General Disclaimer

One or more of the Following Statements may affect this Document

- This document has been reproduced from the best copy furnished by the organizational source. It is being released in the interest of making available as much information as possible.

- This document may contain data, which exceeds the sheet parameters. It was furnished in this condition by the organizational source and is the best copy available.

- This document may contain tone-on-tone or color graphs, charts and/or pictures, which have been reproduced in black and white.

- This document is paginated as submitted by the original source.

- Portions of this document are not fully legible due to the historical nature of some of the material. However, it is the best reproduction available from the original submission.

EVALUATION AND CHARACTERIZATION OF THE METHANE-CARBON DIOXIDE DECOMPOSITION REACTION

(NASA-CR-143890) EVALUATION AND CHARACTERIZATION OF THE METHANE-CARBON DIOXIDE DECOMPOSITION REACTION Final Report, 20 Jun. 1974 - 19 Jun. 1975 (Life Systems, Inc., Cleveland, Ohio.) 81 p HC G3/23

N75-27071

Unclas 29187

FINAL REPORT

by

R.J. Davenport, F.H. Schubert,
J.W. Shumar and T.S. Steenson

June, 1975

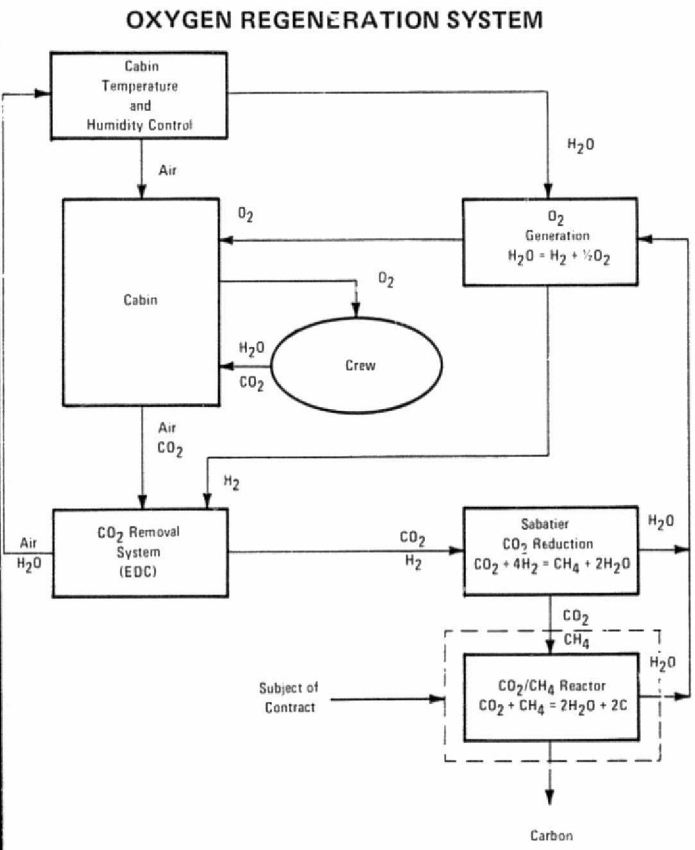

Prepared Under Contract No. NAS8- 30748

by

Life Systems, Inc.
Cleveland, Ohio 44122

for

GEORGE C. MARSHALL SPACE FLIGHT CENTER

National Aeronautics & Space Administration
Marshall Space Flight Center, Alabama 35812

FOREWORD

The analytical and experimental work described herein was performed by Life Systems, Inc. under NASA Contract NAS8-30748 during the period June 20, 1974 to June 19, 1975. The program was directed by F. H. Schubert. Technical effort was completed by R. J. Davenport, T. S. Steeson, and J. W. Shumar.

The Contract Technical Monitor was David C. Clark, Science and Engineering, Astronautics Laboratory, George C. Marshall Space Flight Center, Huntsville, Alabama 35812

TABLE OF CONTENTS

	PAGE
LIST OF FIGURES	iii
LIST OF TABLES	iv
SUMMARY	1
INTRODUCTION	2
METHODS OF CARBON DIOXIDE REDUCTION WITH METHANE	10
Catalytic Reduction Methods	10
Heterogeneous Catalysts	11
Homogeneous Catalysts	11
Gamma Radiation Methods	12
Ultraviolet Radiation Methods	13
Reduction Methods Investigated	13
TEST HARDWARE	14
Catalytic Reactors	15
Reactor Geometry and Sizing	15
Test Stand	15
Reactor Oven	15
Functional Block Diagram of Test Stand	18
Test Stand Construction	18
Ultraviolet Apparatus	20
TEST PROGRAM	20
Test Procedures	20
Definitions	20
Analytical Instrumentation and Procedures	24
Water Generation Rate Measurement	24
Catalyst Pre-Treatment Procedures	25
Baseline Experimental Parameters	25
Test Stand Checkout and Calibration Procedures	28

continued-

Table of Contents - continued

	PAGE
Objective	28
Procedure	28
Results	30
Catalyst Characterization Study	30
Objective	30
Procedure	30
Results	31
Parametric Testing	33
Objective	33
Procedure	33
Results	34
Reactant Gas Flow Rate	43
Reactant Gas Composition	43
Ultraviolet Activation Studies	47
Objective	47
Procedure	47
Results	50
O_2 REGENERATION SYSTEM EMPLOYING THE CO_2/CH_4 REACTOR	53
Electrochemical Depolarized Concentrator (EDC)	58
Sabatier Reactor	58
Solid Electrolyte Water Electrolysis Unit	58
H_2 Separator	63
CO_2/CH_4 Reactor	63
CONCLUSIONS	63
RECOMMENDATIONS	67
REFERENCES	68
APPENDIX 1 - CALIBRATION DATA	A1-1

LIST OF FIGURES

FIGURE		PAGE
1	Water Weight Penalty Versus Time For Six-Man System Employing The "Sabatier-Methane Dump" Concept For Partial O_2 Regeneration	4
2	Comparison Of Sabatier, BCRS And SEORS Systems For CO_2 Reduction	5
3	Bosch Unit Schematic	6
4	Solid Electrolyte O_2 Regeneration System Schematic	7
5	Maximum CO_2-CH_4 Conversion Versus Temperature	9
6	Schematic Of Reactor And Catalyst Bed	16
7	Oven And Exposed Quartz Reactor	17
8	Schematic Of Test Apparatus	19
9	Front Of Test Stand And Gas Chromatograph	21
10	Rear Of Test Stand	22
11	Schematic Of UV Lamp Integrated With Reactor Packed With Catalyst	23
12	Conversion Efficiencies of CO_2 And H_2 In Sabatier Reactor	27
13	Reaction Efficiency Of Linde Catalyst Versus Catalyst Weight	35
14	Reaction Efficiency Of Linde Catalyst Versus Catalyst Weight	37
15	Reactor Temperature Gradient Temperature Versus Distance From Reactor Inlet	38
16	Reaction Efficiency Of Girdler And Linde Catalysts Versus Nominal Reactor Temperature	39
17	Reactor Effluent Composition For Linde Catalyst Versus Nominal Reactor Temperature	41
18	Reactor Effluent Composition For Girdler Catalyst Versus Nominal Reactor emperature	42
19	Effect Of Iron On Reactor Effluent Composition	44
20	Reaction Efficiencies Of Girdler And Linde Catalysts Versus Total Reactant Gas Flow Rate	45
21	Reaction Efficiencies Of Girdler And Linde Catalysts Versus Space Velocity	46
22	Reaction Efficiencies Of Girdler And Linde Catalysts Versus Reactant Gas Composition	48
23	Reaction Efficiencies Of Girdler And Linde Catalysts Versus Reactor Inlet Pressure	49
24	Effects Of UV Activation On Reactor Effluent Composition, Linde Catalyst	51
25	Effects Of UV Activation On Reactor Effluent Composition, Girdler Catalyst	52
26	Schematic Of UV Activation Apparatus Without Catalyst	54

continued-

List of Figures - continued

		PAGE
27	Effects Of UV Activation Without Catalyst On Reactor Effluent Composition	55
28	Comparison Of Water Weight Penalty For Two Partial O_2 Regeneration Concepts	56
29	ORS Block Diagram And Mass Balance	57
30	EDC Cell Schematic	61
31	Sabatier Reactor Configuration	62
32	High Temperature Water Electrolysis Unit Cell Schematic	64
33	H_2 Separator Configuration	65

LIST OF TABLES

TABLE		PAGE
1	Sabatier Subsystem Material Balance For The Four-Man 90-Day, Space Station Simulator Test	3
2	Baseline Values Of The Experimental Parameters	26
3	Parametric Test Instrumentation	29
4	Results of Catalyst Characterization Study	32
5	Operating Characteristics Of The Major ORS Units	59

SUMMARY

A program was conducted to evaluate and characterize the carbon dioxide-methane (CO_2-CH_4) decomposition reaction, i.e., $CO_2 + CH_4 = 2C + 2H_2O$. The primary objective was to determine the feasibility of applying this reaction at low temperatures as a technique for recovering the oxygen (O_2) remaining in the CO_2 which exits mixed with CH_4 from a Sabatier CO_2 Reduction Subsystem as part of an Air Revitalization System (ARS) of a manned spacecraft.

A test unit was designed, fabricated, and assembled for characterizing the performance of various catalysts for the reaction and ultraviolet (UV) activation of the CH_4 and CO_2. The reactor included in the test unit was designed to have sufficient capacity to evaluate catalyst charges of up to 76 g (0.17 lb). The test stand contained the necessary instrumentation and controls to obtain the data required to characterize the performance of the catalysts and sensitizers tested, i.e., flow control and measurement, temperature control and measurement, product and inlet gas analysis, and pressure measurement.

A Product Assurance Program was performed implementing the concepts of quality control and safety into the program effort. The Product Assurance tasks ensured that test procedures were consistent with program objectives and that safety guidelines for program personnel dealing with the test apparatus were followed.

A literature review to identify the catalysts and UV sensitizers which possess the greatest probability for increasing the rate of the low temperature CO_2-CH_4 reaction was performed. Six candidate catalysts were selected and experimentally characterized. The six catalysts were Harshaw nickel (Ni) on kieselguhr, Girdler Ni on kieselguhr, Engelhard palladium (Pd) on alumina, Engelhard ruthenium (Ru) on alumina, Linde Ni on molecular sieves, and Girdler Ni on molecular sieves. The characterization tests involved evaluating each catalyst at one reactant gas mixture composition (3:1 CH_4/CO_2 mole ratio), one reactant flow rate (200 cm^3/min (7.06×10^{-3} cfm)), and two reactor temperatures (673K (752F) and 873K (1112F)).

Extensive parametric testing was conducted on two catalysts which performed best in the characterization study. These catalysts were Girdler Ni on molecular sieves and Linde Ni on molecular sieves. The parametric testing included determining reaction efficiency as a function of temperature from 473K (392F) to 1073K (1472F); as a function of pressure from 108 kN/m^2 (15.7 psia) to 446 kN/m^2 (64.7 psia); as a function of reactant gas composition from a 1:1 to a 7:1 CH_4/CO_2 ratio; and finally, as a function of reactant gas flow rate from 100 cm^3/min (3.53×10^{-3} cfm) to 400 cm^3/min (14.12×10^{-3} cfm).

The parametric test results demonstrated that the catalytic reaction of CO_2 and CH_4 did not occur at low reactor temperatures. To attain a reaction efficiency of 29%, temperatures up to 873K (1112F) were required. The 873K (1112F) CO_2/CH_4 Reactor temperature is comparable to the temperatures required by other carbon forming reactors, e.g., the CO Disproportionator operating temperature is 823K (1022F) and the Bosch Reactor operating temperature is 923K (1202F).

Ultraviolet activation of the CO_2/CH_4 reactant gas mixture, both with and without

catalyst, was evaluated as a possible method of providing necessary energy to the reactants for the low temperature reduction of CO_2.

The UV activation was found to have no significant effect on the reduction of CO_2 with CH_4 when used with or without the Ni on molecular sieve catalysts.

Based on the 29% reaction efficiency obtained with the Linde Ni on molecular sieve catalyst at 873K (1112F), a conceptual O_2 regeneration system involving the integration of the Sabatier reactor and a CO_2/CH_4 reactor was designed.

INTRODUCTION

For future extended duration manned spaceflights there is a definite need for systems that can recover O_2 from expired CO_2. Such a system could reduce flight weight by eliminating the need for carrying stored O_2 (in the form of water or other equivalent) at launch. Several concepts which partially or completely perform this function have been proposed and studied. Some of these are the Fused Salt concept, the Solid Electrolyte concept, the Bosch Reactor concept, the Sabatier-Methane Dump concept, the Sabatier-Methane Decomposition concept, and the Sabatier-Acetylene Dump concept.[1] The Sabatier-Methane Dump concept has been utilized in the Oxygen Recovery System (ORS) for a 90-day Space Station Simulator Test[2] and also was included in the Atmosphere Revitalization Group (ARG) of the Space Station Prototype (SSP).[3] In both applications, a portion of the CO_2 does not react in the Sabatier Reactor because the system lacks sufficient hydrogen (H_2). This is illustrated by Table 1, which is the Sabatier Subsystem Material Balance for the four-man, 90-day, Space Station Simulator Test. The 98.7 kg (217.6 lb) of unreacted CO_2 represents 71.8 kg (158.3 lb) of lost O_2 and would require the storage and electrolysis of 80.8 kg (178.2 lb) of water to compensate for the lost O_2. Figure 1 shows the water weight penalty as a function of time for a six-man mission employing the Sabatier-Methane Dump concept for partial CO_2 reduction.

Two other systems perform the CO_2 reduction process: the Bosch CO_2 Reduction System[4] (BRS) and the Solid Electrolyte O_2 Regeneration System[5] (SEORS). These systems reduce the expired CO_2 either directly to O_2 or to water. The BRS employs a recycle loop with regenerative heat exchangers and water condenser/separators while the SEORS employs a hot recycle loop. A figure showing the relationship between the Sabatier, BRS and SEORS with respect to the CO_2 reduction function is presented in Figure 2. Schematics of the BRS and the SEORS are shown in Figures 3 and 4, respectively. The Sabatier Reactor has several advantages as compared to the BRS and the SEORS. The Sabatier removes carbon in the gaseous state, is a once-through reactor involving the methanation of CO_2 with H_2 (Equation 1), and is accomplished at moderate reactor temperatures.

$$CO_2 + 4H_2 = CH_4 + 2H_2O \qquad (1)$$

However, as previously pointed out, a disadvantage of the Sabatier reactor is that a portion of the expired CO_2 does not react, resulting in lost O_2 when the Sabatier exhaust is dumped. In order to increase the O_2 recovery capability of the Sabatier Reactor, a means for increasing the amount of CO_2 reduced must be established.

TABLE I SABATIER SUBSYSTEM MATERIAL BALANCE
FOR THE FOUR-MAN, 90-DAY, SPACE STATION SIMULATOR TEST

Material In	Weight, kg (Lb)
CO_2	288.9 (636.9)
H_2	36.7 (81.0)
N_2	7.5 (16.6)
O_2	3.7 (8.1)
Water Vapor	2.5 (5.5)
Total:	339.3 (748.1)

Material Out	
Water to Electrolysis Cell	150.6 (332.0)
CH_4	69.2 (152.5)
CO_2	98.7 (217.6)
N_2	7.5 (16.6)
O_2	0.2 (0.5)
H_2	1.7 (3.8)
Water Exhausted	11.4 (25.2)
Total:	339.3 (748.2)

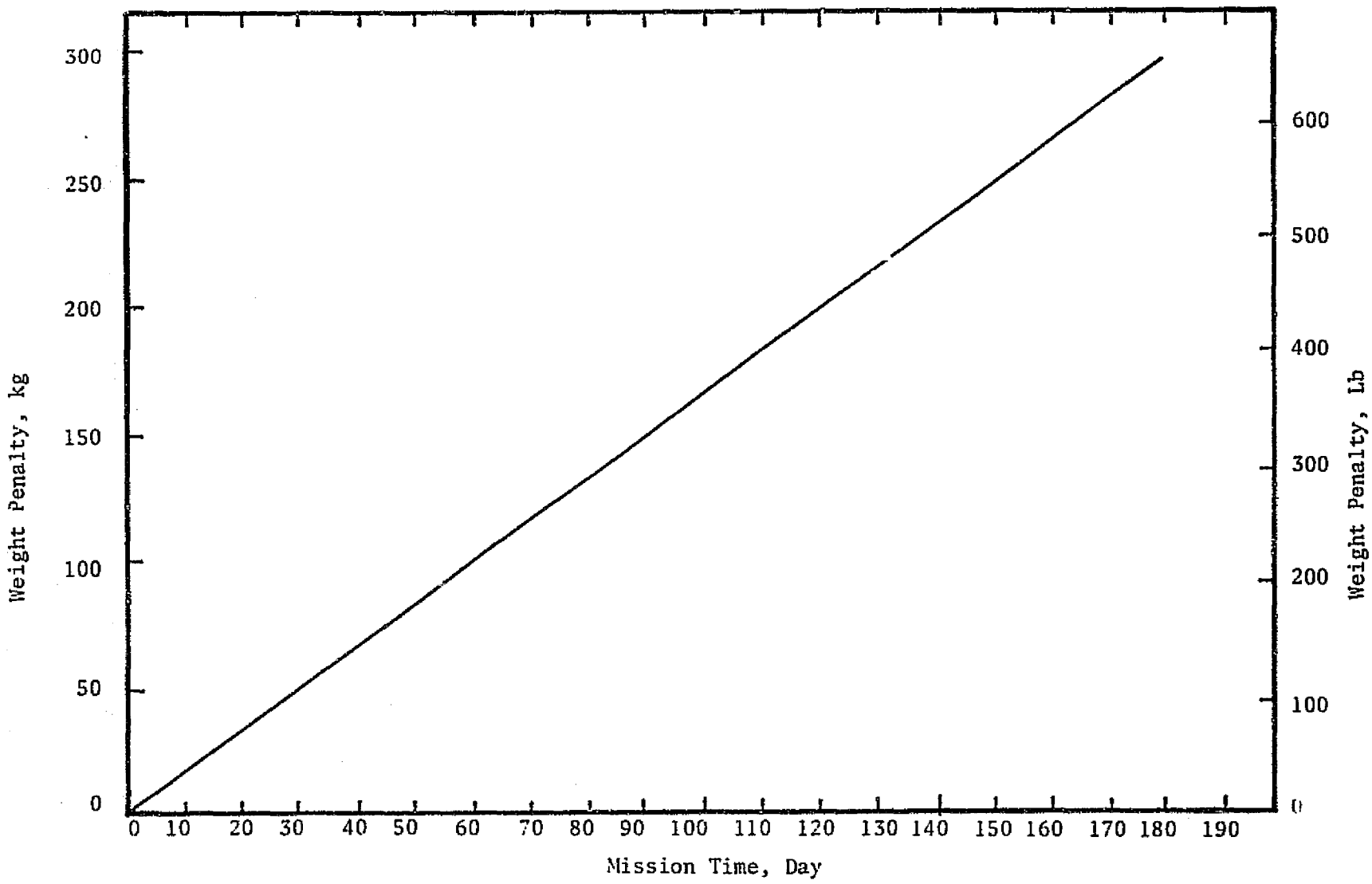

FIGURE 1 WATER WEIGHT PENALTY VERSUS TIME FOR SIX-MAN SYSTEM EMPLOYING THE "SABATIER-METHANE DUMP" CONCEPT FOR PARTIAL O_2 REGENERATION

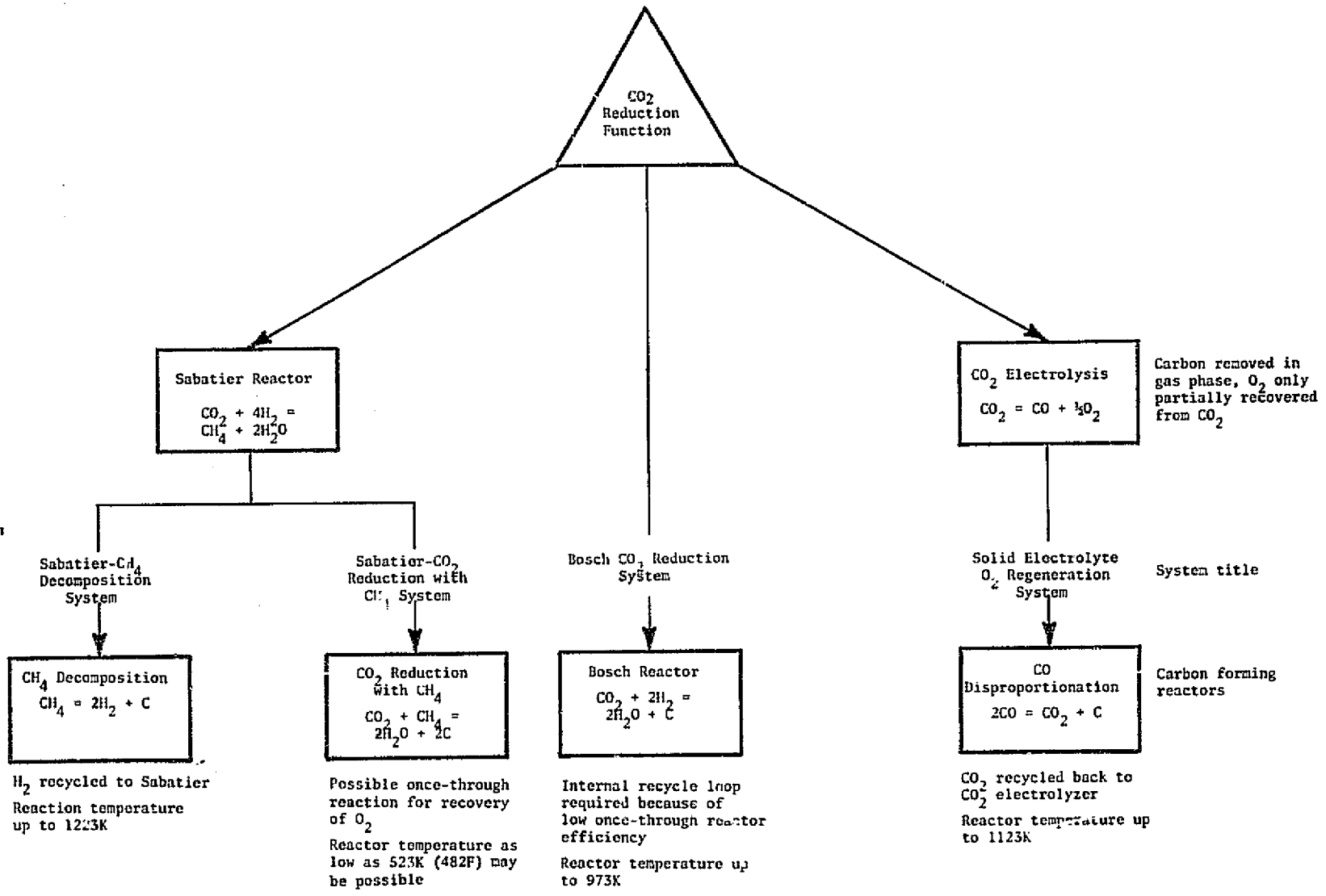

FIGURE 2 COMPARISON OF SABATIER, BCRS AND SEORS SYSTEMS FOR CO_2 REDUCTION

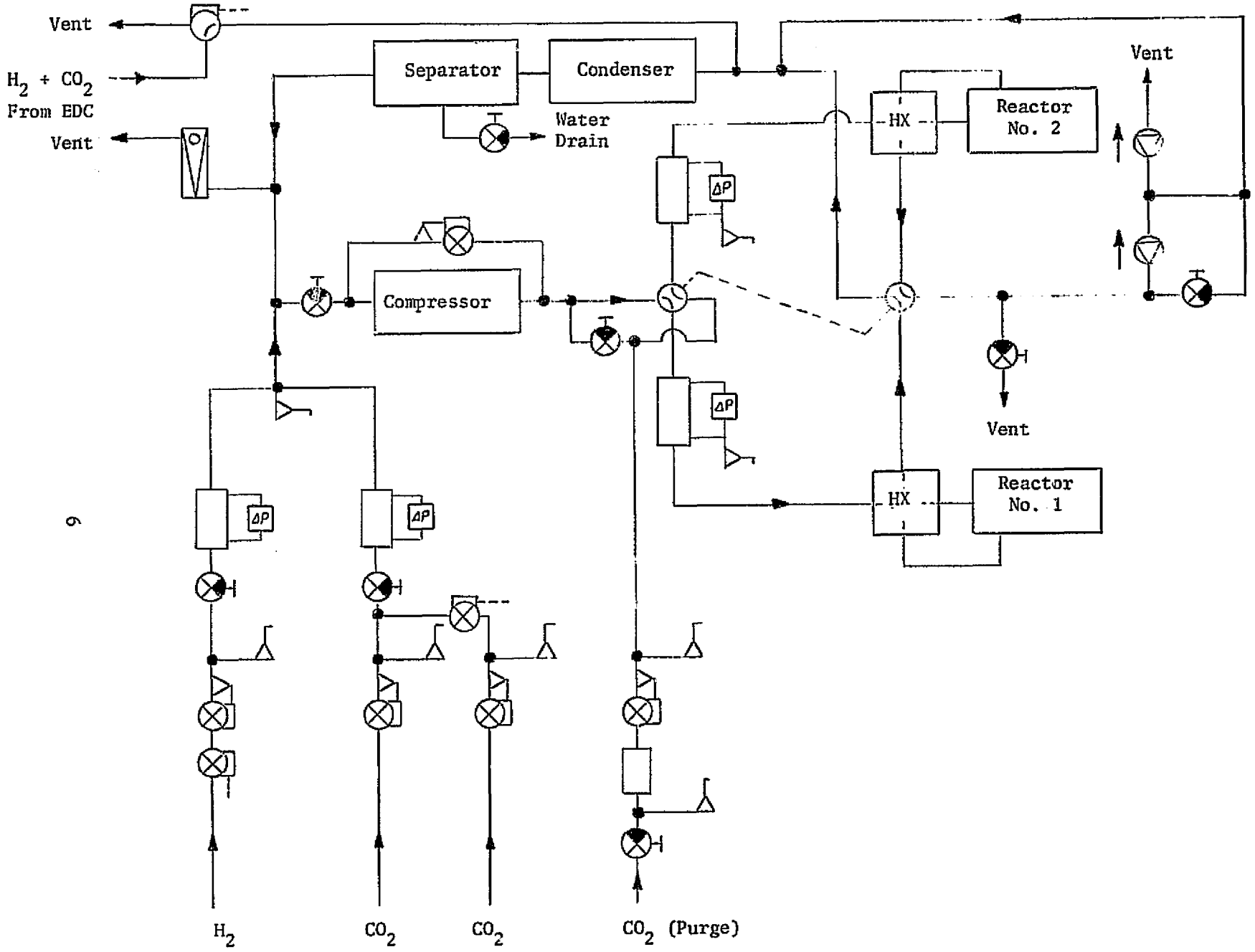

FIGURE 3 BOSCH UNIT SCHEMATIC

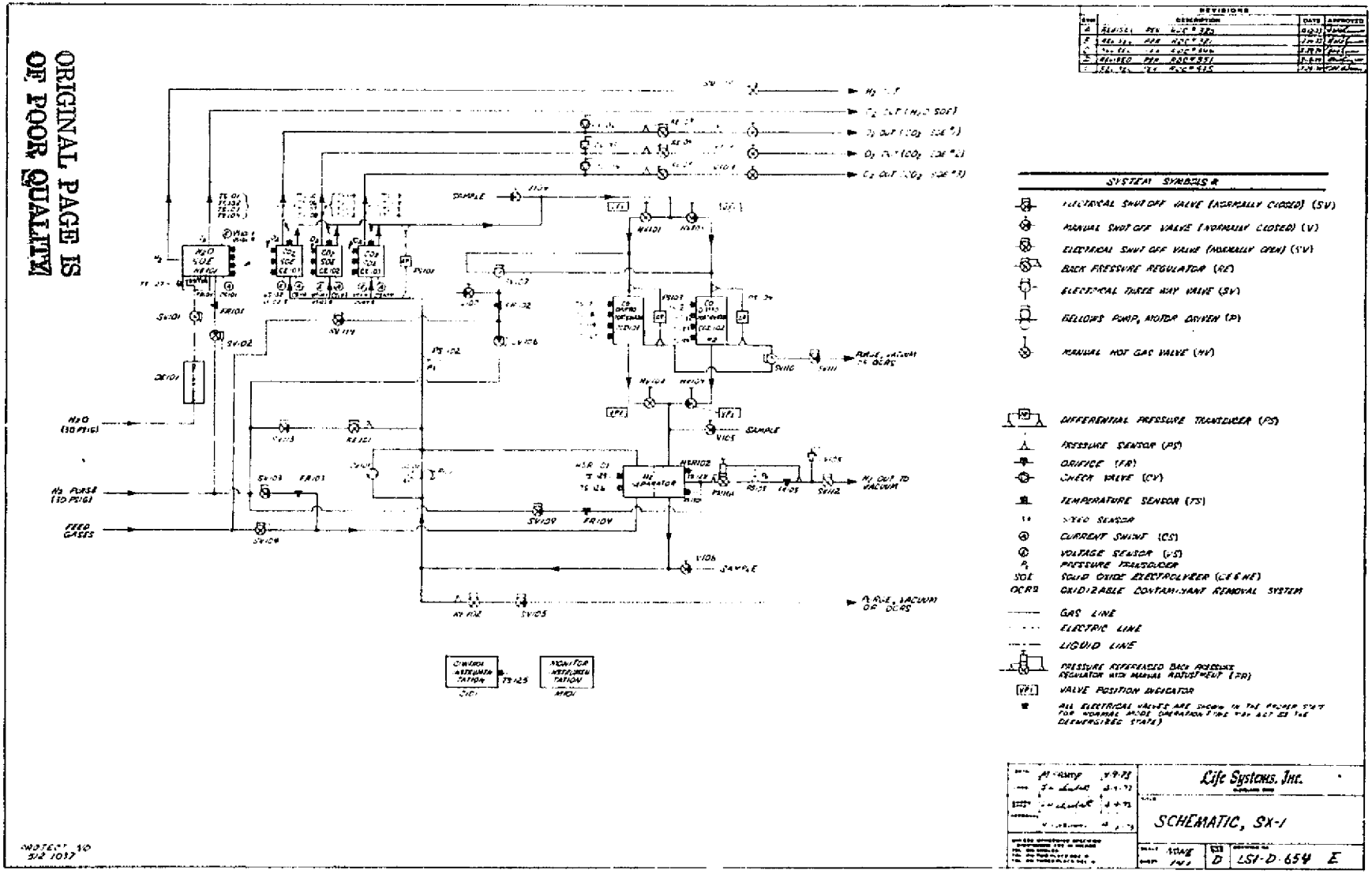

FIGURE 4 SOLID ELECTROLYTE O_2 REGENERATION SYSTEM SCHEMATIC

Two approaches appear feasible for doing this. One approach involves the catalytic decomposition of CH_4 (Equation 2), recycling the H_2 back to the Sabatier Reactor and thereby increasing the volume of CO_2 that reacts in the Sabatier.

$$CH_4 = C + 2H_2 \quad (2)$$

The second approach for the recovery of the O_2 from the CO_2, not reacted in the Sabatier, involves the reaction between CO_2 and CH_4, both of which are present in the Sabatier Reactor exhaust, as shown by the equation below:

$$CO_2 + CH_4 = 2H_2O + 2C \quad (3)$$

The thermodynamics of this reaction indicate that it is favored by low temperatures. Figure 5 is a plot of reaction temperature versus percent maximum theoretical conversion of CO_2 to water and carbon for a stoichiometric mixture of CO_2 and CH_4.[6] Since the CO_2/CH_4 reaction offers a means to completely recover the O_2 of expired CO_2 when integrated with a Sabatier Reactor, and since the reaction is thermodynamically favored by low temperatures, an evaluation and characterization study of the reaction was performed.

The objective of this program was to identify, through a literature review and characterization tests, catalysts and activation techniques effective in initiating the CO_2/CH_4 reaction, and to perform parametric testing on the two most promising catalysts and/or activation techniques as determined by the initial characterization tests. The purpose of the parametric testing was to determine the reaction efficiencies at various temperatures, reactant gas compositions, reactant gas flow rates, and reactor inlet pressures so that the feasibility of integrating a CO_2/CH_4 reactor with a Sabatier Reactor for total O_2 recovery could be determined.

To accomplish the above objectives, the program was divided into five tasks and program management functions. The specific objectives of the five tasks were to:

1.0 Perform a review of literature for identification of possible catalysts and UV sensitizers possessing the greatest probability of high reactivity for the CO_2 reduction with CH_4 reaction.

2.0 Design, develop, fabricate, and assemble an apparatus to test the performance of the various catalyst forms plus various UV sensitization techniques. This apparatus should be of sufficient capacity to evaluate catalyst charges of up to 3.0 g (0.007 lb). The test unit would operate on feed gas flows up to 0.02 kg/h (0.05 lb/hr) CO_2 and 0.20 kg/h)0.05 lb/hr) CH_4. The test unit would contain the necessary instrumentation and controls to gather the data required to characterize the performance of the catalysts and sensitizers selected.

3.0 Establish and implement a mini-Product Assurance Program effort to (a) ensure reproducible reactor performance, (b) ensure that test procedures are consistent with program objectives, and (c) establish safety guidelines for project personnel dealing with the test apparatus.

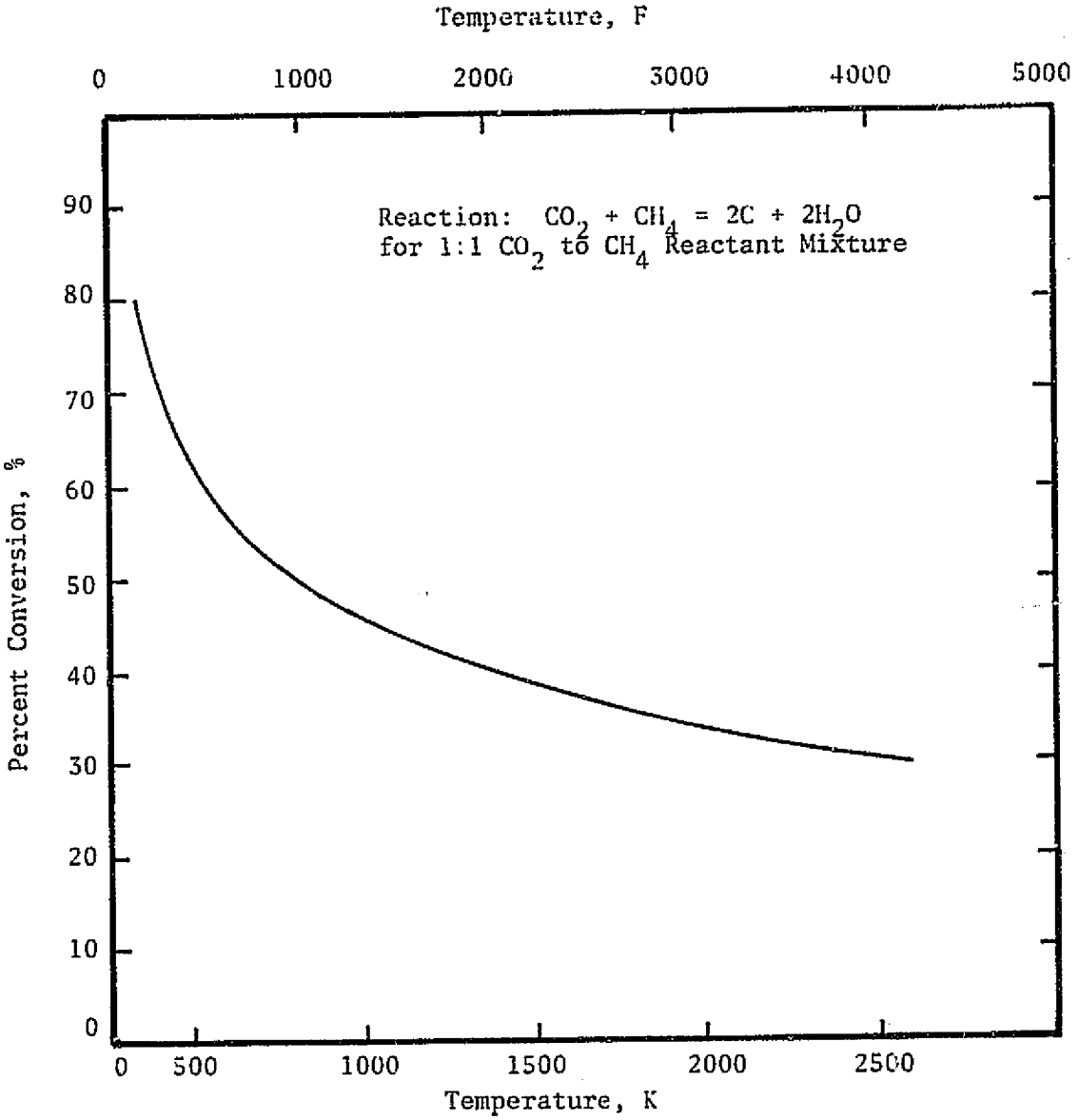

FIGURE 5 MAXIMUM CO_2-CH_4 CONVERSION VERSUS TEMPERATURE

4.0 Perform testing to establish the effects of reaction parameters on the conversion efficiency of CO_2 and CH_4. Tests included calibrations, catalyst and sensitizer characterization tests and parametric testing of selected catalysts and/or sensitizers.

5.0 Conduct supporting studies associated with the identification of an O_2 regeneration Life Support System based upon the integration of the Sabatier Reactor and a CO_2/CH_4 Reactor, including preparation of the system block diagram and calculation of the mass balances based on experimentally determined reactor efficiencies.

The objectives of the program were met. The following sections summarize the work completed and are organized according to the five program tasks.

METHODS OF CARBON DIOXIDE REDUCTION WITH METHANE

The reduction of CO_2 with CH_4 does not occur spontaneously because both reactants are extremely stable.[6] The reaction can only be induced to occur at appreciable rates by activating the reactants. The activation energy can be provided by heating the CO_2 and CH_4, but the reaction equilibrium is favored by low temperatures (Figure 5). It is advantageous, therefore, to employ catalysts that reduce the temperature required for the reaction to proceed at an appreciable rate. The literature of catalysts and catalytic methods applicable to the reduction of CO_2 with CH_4 was reviewed to identify those catalysts to be tested in this program using experimental conditions similar to those conditions anticipated in a CO_2/CH_4 reactor employed in a spacecraft ARS.

Carbon dioxide and CH_4 are activated by electromagnetic radiation in the gamma ray and UV wavelength region as well as by heat. Activation by gamma ray or UV radiation transfers little heat to the gases. Therefore, the possibility exists for activation of CO_2 and CH_4 at ambient temperatures, and since the equilibrium is favored by low temperature, the reduction of CO_2 would be essentially complete. Because of the possibility of high coversion efficiencies, gamma ray and UV methods for activation of CO_2 and CH_4, reported in the literature, were reviewed to ascertain the feasibility of the application of these methods to the reduction of CO_2 with CH_4.

Catalytic Reduction Methods

Heterogeneous catalysts that have been effective in the reduction of CO_2 with CH_4 were reviewed to identify the catalysts producing the greatest reaction efficiencies (i.e., conversion of CO_2 to water and carbon) at low temperatures.

Homogeneous catalysis was considered as an alternative because heterogeneous catalysts may be coated and ultimately inactivated by the carbon formed during the reduction of CO_2 with CH_4. The use of a homogeneous catalyst that would continuously flow through the reactor with the reactants was considered as a method of avoiding lowered reaction efficiencies due to carbon inactivation of the catalyst. The reactor would contain a fresh supply of the catalyst at all times, eliminating the possible reduced activity resulting from carbon formation on stationary catalyst particles.

Heterogeneous Catalysts

A limited amount of data has been reported regarding the heterogeneous catalysis of the reduction of CO_2 with CH_4. Most of the data reported was obtained using a reactant mixture having a 1:1 CH_4/CO_2 mole ratio. None of the data was obtained using the 3:1 mixture of CH_4 and CO_2 that simulates the anticipated composition of the Sabatier exhaust (see Section on Reactant Gas Composition). However, general trends can be recognized in the activity of various catalyst materials and supports, and the optimum reported reaction temperatures.

The catalyst material generally most active in the reduction of CO_2 with CH_4 is Ni.[7] However, this applies only to Ni supported on certain high surface area catalyst supports. Nickel shot and Ni felt metal exhibit little or no activity. The catalyst support that provides the greatest activity so far reported for Ni is molecular sieves. The maximum efficiencies of CO_2 conversion reported for the Ni on molecular sieves range from 13 to 24%.[7] The temperatures required for these maximum efficiencies are in the range of 808 to 977K (995 to 1200F), with space velocities of the 1:1 CH_4/CO_2 reactant mixture in the range of 220 to 420 hours^{-1}. Using similar experimental conditions, Ni on kieselguhr catalysts produced 4 to 14% conversion efficiencies, and the conversion efficiencies of Ni on alumina catalysts was 8 to 11%. Nickel on asbestos was found to be unreactive.

Other catalyst materials are somewhat reactive. Platinum (Pt) on silica gel produced 5% efficiency at 838K (1050F); however, Pt on alumina was not reactive.[7,8] Cobalt (Co) on silica produced 8% conversion at 838K (1050F), but Co metal, Co oxide catalysts, and Co thoria were not reactive.[7] Engelhard Pd on asbestos produced 4% conversion at 977K (1300F), but Pd on asbestos and Pd on alumina catalysts from Harshaw were unreactive.[7] Other catalysts that were unreactive are iron (Fe) metal and rhodium (Rh) on molecular sieves.[7]

Homogeneous Catalysts

Homogeneous catalysts for the reduction of CO_2 with CH_4 have not been reported. However, Ni carbonyl ($Ni(CO)_4$) and Fe pentacarbonyl ($Fe(CO)_5$) were considered as homogenous catalysts for the decomposition of CH_4, and the catalysis of the reaction by $Fe(CO)_5$ was experimentally investigated.[7]

When heated to more than 430K (266F), $Fe(CO)_5$ decomposes to extremely fine Fe powder and carbon monoxide (CO). It was the Fe powder that catalyzed the decomposition of CH_4. In the study, CH_4 was mixed with $Fe(CO)_5$ and heated to 1088K (1500F). The efficiency of the reaction was 2% over the range of space velocities from 16 to 65 hours^{-1}, and the Fe powder was converted during the reaction to a carbide having an approximate composition of FeC_4.

Although metal carbonyls have not been used to catalyze the reduction of CO_2 with CH_4, certain conclusions can be drawn from their use in the CH_4 decomposition reaction. First, $Ni(CO)_4$ would probably be a more active catalyst than $Fe(CO)_5$ since Ni heterogeneous catalysts are more active than Fe catalysts. The reaction temperature producing the maximum conversion efficiency would be approximately the same as for the Ni heterogeneous catalysts since Ni is

the catalyst material in both cases.[9] However, $Ni(CO)_4$ is extremely toxic and explodes in air at 333K (140F).[9] Therefore, stringent safety requirements would have to be met before a system utilizing $Ni(CO)_4$ could be used aboard a spacecraft. Iron pentacarbonyl is less toxic than $Ni(CO)_4$ and does not explode in air, although it is pyrophoric.[9] Therefore, a system employing $Fe(CO)_5$ could be integrated into a spacecraft ARS more easily than the one using $Ni(CO)_4$. The $Fe(CO)_5$ is consumed in the CH_4 decomposition reaction and cannot be reused. If it were used to catalyze the reduction of CO_2 with CH_4, the overall reaction would be that shown in Equation 4 if the Fe carbide produced had the composition reported for the CH_4 decomposition.

$$2CO_2 + 2CH_4 + Fe(CO)_5 = FeC_4 + 4H_2O + 5CO \qquad (4)$$

From the stoichiometry of the reaction it can be calculated that for each kg (2.2 lb) of CO_2 reduced, 1.1 kg (2.4 lb) of $Fe(CO)_5$ would be consumed. The nominal performance specifications of a six-man Sabatier Reactor in a spacecraft ARS show that 1.43 moles of CO_2 will be discharged per hour.[10-11] This equals an output of 45 kg (100 lb) of CO_2 per 180 man-days. At this rate of CO_2 reduction, 50 kg (110 lb) of $Fe(CO)_5$ would be required each 180 man-days.

The metal carbonyls were not chosen for experimental evaluation because they offer no advantage over heterogeneous catalysts with respect to operating temperatures. Also, the high consumption rate and the toxic and explosive or pyrophoric natures of the carbonyls may outweigh any advantage they have over heterogeneous catalysts with respect to carbon fouling.

Gamma Radiation Methods

Radiation with gamma rays was considered as one method to provide activation energy to mixtures of CO_2 and CH_4 at low temperature. When a mixture of CO_2 and CH_4 is irradiated with gamma rays a number of products are formed. The products can be grouped into three phases: a phase that is condensable at 195K (-108F), a phase that is not condensable at 195K (-108F), and a viscous oil.[12] The condensable phase contains approximately 20 different compounds. About 75% of the phase is a mixture of dimethylketone and methylethylketone. The noncondensable phase is mostly CO and ethane (C_2H_6). The viscous oil is a polyketene type of polymer. Hydrogen and water have been reported to be only minor products.[13]

It can be concluded from these results that gamma radiation methods, as applied to the recovery of O_2 from the Sabatier Reactor exhaust, would produce a large number of products. Oxygen and water would not be produced to an appreciable extent since the majority of O_2 originally in the form of CO_2 is retained in the CO, ketones, and the polymer. The reaction efficiency of the reaction would therefore be low. Also, elaborate safety requirements would be necessary to contain the gamma radiation safely in the spacecraft environment. Because of these considerations, gamma radiation methods are not considered to be practical alternatives to the heterogeneous catalytic methods discussed above.

Ultraviolet Radiation Methods

Ultraviolet photolysis was considered as an alternative method to gamma ray radiation for providing activation energy to mixtures of CO_2 and CH_4 at low temperatures. Only a few investigations of the photolysis of mixtures of CO_2 and CH_4 have been reported. In one study, a mixture of CO_2, CH_4 and water was irradiated with 127 nm light.[14] Hydrogen and hydroxyl radicals were observed to be formed immediately upon photolysis. Radicals of this sort are extremely reactive species that would be anticipated to react with CO_2 and CH_4 to form the variety of products observed after gamma ray radiation. In other studies, the photolysis of pure CH_4 produced H_2, C_2H_6, ethylene (C_2H_4) and acetylene (C_2H_2),[15-16] with C_2H_4 being the main hydrocarbon product.[17] Again, these are the same types of products formed in the radiation of CH_4 with gamma rays. These results indicate that the long-term photolysis of mixtures of CO_2 and CH_4 would probably produce the variety of ketones, hydrocarbons and the polymer produced by gamma ray radiation.

Photochemical reactions can be catalyzed by certain species called UV sensitizers. Sensitizers catalyze the reaction by absorbing energy from the UV radiation and transmitting the absorbed energy to the chemical reactant causing the reaction to proceed. The use of UV sensitizers as they might be applied to the reduction of CO_2 with CH_4 was reviewed. Mercury (Hg) vapor was found to be a sensitizer effective in the photolysis of CH_4.[18] For partial pressures of Hg vapor over the range of 13 to 130 kN/m^2 (100 to 1000 mm Hg), the main products formed are C_2H_6 and H_2. The quantum yield of the reaction (i.e., number of molecules that reacts per quantum of light absorbed) is temperature-dependent. At 371K (208F), the quantum yield is 0.004, while at 673K (752F) the quantum yield is approximately one. The reaction therefore requires elevated temperatures for efficient conversion.

Ultraviolet photolysis does activate mixtures of CO_2 and CH_4 at low temperatures. However, the photochemical reaction is not as selective as the heterogeneous catalytic reduction of CO_2 with CH_4, and a wide variety of products are formed. Mercury vapor catalyzes the photochemical reaction, especially at elevated temperatures but produces the same kinds of products formed without photo sensitization. The reaction products formed after photochemical activation of CO_2 and CH_4 do not consist of significant quantities of water or O_2. Therefore, the photolysis method, without some mechanism to selectively convert the O_2 in the CO_2 to water or O_2, cannot be efficiently applied to a spacecraft ARS. Ultraviolet photolysis combined with heterogeneous catalysis, however, may permit low temperature activation and selective production of water.

Reduction Methods Investigated

As the result of the literature review, the heterogeneous catalytic method for the reduction of CO_2 with CH_4 was selected for experimental evaluation during this testing program. Six candidate catalysts were chosen for an initial characterization to identify the most active low temperature catalysts for the reduction of CO_2. The reactant gas mixture had the anticipated composition of the Sabatier reactor exhaust so that the performance of the catalysts in an ARS was approximated. The first catalysts characterized were Harshaw

NI0104T1/8 and Girdler G-49A. Both of these are Ni on kieselguhr catalysts. They were chosen because Ni on kieselguhr catalysts were reported to have relatively high conversion efficiencies and because these catalysts are readily available from commercial sources. Because of their availability, these catalysts were used during the initial checkout of the test stand and catalytic reactor. They also provided a baseline for comparision of reaction efficiencies with the efficiencies of the other Ni catalysts evaluated.

The most reactive Ni catalysts so far reported are Ni on molecular sieves. However, these catalysts are not routinely available from commercial manufacturers. Limited quantities of two Ni on molecular sieve catalysts were obtained for evaluation. One catalyst contained 10% Ni on molecular sieve and was obtained from Linde Div. of Union Carbide Corp. The other catalyst was obtained from Girdler Chemical Inc. and contained 20% Ni on molecular sieve.

Another catalyst chosen for evaluation was Engelhard 0.5% Pd on alumina. This catalyst was chosen because an Engelhard Pd on asbestos catalyst was reported to be reactive.[7] In the case of Ni catalysts, asbestos supports produced less active catalysts than alumina or silica. Therefore, an Englehard Pd on alumina catalyst possibly would provide greater reactivity than Pd on asbestos. However, Harshaw Pd on asbestos and Pd on alumina catalysts were both reported to be inactive. This inactivity possibly may be the result of a manufacturing treatment or process used on Harshaw Pd catalysts.

Nickel is an active catalyst for the methanation reaction (Equation 1), as well as the reduction of CO_2 with CH_4, and Ni is often used in Sabatier Reactors.[19-20]

Ruthenium (Ru) is also a very active methanation catalyst.[19-22] In fact, with stoichiometric reactant gases, a Ru catalyst has been reported to produce 94.8% reaction efficiency in a Sabatier Reactor while a Ni catalyst produced only 90.7% efficiency under identical conditions.[22] The application of Ru catalysts to the reduction of CO_2 with CH_4 has not been reported in the literature, however. To investigate the possibility that Ru, like Ni, may catalyze the CO_2 reduction as well as the CO_2 methanation reactions, an Englehard 20% Ru on alumina catalyst was selected for use in the characterization study.

Catalytic methods have been demonstrated to selectively produce water from CO_2 and CH_4 at elevated temperatures. Ultraviolet activation of CO_2 and CH_4 at low temperatures has been demonstrated to occur, but results in a variety of organic compounds and low efficiency for the production of O_2 or water. The combination of UV activation with heterogeneous catalysis was considered as a possible means of providing activation energy to the reactant gases at low temperatures, allowing the catalyst to possibly operate at lower temperatures than required without the UV activation. Therefore, the use of UV activation in conjunction with heterogeneous catalysis was selected for evaluation in addition to the heterogeneous catalytic methods.

TEST HARDWARE

The test hardware was designed to allow accurate comparison of catalyst activities

and analysis of the reactant gas mixture and reaction products. The test hardware consisted of a breadboard catalytic reactor, the test stand, and analytical instrumentation.

Catalytic Reactors

Two reactors were used during the test program. A copper tubular reactor was used during the characterization and parametric testing studies. The copper reactor was required to withstand the elevated pressures used during the parametric tests. The second reactor was a quartz tube and was used during the UV activation tests because quartz is transparent to the UV radiation at the wavelengths used in the test.

Reactor Geometry and Sizing

A requirement for the choice of geometry of the catalytic reactor was that it allow the reactor to be loaded with catalysts in a reproducible manner, producing precise experimental results and permitting the accurate comparison of the efficiencies of the six catalysts. Therefore, no attempt was made to design a reactor geometry for optimum reaction efficiency.

A tubular geometry was chosen for the reactor because it afforded a convenient and reproducible catalyst loading procedure. Also, the major gradients of temperature and pressure exist along the longitudinal axis of the reactor, simplifying the consideration of the effects of those gradients on catalyst efficiencies.

Both reactors had outside diameters of 2.54 cm (1.0 in). The length of the copper reactor was 61 cm (24 in) and it had a wall thickness of 0.89 mm (0.035 in). The quartz reactor was 91 cm (36 in) in length and had a wall thickness of 1.5 mm (0.060 in). Both reactors were connected to the test stand with brass fittings. Teflon and Kel-F ferrules were used on the quartz reactor while brass ferrules were used to secure the copper reactor. The catalyst was retained in both reactors by rolled quartz wool plugs as shown in Figure 6. This arrangement produced very low pressure drops to the reactor and permitted rapid replacement of the catalyst.

Test Stand

The test stand was designed to control the experimental parameters of reactant gas composition, flow rate, reactor inlet pressure, and reactor temperature. The test stand was also designed to allow the measurement of water generation rates over the wide range of values possibly encountered during the test program. The test stand was interfaced to a gas chromatograph for the analysis of the reactant and product gas mixtures.

Reactor Oven

The oven used to heat the catalyst reactor was a Lindburgh Model 55035-A tube furnace. The furnace was sized to contain a tubular reactor with an outer diameter of 2.54 cm (1 in) and was capable of heating the reactor over a length of 33 cm (13 in). Figure 7 shows the quartz reactor containing catalyst and

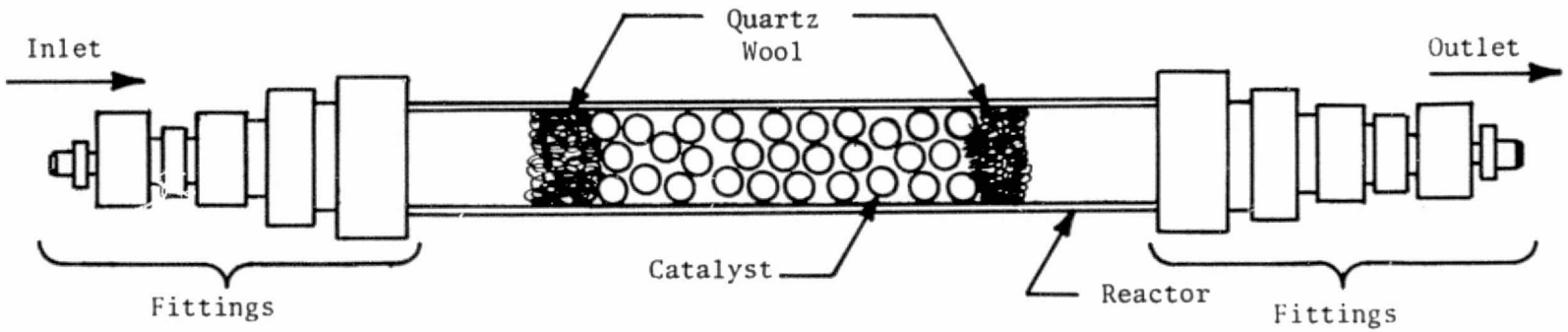

FIGURE 6 SCHEMATIC OF REACTOR AND CATALYST BED

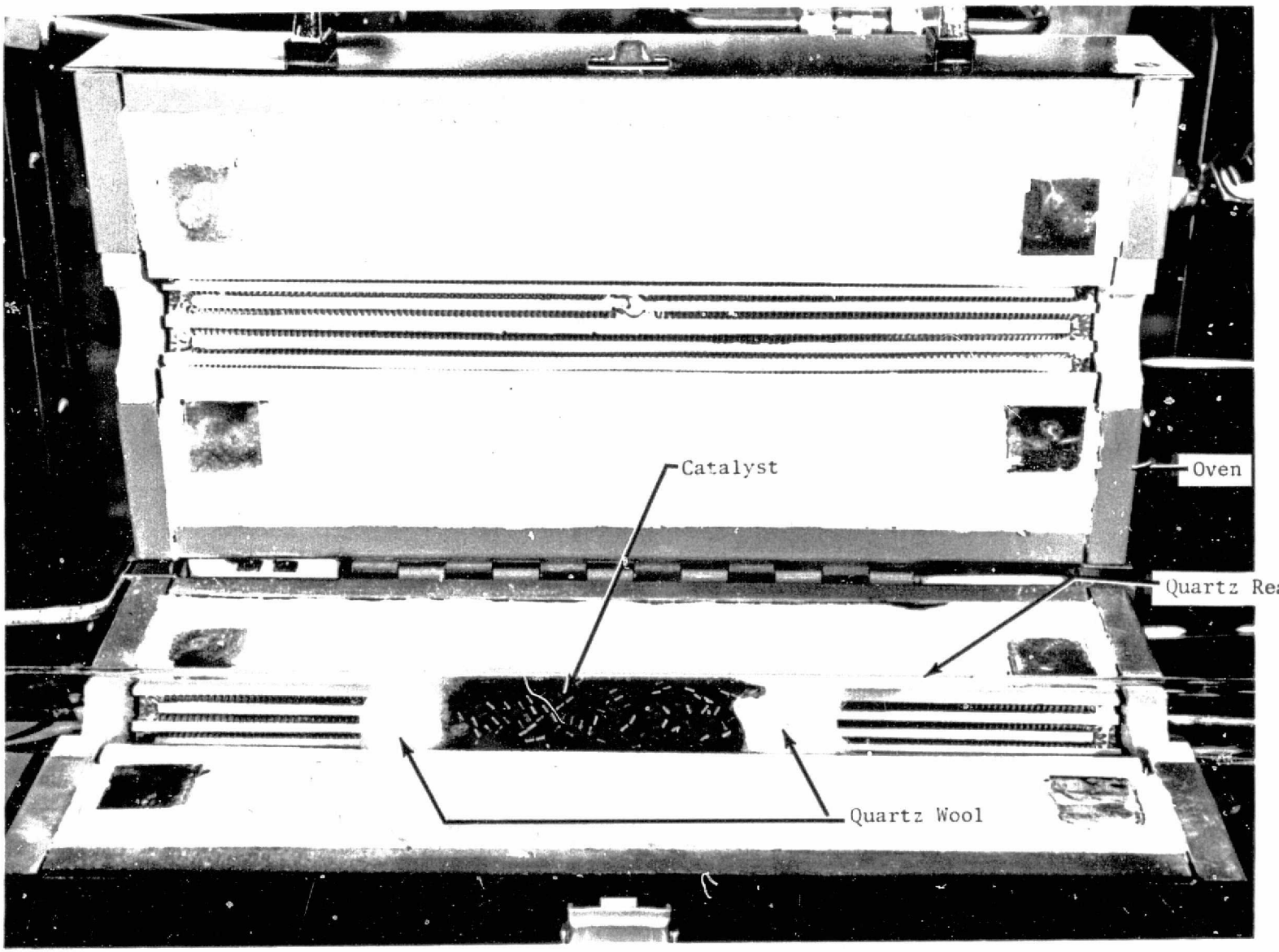

FIGURE 7 OVEN AND EXPOSED QUARTZ REACTOR

quartz wool plugs mounted in the opened reactor oven.

Functional Block Diagram of Test Stand

Figure 8 is a functional schematic of the test stand, reactor, and oven. The reactant mixture of CO_2 and CH_4 entered the test stand from the gas cylinders through valves V1 and V2 and flowmeters FM1 and FM2. During the initial catalyst pretreatment step, H_2 was directed to the reactor through V3 and FM2. All gases flowed through the gas purifier tube that dried the gases to prevent water vapor from entering the test stand and insured thorough mixing of the reactant gases. Valve V4 directed the reactant gas mixture to the reactor, or through V9 to the gas chromatograph for analysis. The reactor inlet pressure was measured with pressure gauge PG1, while the pressure drop across the reactor was measured with PG2.

For water generation rates greater than 5 g/hr (0.01 lb/hr), the product gases and water vapor from the reactor were directed through valve V5 to a condensing heat exchanger where the water vapor was condensed and collected in a graduated cylinder retained in a sealed flask. Cooling water entered the heat exchanger through V10 and the product gases vented from the flask through pressure regulator R1.

For water generation rates less than 5 g/hr (0.01 lb/hr), the product gases from the reactor were directed through valves V6 and V7 to a gas drying tube containing a dessicant (Drierite). The water vapor was collected on the Drierite, and the dried product gases exited through valve V8. A bypass was provided around the gas drying tube to allow operation of the test stand while the gas drying tube was removed for weighing. The product gases and water vapor could be directed through the bypass through valves V7 and V8.

In addition to the drying tube, the gas chromatograph was capable of determining the quantity of water produced in the reactor for very small water generation rates. The gas chromatograph was used to analyze the dried product gases directed through the gas drying tube and V8 into the gas sample loop of the chromatograph. The exit of the gas sample loop was connected to R1 to maintain the system pressure. When the dried product gases were not being analyzed, they were directed through V8 directly to R1 and the vent.

Accurate measurement of water generation rates necessitated heating of the tubing upstream of heat exchanger and the gas drying tube using heating tapes to maintain the product water in the vapor phase in those sections of the tubing. This prevented the accumulation of water in the tubing from one measurement to the next. The tapes were heated to 363K (194F) and controlled with a Variac and automatic temperature controller.

Test Stand Construction

The tubing used in the test stand was 0.64 cm (1/4 in) OD copper, except for the tubing leading from the reactor outlet to the differential pressure gauge. This tubing was 0.32 cm (1/8 in) OD. Fittings and valves used in the test stand were brass. The use of stainless steel was minimized in the heated portions of the test stand and reactor to prevent possible catalysis of the

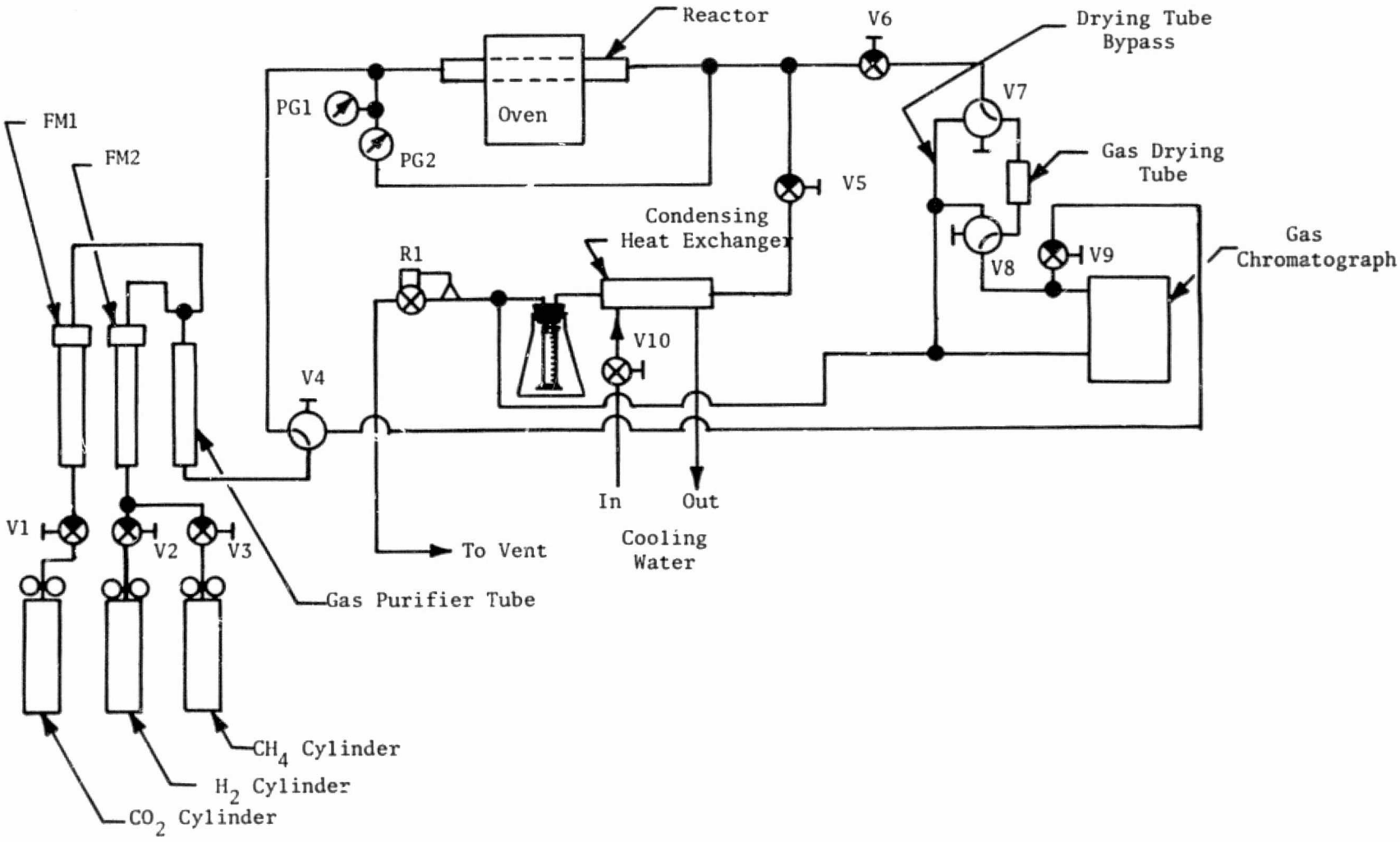

FIGURE 8 SCHEMATIC OF TEST APPARATUS

CO_2 reduction or CH_4 decomposition by the Ni and Fe in the stainless steel.

The test stand in the configuration used in the characterization studies and parametric testing is shown in Figure 9. The front panel of the test stand, the gas chromatograph, and the strip chart recorder are shown. The cylinders of CO_2, CH_4, and H_2 are at the extreme left of the figure. Cooling water for heat exchanger leads to the test stand from the top of the picture. Water condensed in the heat exchanger was collected in the graduated cylinder in the flask to the left of the front panel. The rear of the test stand and the reactor and oven are shown in Figure 10. The controller and Variac used with the heating tapes to heat the tubing are shown in the bottom center of the picture.

Ultraviolet Apparatus

The UV lamp used in the UV activation study was a UV Products Inc. Model PCQ-024S. The lamp consisted of a 0.64 cm (1/4 in) OD tube in a spiral configuration, 15 cm (6 in) long and had an interior diameter of 5.1 cm (2 in). The lamp produced more than 5 watts at 2537 A for an intensity of approximately 30,000 $\mu W/cm^2$ in the center of the lamp. The quartz tubular reactor was positioned through the center of the lamp spiral and the lamp was attached to a test stand within 1.3 cm (0.5 in) of the inlet of the reactor oven as shown in Figure 11. To shield the operator from the UV radiation, the lamp and irradiated portion of the quartz reactor were contained in an aluminum box, sealed against the furnace with Viton A gasket material. The interior surfaces of the box were reflective. The leads from the power supply to the lamp entered the box through grommeted holes. The only required modification to the test stand was a lengthened reactor inlet tube leading from V4 to the inlet of the quartz tube to accommodate the 91 cm (36 in) long quartz reactor.

TEST PROGRAM

The test program was designed to identify the two most active low temperature catalysts for the reduction of CO_2 with CH_4 from the six candidate catalysts chosen for characterization. The two optimum catalysts were then extensively tested to determine the effects of changes in reactor temperature, reactant gas composition, flow rate and pressure on their performance. The effect of UV activation of the reactant gas mixture on the efficiency of the catalysts was also evaluated.

Test Procedures

The test program consisted of (1) an initial checkout of the system and calibration of the parametric measuring devices incorporated in the test stand, (2) a characterization study of six catalysts, (3) the parametric testing of the two optimum catalysts, and (4) the UV activation studies. Procedures for each part of the test program were developed to ensure the collection of data accurately reflecting the performance of the catalysts in the reduction of CO_2 with CH_4 with the simulated exhaust gas of a Sabatier reactor.

Definitions

The terms below are defined as they were used during the test program.

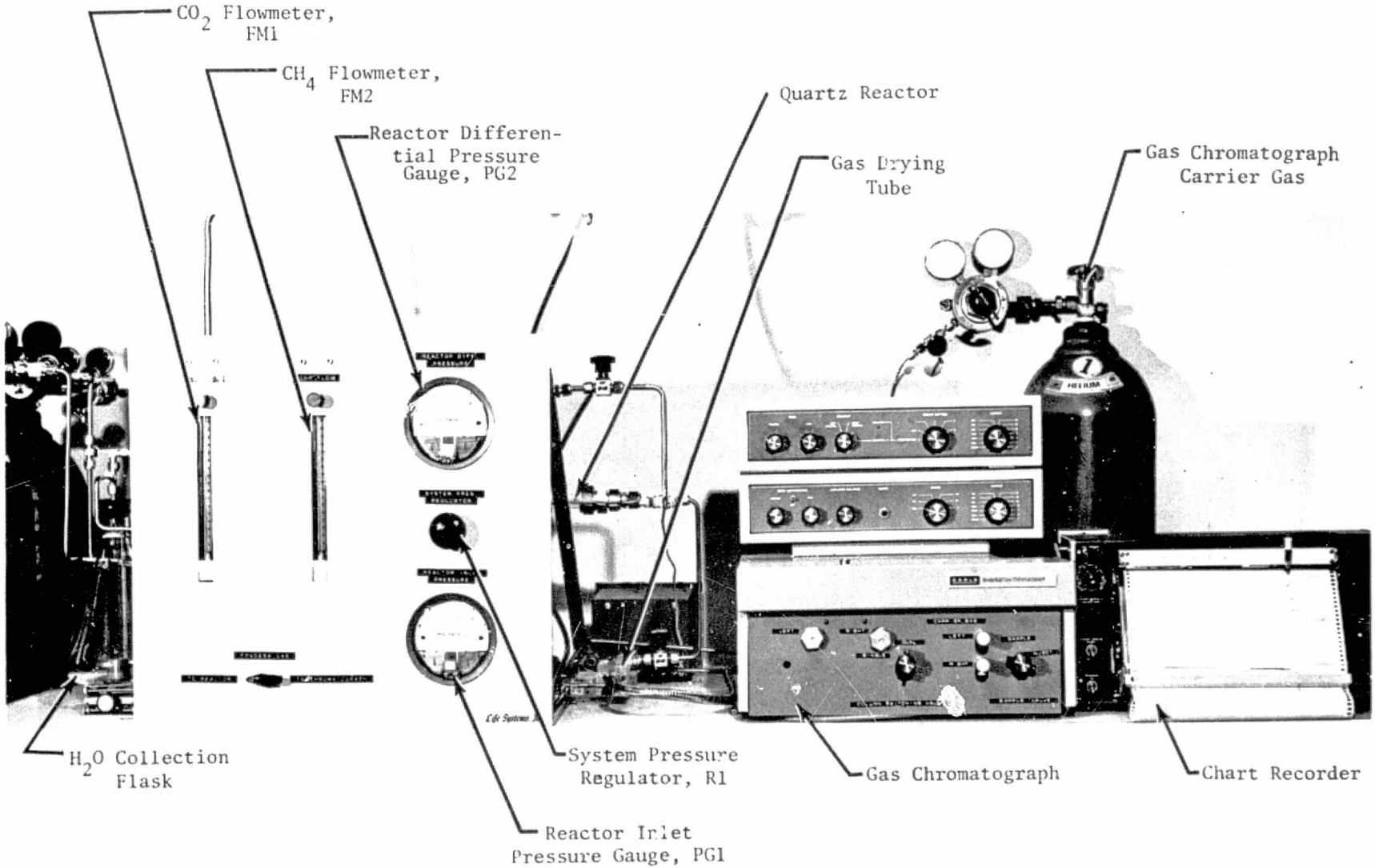

FIGURE 9 FRONT OF TEST STAND AND GAS CHROMATOGRAPH

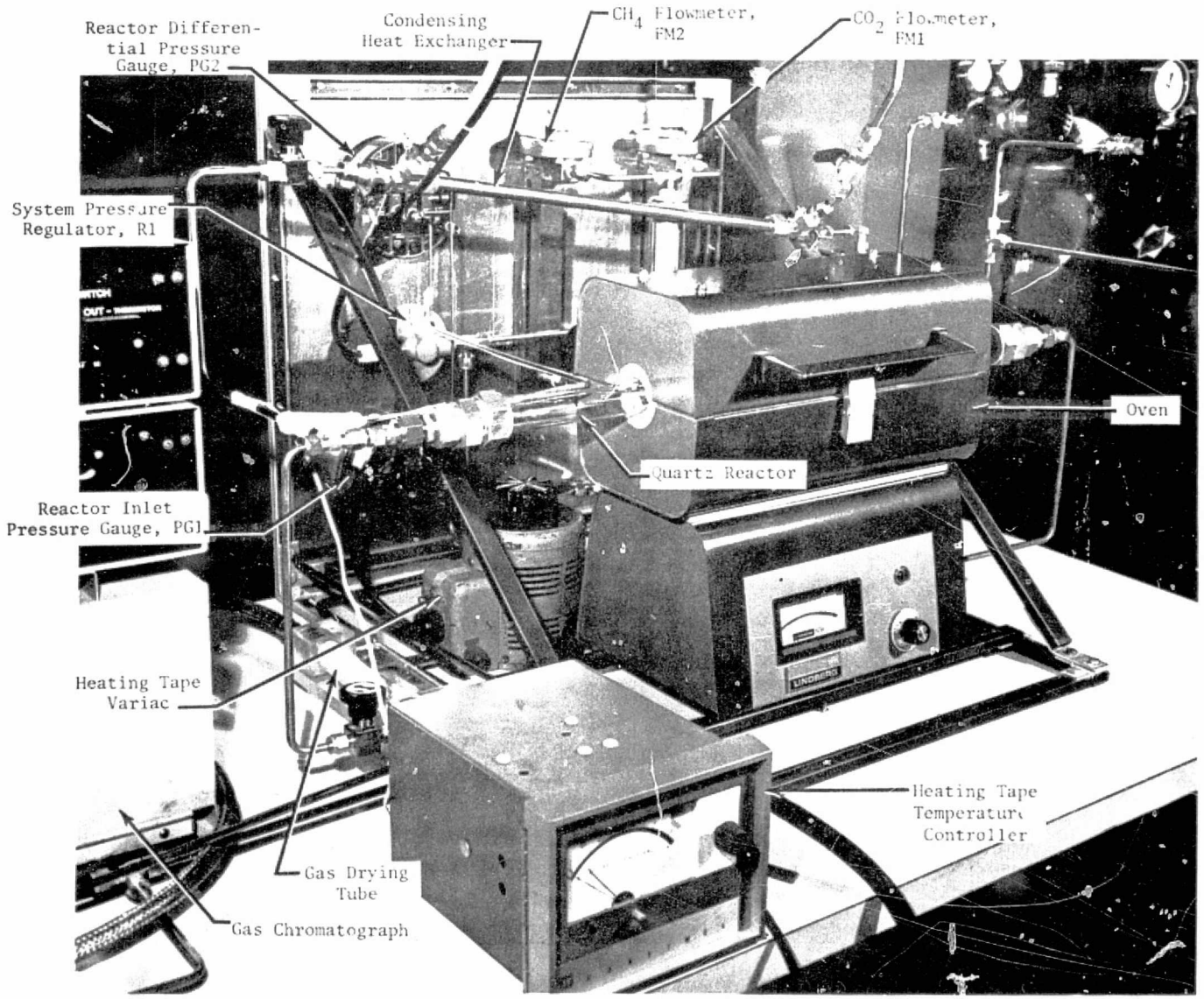

FIGURE 10 REAR OF TEST STAND

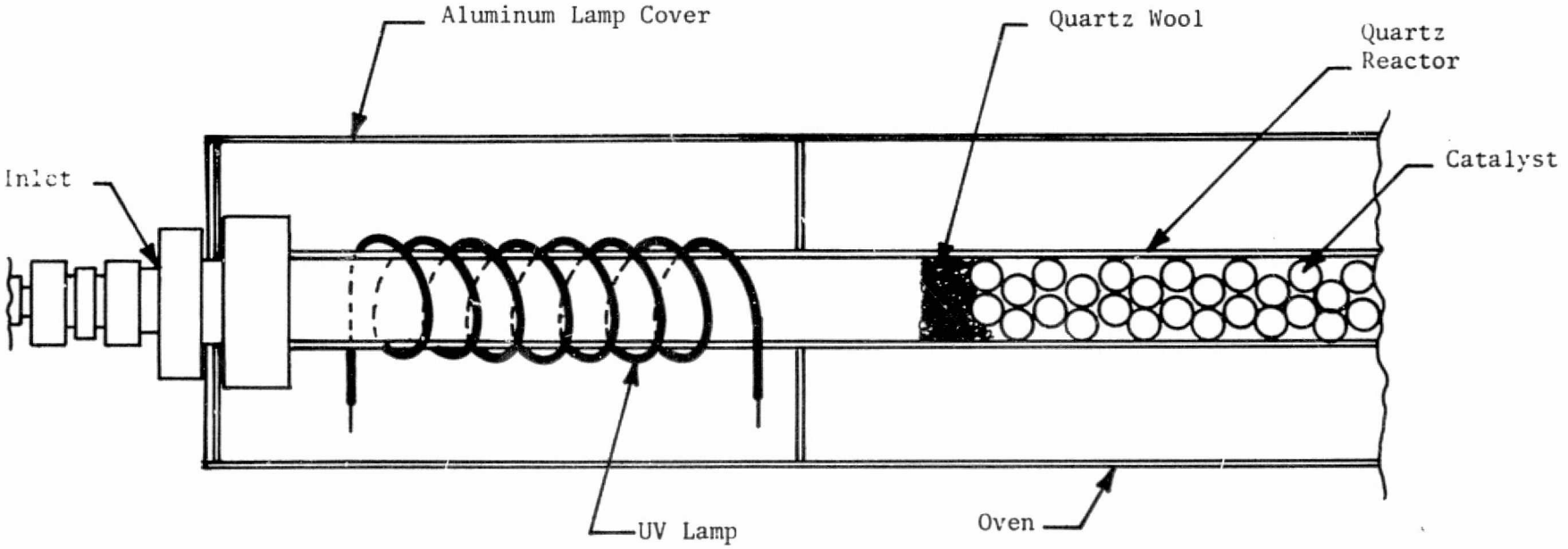

FIGURE 11 SCHEMATIC OF UV LAMP INTEGRATED WITH REACTOR PACKED WITH CATALYST

1. Space Velocity - The space velocity of the reactant gas mixture equals the apparent catalyst bed volume (in cm^3) divided by the volumetric flow rate of the gas mixture (in cm^3/hr). Units of space velocity are $hour^{-1}$.

2. Reaction Efficiency - The reaction efficiency is defined in this program as the weight percent of the total quantity of CO_2 entering the catalytic reactor that reacts to form water.

3. Conversion Rate - Conversion rate is the weight of CO_2 converted to water per hour, divided by the weight of catalyst in the reactor.

Analytical Instrumentation and Procedures

The analytical measurements made during the program consisted of the analysis of the reactant and product gas mixtures and determination of the rate of water generation from the reduction of CO_2.

Gas Analysis. The composition of the reactant and product gas mixtures were determined using a Carle Model 311 analytical gas chromatograph. The chromatograph was fitted with a dual filament thermal conductivity detector and a gas sampling valve which was interfaced to the test stand as shown in Figure 8. The analytical columns in the chromatograph were a 1.7 m x 0.64 cm (6 ft x 1/4 in) column of 30% Di(2-ethylhexyl)Sebacate(DEHS) on 60-80 mesh Chromasorb P and a 3.0 m x 0.64 cm (10 ft x 1/4) in column of 80-100 mesh molecular sieve 13X. A three-way valve between the columns was used to direct each gas sample from the DEHS column to the detector, or to the molecular sieve column, and then to the detector. The DEHS column separated CO_2 from the other gases in the gas sample, and therefore allowed determination of the concentration of CO_2 in the sample. To determine the concentration of the gases other than CO_2, the sample was directed through both the DEHS and molecular sieve columns. The latter column separated H_2, CH_4 and CO while it absorbed the CO_2 in the sample. The carrier gas used during the analysis was 8% H_2 in He at a flow rate of 15 cm^3/min (5.3×10^{-4} cfm) with a column temperature of 298K (77F).

The detector output of the chromatograph, consisting of chromatographic peaks for each component of the gas mixture, was recorded on a Hewlett-Packard Model 17501A strip chart recorder. The chromatographic detector response factors for each compound in the gas mixture were calculated from the chromatograms of the pure compounds. Chromatographic peak areas were then used to calculate the composition of the reactant and product gas mixtures.

Water Generation Rate Measurement

The rate of water generation with all the catalysts was sufficient to collect the water from the product gas stream in the gas drying tube shown in Figure 8. A lightweight drying tube, used in all testing except the pressure test, was constructed of a polyethylene tube 19 cm (7-1/2 in) long with a diameter of 1.9 cm (3/4 in). Each end of the tube was plugged with rubber stoppers through which copper tubes were inserted, allowing attachment of the drying

tube to the test stand. The polyethylene tube used for the pressure test was also 19 cm (7-1/2 in) long with a 1.3 cm (1/2 in) OD and was attached directly to the test stand with brass fittings and ferrules. Both tubes were filled with Drierite, retained with glass wool plugs. Water generation rates were calculated from the weight gain of the tube during water collection periods of 20 minutes to 2 hours, depending on the activity of the catalyst and the flow rate of the reactant gases.

Catalyst Pre-Treatment Procedures

Each catalyst sample loaded in the reactor was pre-treated before data was obtained with it by chemically reducing the catalyst under standardized conditions. Pre-treatment assured reproducible results and allowed accurate comparison of the performance of each catalyst. The procedure used to pre-treat each catalyst consisted of a 15 minute purge of the reactor, heated to 673K (752F), with a flow of CH_4 at 300 cm^3/min (1.06×10^{-2} cfm). The CH_4 purge removed air from the reactor and was followed by a 30 min reduction of the catalyst with H_2 flowing at 150 cm^3/min (5.30×10^{-3} cfm). The H_2 was then purged from the reactor with a flow of CH_4 at 150 cm^3/min (5.30×10^{-3} cfm), while the temperature of the reactor was adjusted to the required temperature for the subsequent test. During this 30-min period, thermal equilibrium in the reactor was attained. At the beginning of the test, the flows of CO_2 and CH_4 and the other experimental parameters were adjusted to the required values.

Baseline Experimental Parameters

The baseline experimental parameters chosen are consistent with the anticipated composition and pressure of the Sabatier Reactor exhaust. The space velocity of the reactant gases was selected on the basis of the anticipated catalyst activities. The space velocity and reactor volume determined the baseline reactant gas flow rates. The baseline parameters are listed in Table 2.

Reactant Gas Composition. The composition of the reactant gas mixture used for testing the catalysts simulated the composition of the exhaust of a Sabatier reactor interfaced with an Electrochemical Depolarized Concentrator (EDC). The nominal output of a six-man EDC is 7.16 l/min (0.036 kg/hr) H_2 and 2.28 l/min (0.249 kg/hr) CO_2. The mole ratio of H_2 to CO_2 in the EDC exhaust is 3.14:1 at these nominal values.[11]

The conversion efficiency of a Sabatier Reactor as a function of the ratio of H_2 to CO_2 in the Sabatier reactant gases is shown in Figure 12.[10] As shown in the figure, the efficiency of conversion at the nominal H_2:CO_2 molar ratio is 94% for H_2 and 74% for conversion of the CO_2. These conversion efficiencies correspond to a Sabatier exhaust output of 4.23 moles CH_4/hr, 1.43 moles CO_2/hr, and 1.1 moles H_2/hr. The CH_4 to CO_2 mole ratio in the Sabatier exhaust, therefore, is 3.0:1, and this composition was selected for the reactant gas mixture used for the testing of the candidate catalyst for the reduction of CO_2 with CH_4.

Reactant Gas Flow Rate. The approximate space velocity used to initially size the catalyst bed volume and reactant gas flow rate was 250 hr^{-1}. This

TABLE 2 BASELINE VALUES OF THE EXPERIMENTAL PARAMETERS

Parameter	Value
Reactant Gas Composition, Mole Ratio, CH_4:CO_2	3:1
Total Reactant Gas Flow Rate, cm^3/min (Cfm)	200 (7.06×10^{-3})
Reactor Inlet Pressure, kN/m^2 (Psia)	108.1 (15.7)

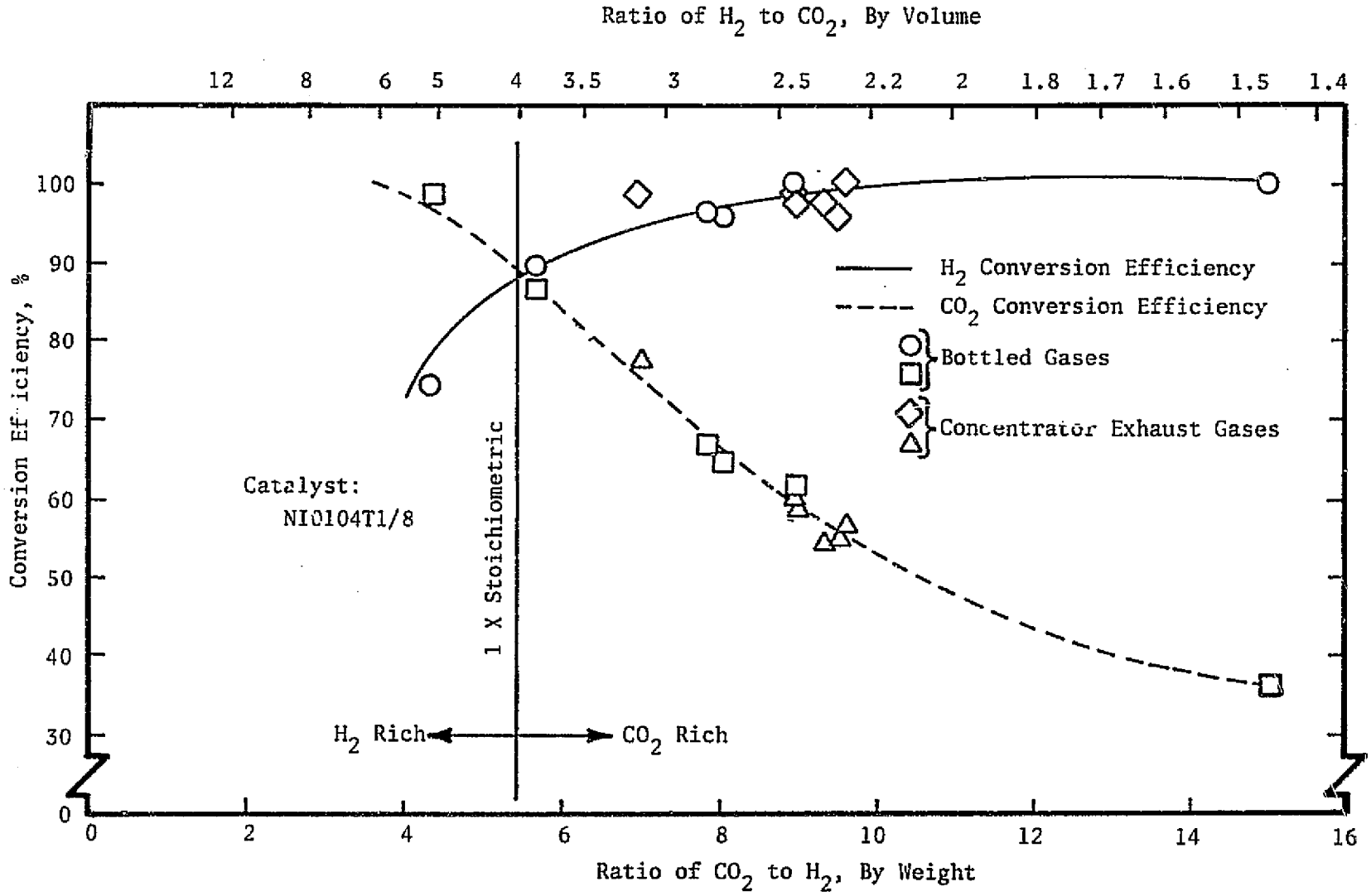

FIGURE 12 CONVERSION EFFICIENCIES OF CO_2 AND H_2 IN SABATIER REACTOR

space velocity was selected because it would produce sufficient water for accurate measurement during water collection periods of reasonable length, assuming reaction efficiencies and water generation rate values similar to those previously reported. A catalyst bed volume of 50 cm^3 (3.0 in^3) could be contained in a length of the reactor equal to approximately 10 cm (4.0 in). This volume of catalyst could be contained in the center of the heated zone of the reactor, where temperature gradients would be minimized. Therefore, the baseline reactant gas flow rate of 200 cm^3/min (7.06 x 10^{-3} cfm) was selected because it resulted in a space velocity of 240 hr^{-1} for a bed volume of 50 cm^3 (3.0 in^3). To attain the 3:1 molar ratio of CH_4 to CO_2, the baseline flow rate of CH_4 was 150 cm^3/min (5.3 x 10^{-3} cfm) and the flow rate of CO_2 was 50 cm^3/min (1.8 x 10^{-3} cfm).

Reactor Inlet Pressure. The baseline reactor inlet pressure was 108 kN/m^2 (15.7 psia). The differential pressure through the reactor was anticipated to vary for each of the six candidate catalysts because they had different catalyst supports and particle dimensions. The use of a small but constant inlet pressure was anticipated to produce more precise data if the reactor pressure affected catalyst performance.

Test Stand Checkout and Calibration Procedures

The first part of the test program was a checkout and calibration of the test hardware.

Objective

The objectives of the first part of the test program was the calibration and checkout of the parametric devices on the test stand to insure proper operation. The parametric measuring devices are listed in Table 3 with their locations and anticipated accuracies. Water collection methods to be used were checked out by methanating CO_2 with H_2 in the reactor (Equation 1). The methanation reaction is known to produce sufficient water to allow checkout of the heat exchanger for water collection as well as the gas drying tube.

Procedure

1. Following assembly of the test stand, the pressure gauges (PG1 and PG2), flowmeters (FM1 and FM2), and the reactor oven thermocouple and temperature readout were calibrated. The calibration curves for these parametric measuring devices are shown in Appendix 1.

2. Fill copper tubular reactor with 40 g (0.088 lb) of NI0104T1/8 catalyst.

3. Attach reactor to test stand.

4. Cap vent downstream of regulator R1. Pressurize reactor to 515 kN/m^2 (74.7 psia) with CO_2. Check for leaks.

5. Uncap vent and reduce pressure in test stand. Pretreat catalyst using baseline pre-treatment procedure.

TABLE 3 PARAMETRIC TEST INSTRUMENTATION

Type of Measurement	Type of Instrument	Measurement Location	Expected Accuracy
Temperature	Honeywell Temperature Controller	Downstream of Reactor	±2% Full Scale
Pressure	Magnehelic Pressure Gauge, No. 2205, 0 to 5 Psig	Upstream of Reactor	±2% Full Scale
Pressure	Ashcroft Pressure Gauge, 0 to 60 Psig	Upstream of Reactor	±2% Full Scale
Pressure	Magnehelic Pressure Gauge, No. 2005, 0 to 5 In of Water	Across Reactor	±2% Full Scale
Flow Rate	Skanflo 175, Flow Controller, 0 to 180 Psig	Upstream of Reactor	±2% Full Scale
Reactor Effluent Composition	Carle Gas Chromatograph Model 311	Downstream of Reactor	±5% Full Scale of value

6. Initiate gas flow through reactor consisting of 50 cm^3/min (1.8 x 10^{-3} cfm) CO_2 and 200 cm^3/min (7.06 x 10^{-3} cfm) H_2. Adjust the location and temperature control of the heating tapes to prevent condensation in tubing upstream of heat exchanger and gas drying tube.

7. Verify operation of heat exchanger and gas drying tube for water collection.

Results

Placement of the heating tapes, adjusted to 363K (194F), from the reactor outlet to the inlet of the heat exchanger and gas drying tube was sufficient to prevent water condensation in the tubing in that region of the test stand.

With condensation in the test stand eliminated, the precision of the water generation rate measurements was equal to the precision obtainable in using the water measuring devices. The precision of water generation rate measurements made with the graduated cylinder, following condensation of the water vapor in the heat exchanger, was determined during the checkout of the test stand. The uncertainty of the method was approximately ±5% over the generation rate range of 5 to 10 g water/hr (1.1 to 2.2 x 10^{-2} lb/hr).

The precision of the water generation rate computed from the weight of water collected in the gas drying tube was calculated from repetitive measurements made during the characterization study. One typical set of measurements resulted in an average generation rate value of 2.06 g water/hr (4.53 x 10^{-3} lb/hr) with a relative standard deviation of 4.4%. Because the water generation rate measurements have an uncertainty of from 4 to 5% and chromatographic data has uncertainties of 5% or less, the experimental measurements of reaction efficiencies and product gas compositions are anticipated to be accurate to within ±5%.

Catalyst Characterization Study

The second part of the testing program was the catalyst characterization.

Objective

The objective of the catalyst characterization study was the direct comparison of the reaction efficiencies and conversion rates of the six candidate catalysts selected for evaluation. The activities of the catalysts were compared at two temperatures. Because the temperature for maximum activity of each catalyst was not known, data obtained at two temperatures was anticipated to provide more representative information on the performance of the catalysts. Based on the results obtained in the characterization study, the two catalysts most active at low temperatures were identified.

Procedure

The procedure used to characterize the activity of each catalyst is given below.

1. Weigh the catalyst sample and pack it in the reactor. Attach reactor to test stand.

2. Adjust reactor oven temperature to 673K (752F) and pre-treat the catalyst.

3. Following pre-treatment, adjust the experimental parameters to the baseline values listed in Table 2 and adjust oven temperature to 673K (752F).

4. Weigh gas drying tube and attach tube to test stand.

5. Operate the reactor for one hour to allow the system to reach a steady-state condition, and bypass the product gases and water vapor around the gas drying tube using valves V7 and V8 (Figure 8).

6. After one hour, direct product gases and water vapor through gas drying tube for 20 minutes.

7. After the water collection period, direct product gases through the gas drying tube bypass. Remove and weigh tube to determine the weight of water collected.

8. Reconnect drying tube and repeat Steps 6 and 7 to obtain second water generation rate data point.

9. Adjust oven temperature to 873K (1112F) and purge system with CH_4 at 150 cm^3/min (5.30×10^{-3} cfm) for 30 minutes to remove residual water vapor from the system.

10. Resume flow of CO_2 at 50 cm^3/min (1.8×10^{-3} cfm) and repeat Steps 5 through 8 to obtain water generation data at 873K (1112F).

11. Shut down test stand by closing gas cylinder valves and turning off reactor oven and heating tapes.

12. Repeat Steps 1 through 11 for next candidate catalyst sample.

Results

The reaction efficiencies and conversion rates measured at 673K (752F) and 873K (1112F) for the candidate catalysts are listed in Table 4. The activities of all the catalysts are greater at 873K (1112F) than at 673K (752F). The efficiencies of the Ni catalysts range from 13.8 to 21.6% at 873K (1112F), whereas the efficiencies of the Ru and Pd catalysts are only 3.6 and 2.7%, respectively. At 673K (752F), the Ni on molecular sieve catalysts retain more activity than the other catalysts. The Linde catalyst exhibits an efficiency of 7.1% at 673K (752F), while the Girdler Ni on molecular sieve catalyst converts 6.2% of the CO_2. The remaining Ni catalysts and the Ru catalyst have efficiencies of approximately 2% and the Pd catalyst has negligible activity.

TABLE 4 RESULTS OF CATALYST CHARACTERIZATION STUDY

Catalyst	Catalyst Weight, g (Lb)	Bed Volume, cm^3 (In^3)	Space Velocity, Hr^{-1}	Reaction Efficiency, %		Conversion Rate, g CO_2/g Catalyst-Hr	
				673K (752F)	873K (1112F)	673K (752F)	873K (1112F)
Harshaw NI0104	41.40 (0.091)	28.4 (1.73)	422	2.4	14.9	3.2×10^{-3}	2.0×10^{-2}
Girdler G-49A	37.70 (0.083)	38.5 (2.35)	312	1.8	13.8	2.6×10^{-3}	2.0×10^{-2}
Linde Ni on Molecular Sieve	44.99 (0.099)	77.4 (4.72)	155	7.1	21.6	8.7×10^{-3}	2.6×10^{-2}
Girdler Ni on Molecular Sieve	36.78 (0.081)	45.7 (2.79)	262	6.2	14.2	9.3×10^{-3}	2.1×10^{-2}
Engelhard Pd on Alumina	38.65 (0.085)	39.8 (2.43)	302	0.2	2.7	2.8×10^{-4}	5.0×10^{-4}
Engelhard Ru on Alumina	35.13 (0.077)	36.0 (2.20)	333	2.0	3.6	3.1×10^{-3}	5.6×10^{-3}

The activities of the catalysts are also given in terms of conversion rate in Table 4. The conversion rate is a way of expressing the activity of the catalyst, partially normalized on the basis of the weight of catalyst used in each test. The conversion rate expresses the efficiency in terms of weight of CO_2 converted to water per hour, divided by the weight of the catalyst in the reactor. The catalyst weight is not related to the quantity of catalyst consumed or inactivated in the reaction.

The conversion rates of the four Ni catalysts are approximately equal at 873K (1112F). The values range from 2.0×10^{-2} to 2.6×10^{-2} g CO_2/g catalyst-hr. The values of the conversion rates of the Ru and Pd catalysts are only 5.6×10^{-3} and 5.0×10^{-4} g CO_2/g catalyst-hr, respectively. Therefore, the conversion rate values show the same trends in catalyst activity as the reaction efficiency.

At 673K (752F), the Linde and Girdler Ni on molecular sieve catalysts produce conversion rates of 8.7×10^{-3} and 9.3×10^{-3} g CO_2/g catalyst-hr, respectively. These values are greater than those of any other catalyst evaluated by a factor of three or more. These conversion rate values show the two Ni on molecular sieve catalyst to be the catalysts most active at low temperatures. Low temperature operation of catalytic reactors reduces power consumption and, in the case of the reduction of CO_2 with CH_4, makes higher conversion efficiencies possible. Therefore, the Ni on molecular sieve catalysts were selected for use in the parametric testing studies.

Parametric Testing

The third part of the testing program was the parametric testing studies.

Objective

The objective of the parametric testing was to quantify the effects of four main reaction parameters on the performance of the two most active catalysts identified in the characterization studies. The four parameters were reactor temperature, reactant gas flow rate, reactant gas composition, and reactor inlet pressure. The data obtained from this study would aid in determining the conditions that result in maximum reaction efficiencies. A preliminary study was also made to determine the optimum weight of catalysts to be used in the breadboard reactor during the parametric testing and subsequent tests.

Procedure

The procedure used during the parametric tests is given below.

1. Weigh the catalyst and pack reactor. Mount reactor in oven and connect reactor inlet and outlet to test stand.

2. Pretreat catalyst using baseline procedure.

3. After the catalyst pretreatment, establish the required experimental parameters.

4. Operate the system for 15 to 30 minutes until steady-state performance is obtained. During this time, direct the product gases and water vapor through the gas drying tube bypass.

5. Weigh the gas drying tube and mount it on the test stand while the reactor is reaching steady-state performance.

6. Direct the product gases and water vapor through the gas drying tube for one hour.

7. During the one hour water collection period, obtain two sets of chromatograms of the product gases exiting the gas drying tube. Each set of chromatograms consists of a chromatogram obtained with the DEHS column, and the molecular sieve column in series with the DEHS.

8. Direct the product gases through the drying tube bypass. Remove and weigh the drying tube to calculate the weight of collected water.

9. Reconnect the drying tube. Repeat Steps 6 and 8 to obtain a second water generation rate value.

10. Adjust the experimental parameters to the next set of required values and repeat Steps 4 through 9.

11. At end of daily test activities, shut down the chromatograph, close all gas cylinder valves, turn off reactor oven and heating tape temperature controller.

Results

The optimum quantity of catalyst to be used in the breadboard reactor was determined. The effects of reactor temperature, reactant gas flow rate and composition, and reactor inlet pressure on each catalyst was then quantified using the optimum weight of catalysts.

Catalyst Weight. The characterization study was performed with approximately 40 g (0.09 lb) of each catalyst. Prior to parametric testing, an investigation was performed to determine if greater conversion efficiencies could be achieved by increasing the amount of catalyst in the reactor. The Linde Ni on molecular sieve catalyst was used for this study because it had exhibited the greatest reaction efficiency in the characterization studies. In Figure 13, the reaction efficiency at 873K (1112F) is shown as a function of the weight of catalyst in the reactor. The maximum measured efficiency was 27% with 75 g (0.16 lb) of catalyst, the maximum weight of catalyst that could be held in a heated volume of the reactor. An extrapolation of the curve shows that the reaction efficiency approaches the maximum value of 30% for a weight of catalyst equalling approximately 130 g (0.29 lb).

Although adding catalyst to the reactor increases the reaction efficiency, the

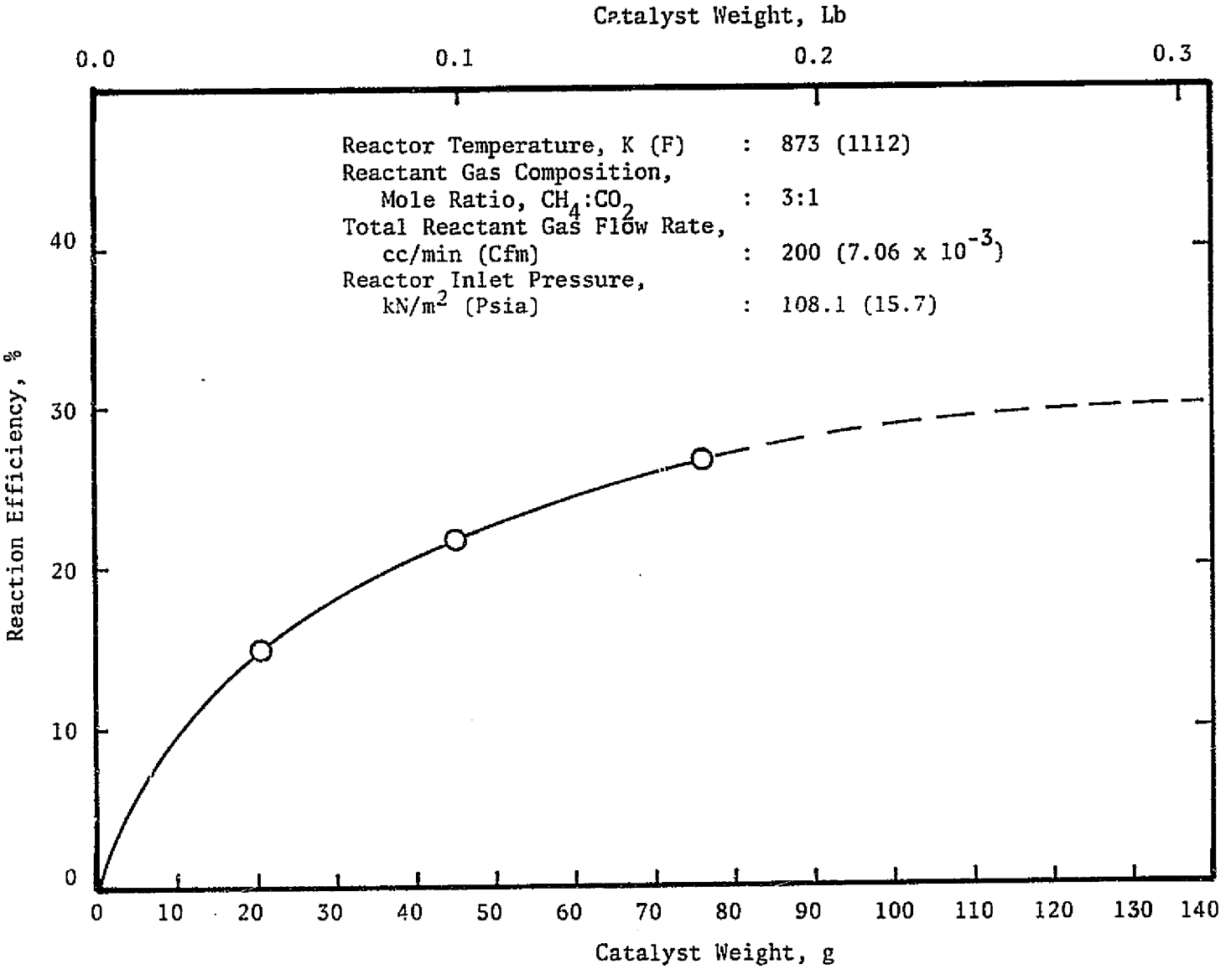

FIGURE 13 REACTION EFFICIENCY OF LINDE CATALYST VERSUS CATALYST WEIGHT

efficiency increases less than the weight of added catalyst. This is illustrated by Figure 14 showing conversion rate as a function of the weight of Linde catalyst in the reactor. The conversion rate decreases as catalyst is added because the average activity of the catalyst decreases as catalyst is added to the reactor. Figure 13 shows that the first 20 g (0.044 lb) of catalyst converts 14.7% of the CO_2 entering the reactor. When an additional 20 g (0.044 lb) of catalyst is added, the reaction efficiency increases only 5.9% to 20.6%. Therefore, the factor that equals the catalyst weight in the denominator of the conversion rate computation increases more than the factor in the numerator, equaling the weight of CO_2 converted per hour.

A possible reason that the catalyst is less effective as the weight of catalyst is increased is because the temperature gradient anticipated to exist along the longitudinal axis of the reactor causes the catalyst added to the ends of the catalyst bed to exist at a significantly different temperature than the catalyst originally in the center of the reactor. The temperature of the ends of the catalyst bed may be less favorable for reaction efficiency than the temperature of the center of the reactor, so that adding catalyst to the bed places that catalyst in a temperature zone in which it is less reactive than the catalyst already in the center. The catalyst therefore would become less efficient as the weight of catalyst in the reactor is increased.

This possibility was tested by inserting a thermocouple longitudinally through the reactor which was completely filled with catalyst. The flow of reacting gases was simulated by a flow of 200 cm^3/min (7.06×10^{-3} cfm) of CH_4 and the furnace temperature readout was adjusted to 873K (1112F). The longitudinal temperature gradient through the reactor is shown in Figure 15. The ends of the catalyst were approximately 100K (212F) lower in temperature than the center which was at 871K (1036F). The reduction of CO_2 with CH_4 appears to require the more elevated temperatures at the center of the reactor bed. The temperature gradient is significant and therefore may be the cause of the decreasing conversion rate of CO_2 with increased catalyst weight.

The use of more than the 40 g (0.088 lb) of catalyst used in the characterization study, increased the water generation rates, making those measurements more precise. The higher conversion efficiencies are also more representative of the reactor performance if it was integrated in a spacecraft ARS. Therefore, 65 g (0.14 lb) of each of the Ni on molecular sieve catalysts was used in subsequent tests. That weight was chosen because it equalled the maximum amount of the Linde catalyst that could be packed in the reactor without the ends of the catalyst bed being close to the cooler extremities of the reactor.

Temperature Study. The catalysis of the reduction of CO_2 with CH_4 by the Ni on molecular sieve catalysts is temperature dependent, and there is a temperature for each catalyst at which the reaction efficiency is a maximum. With the baseline experimental parameters and 65 g (0.14 lb) of each catalyst in the reactor, the catalysts exhibit identical temperature dependence below 700K (801F) (Figure 16) and produce efficiencies of less than 5%. At higher temperatures, the Linde catalyst is significantly more active than the Girdler catalyst. The Linde catalyst obtains a maximum efficiency of 29.9% at 950K (1251F) and the Girdler produces an efficiency of 21.7% at 873K (1112F).

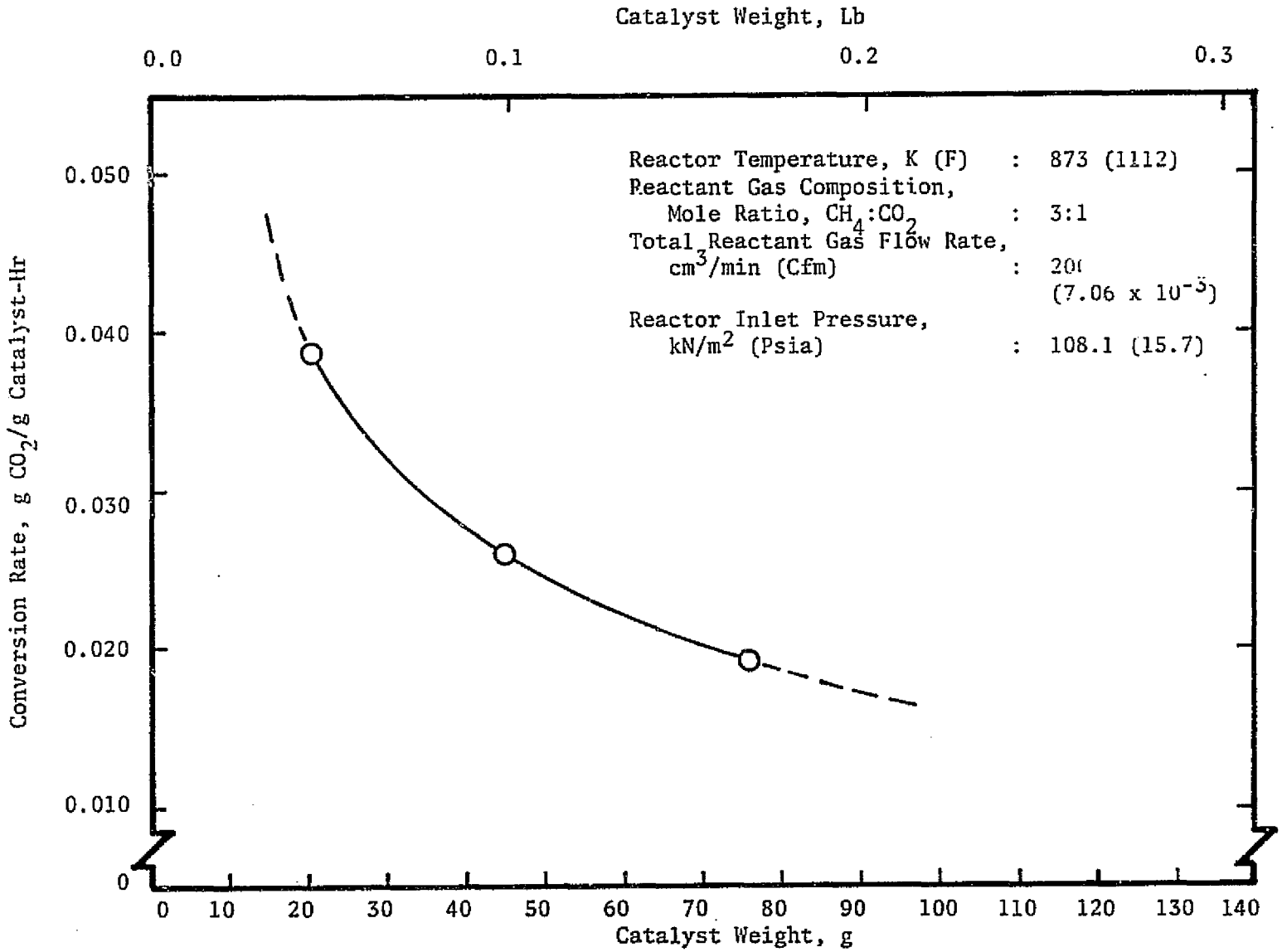

FIGURE 14 REACTION EFFICIENCY OF LINDE CATALYST VERSUS CATALYST WEIGHT

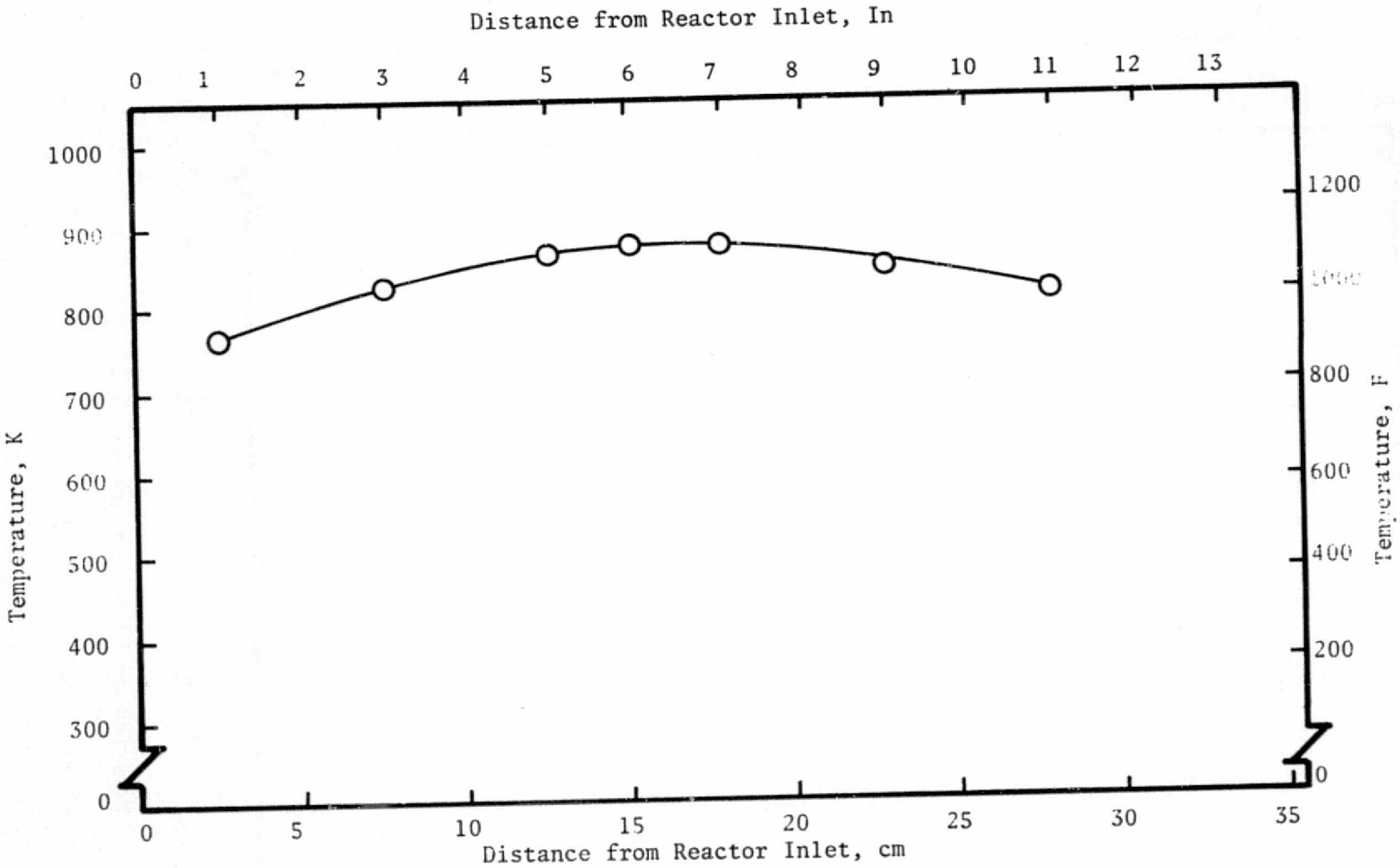

FIGURE 15 REACTOR TEMPERATURE GRADIENT TEMPERATURE VERSUS DISTANCE FROM REACTOR INLET

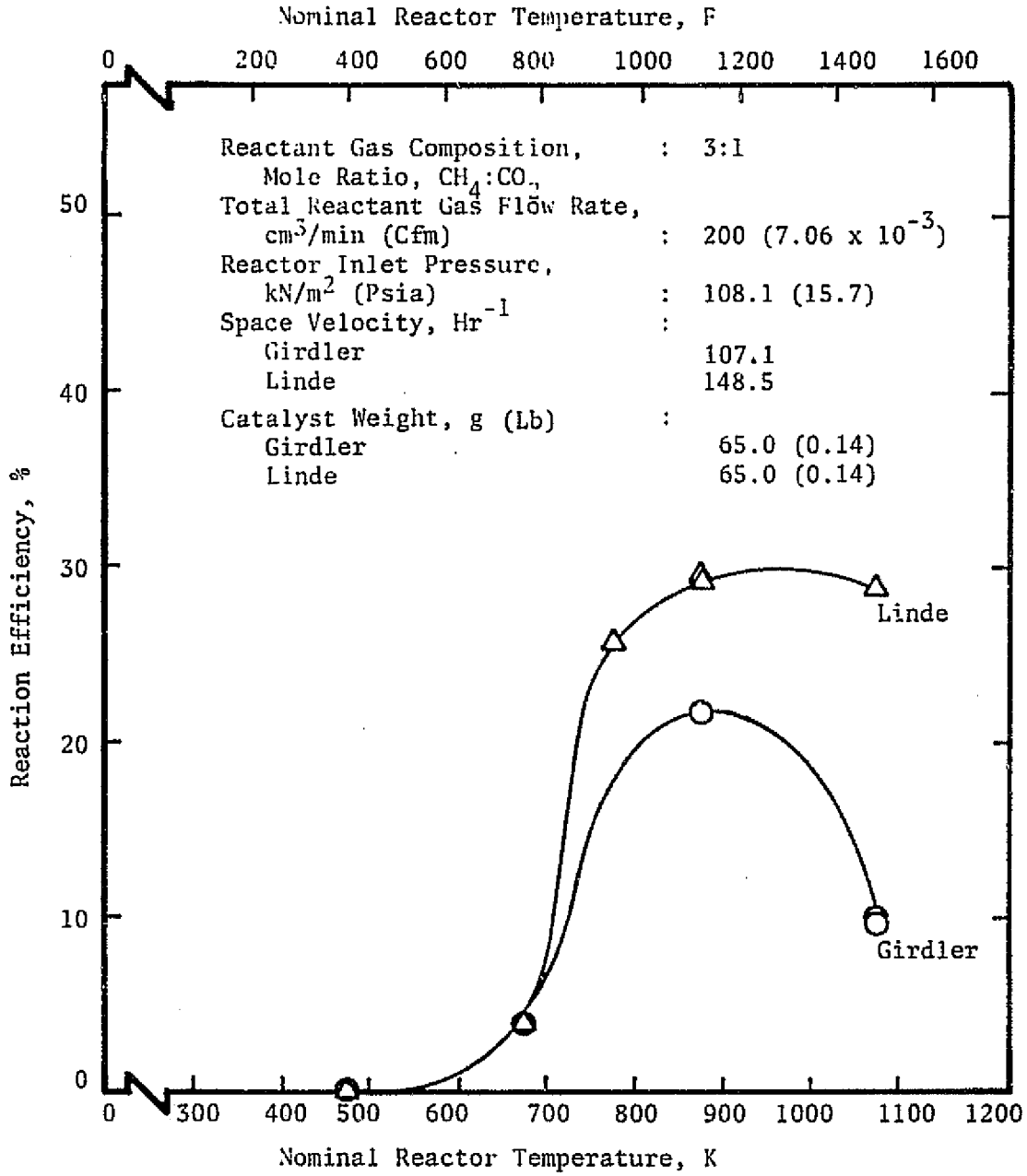

FIGURE 16 REACTION EFFICIENCY OF GIRDLER AND LINDE CATALYSTS VERSUS NOMINAL REACTOR TEMPERATURE

The composition of the product gases was determined chromatographically for both catalysts for the range of reactor temperatures of 273 to 173K (77 to 1442F). The product gas composition, in mole percent, is presented in Figures 17 and 18 for the Linde and Girdler catalysts, respectively. The water output and the mole percent of carbon formed in the reactor are also shown. The mole percent of carbon was calculated from the composition of the reactant and product gas streams and water generation rate data.

Figures 17 and 18 are very similar for the two catalysts. However, CO_2 and CH_4 react at somewhat lower temperatures at the Girdler catalyst, forming CO and H_2. Nickel catalysts are known to catalyze the production of CO and H_2 shown in Equation 5.[23-24]

$$CH_4 + CO_2 = 2CO + 2H_2 \qquad (5)$$

This side reaction is apparently more actively catalyzed at low temperatures by the Girdler catalyst, but it occurs at higher tempeatures at both catalysts, as indicated by the significant concentrations of H_2 and CO shown in Figures 17 and 18.

The water production has been shown to reach a maximum rate at 950K (1251F) for the Linde catalyst and 873K (1112F) for the Girdler catalyst (Figure 16). However, CH_4 reacts at a higher rate at temperatures above the maximum temperature for water production. Hydrogen and carbon are major products at these temperatures, indicating that the decomposition of CH_4 (Equation 2) is a major side reaction in the reactor. The decomposition of CH_4 at Ni catalysts has been reported to occur at temperatures between 973 and 1223K (1292 and 1742F).[25-27]

The data in Figures 17 and 18 show that the Ni on molecular sieve catalysts catalyze three major reactions. The formation of CO and H_2 from CO_2 and CH_4 is catalyzed at all temperatures above 500K (441F) and 620K (657F) for the Girdler and Linde catalysts, respectively. The production of water and carbon is catalyzed primarily between the temperatures of 750 and 1050K (891 and 1431F) for both catalysts, and the decomposition of CH_4 is catalyzed at temperatures around 900K (1161F) and greater.

The Ni on molecular sieve catalysts produce significant quantities of CO and H_2, although Ni catalysts are known to be effective in catalyzing the methanation of Co with H_2.[19] If the residual CO was reduced with the H_2, water production and the overall reaction efficiency would be increased. Another catalyst, more capable of catalyzing the reduction of the residual CO, was sought to quantify the improved efficiency, if any, resulting from the addition of that catalyst to the downstream end of the Ni on molecular sieve catalyst bed.

Iron wool is known to catalyze the reduction of CO with H_2[4], and was therefore used for this investigation. The Fe wool was pre-treated with a rinse in hydrochloric acid (HCl) and distilled water before use. Pieces of the wool (approximately 1 cm (0.4 in) dia.), totalling 2.40 g, were added to the downstream end of the catalyst bed, that contained 65.1 g of the Girdler Ni on molecular

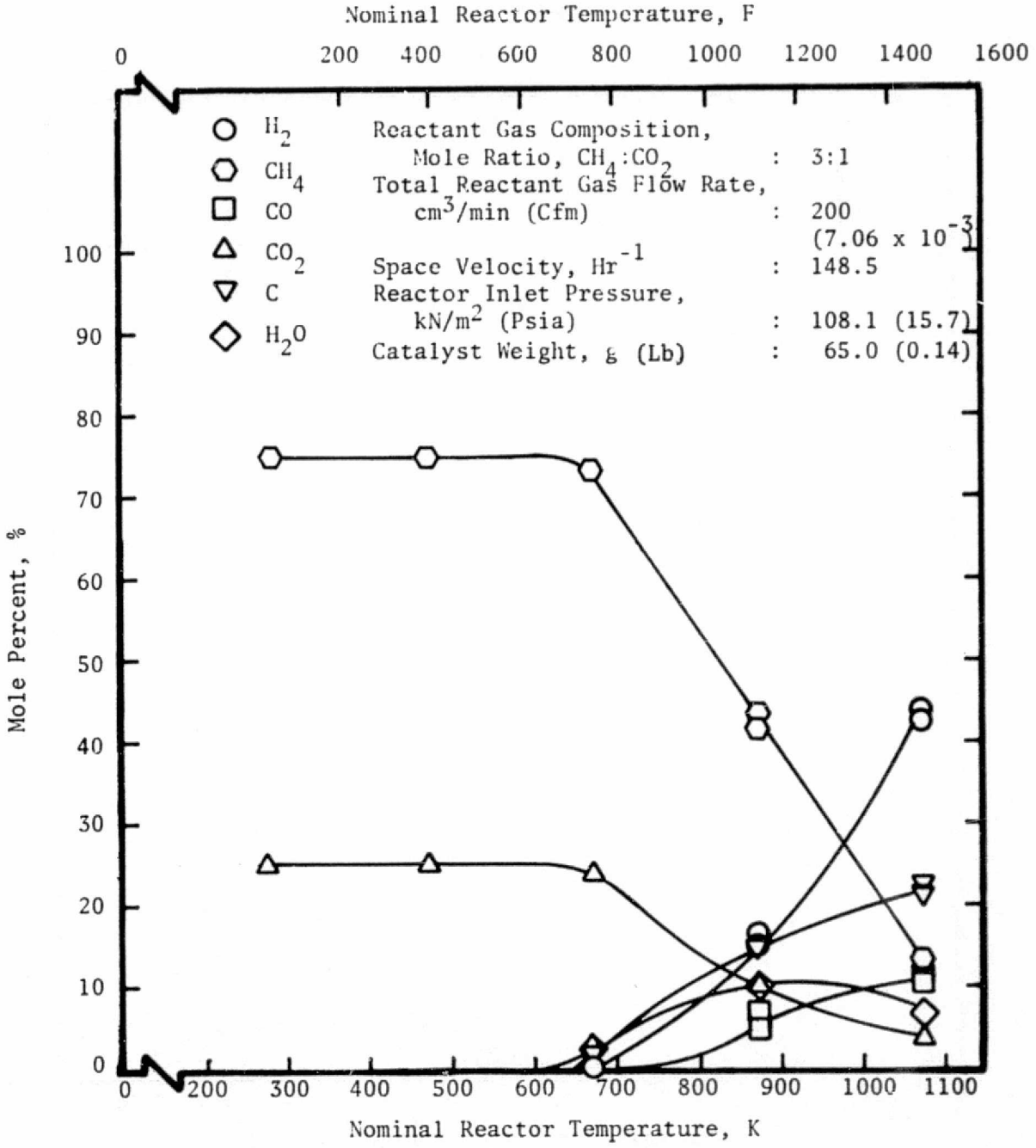

FIGURE 17 REACTOR EFFLUENT COMPOSITION FOR LINDE CATALYST VERSUS NOMINAL REACTOR TEMPERATURE

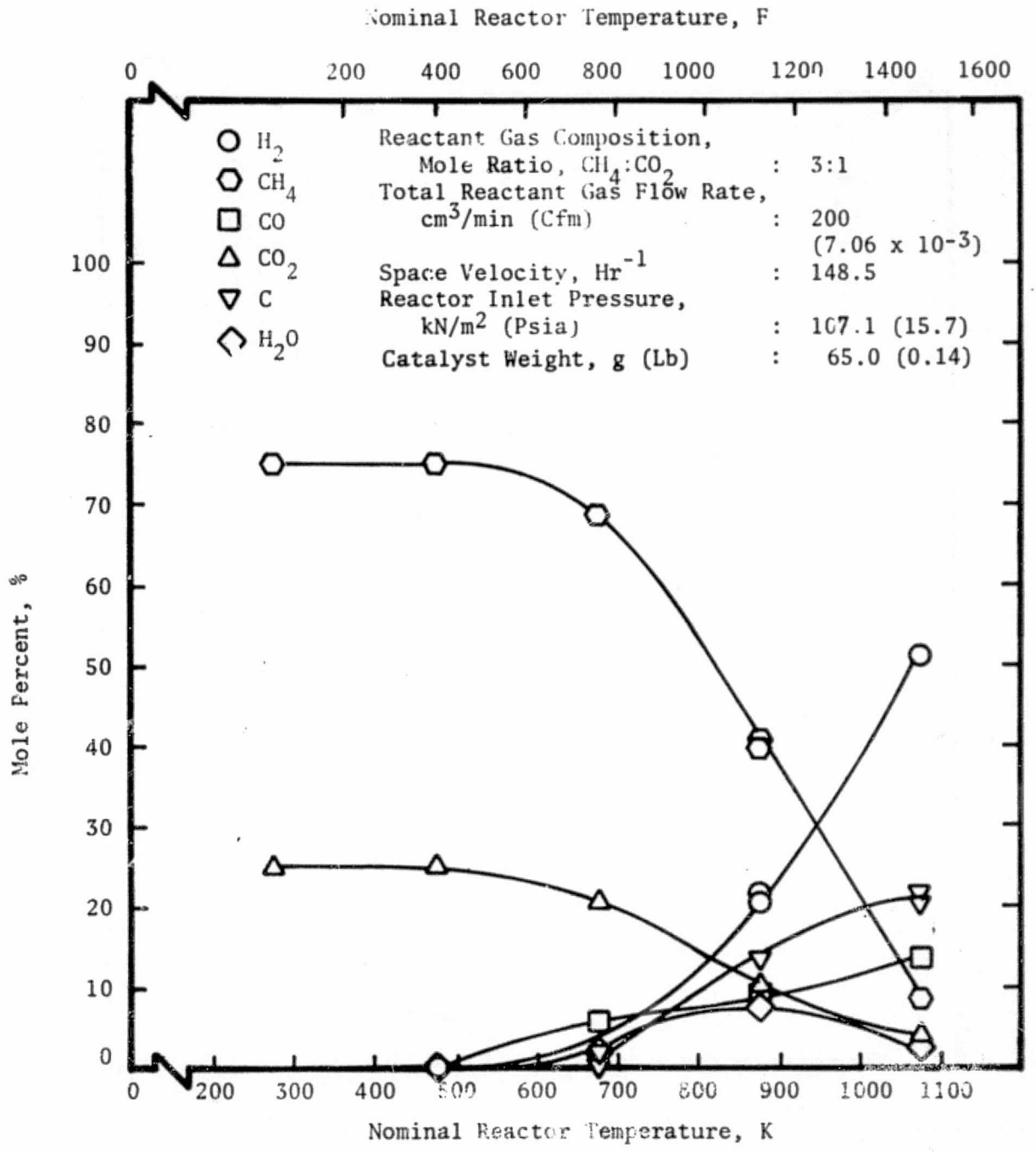

FIGURE 18 REACTOR EFFLUENT COMPOSITION FOR GIRDLER CATALYST VERSUS NOMINAL REACTOR TEMPERATURE

sieve catalyst. With the baseline experimental parameters, the Fe wool increased the reaction efficiency from 21.8 to 27.3%. A comparison of the reactor effluent composition with and without the Fe wool (Figure 19) shows that the addition of the Fe wool decreased the CO concentration from 9 to 3% and the H_2 concentration from 21 to 4%. Simultaneously, the CH_4 concentration increased from 40 to 57% and the water from 7 to 11%. These results show that Fe wool is effective in reducing the residual CO in the CO_2/CH_4 reactor effluent, and the major reaction products are CH_4 and water.

During the temperature study, the Linde catalyst rapidly deteriorated at 873K (1112F) and higher temperatures. The catalyst bed became plugged with small particles of the catalyst and carbon, and the pressure drop through the reactor increased until gas flow could not be maintained at the baseline reactor inlet pressure. The Girdler catalyst did not degrade noticeably, although carbon particles were formed. The degradation of the Linde catalyst decreased greatly at 773K (932F). The efficiency of the reactor at this temperature (25.5% for 65 g of catalyst with the baseline experimental parameters) was nearly equal to the maximum value at 950K (1251F). Therefore, to minimize the catalyst degradation and because of the goal of the program was to identify catalysts that could be operated at low temperatures, the reactor temperature used in all subsequent studies of the Linde catalyst was 773K (932F). The temperature used for the Girdler catalyst remained 873K (1112F).

Reactant Gas Flow Rate

The total flow rate of the reactant gas mixture was anticipated to affect the reaction efficiency and would be useful in future sizing of CO_2/CH_4 reactors. Figure 20 shows the reaction efficiencies as a function of the reactant gas flow rate for the Linde and Girdler catalysts. The composition of the reactant gas at all flow rates was a 3:1 mole ratio of CH_4 to CO_2. The efficiencies of both catalysts is 25.4% at 100 cm^3/min (3.53×10^{-3} cfm), the lowest flow rate investigated. This reaction efficiency is maintained by the Linde catalyst up to flow rates of 175 cm^3/min (6.18×10^{-3} cfm). The efficiency then falls to a value of 15% at 400 cm^3/min (1.41×10^{-2} cfm). The efficiency of the Girdler catalyst falls more quickly from the maximum value of 24.4% at 100 cm^3/min (3.53×10^{-3} cfm) to a flow rate independent value of 13.6%.

The space velocities for the two catalysts at a given flow rate differ because the apparent densities of the catalysts are different. The Linde catalyst has an apparent density of 0.581 g/cm^3 (2.10×10^{-2} lb/in^3) while the density of the Girdler catalyst is 0.805 g/cm^3 (2.91×10^{-2} lb/in^3). Therefore, the space velocity of reactant gas at a given flow rate is greater for a reactor containing 65 g (0.14 lb) of the Girdler catalyst than for 65 g (0.14 lb) of the Linde catalyst. Figure 21 shows that the relationship between reaction efficiency and space velocity is the same for the two catalysts. The figure also shows that maximum efficiency is obtained at space velocities less than 100 hr^{-1}.

Reactant Gas Composition

The composition of the reactant gases was anticipated to affect the catalytic

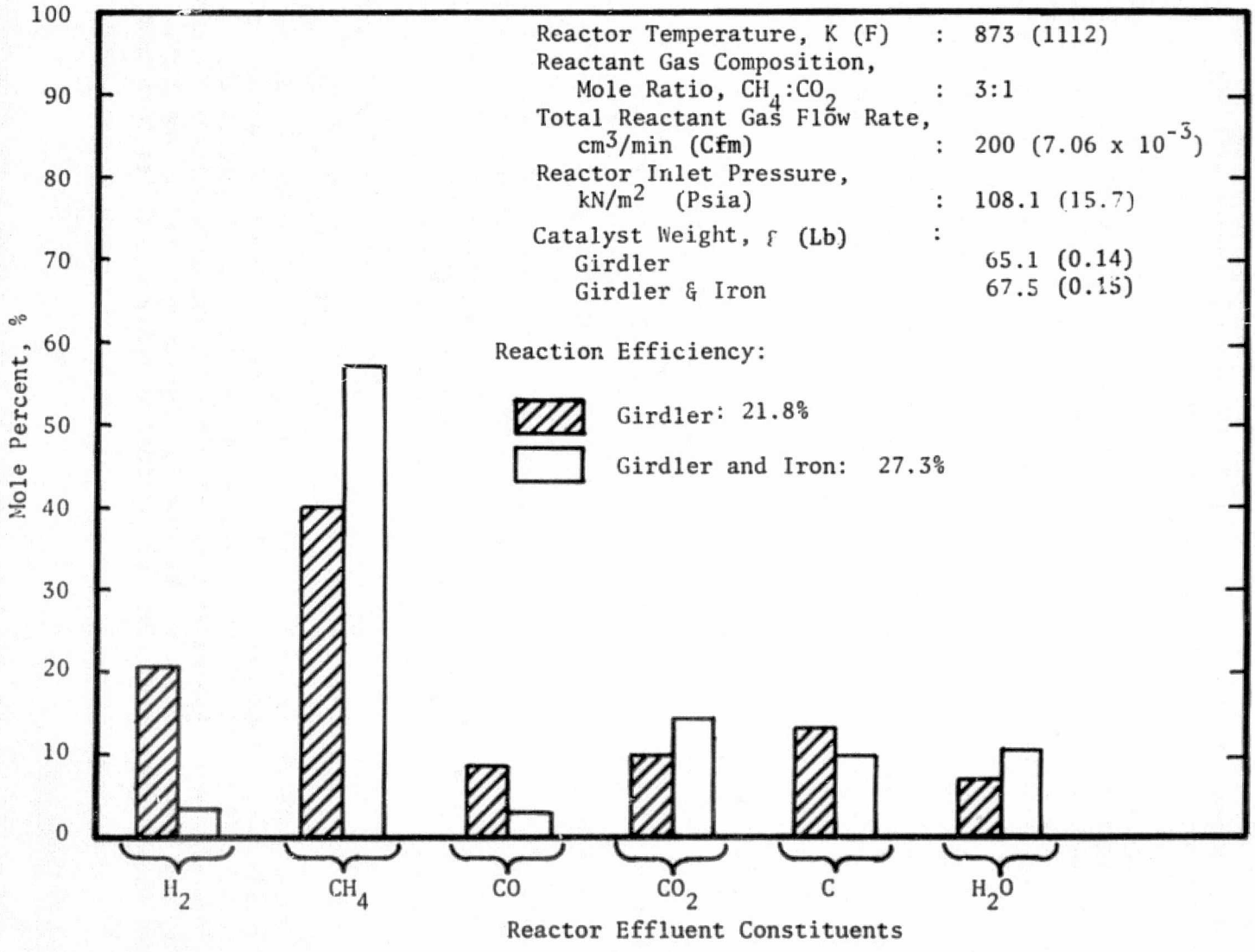

FIGURE 19 EFFECT OF IRON ON REACTOR EFFLUENT COMPOSITION

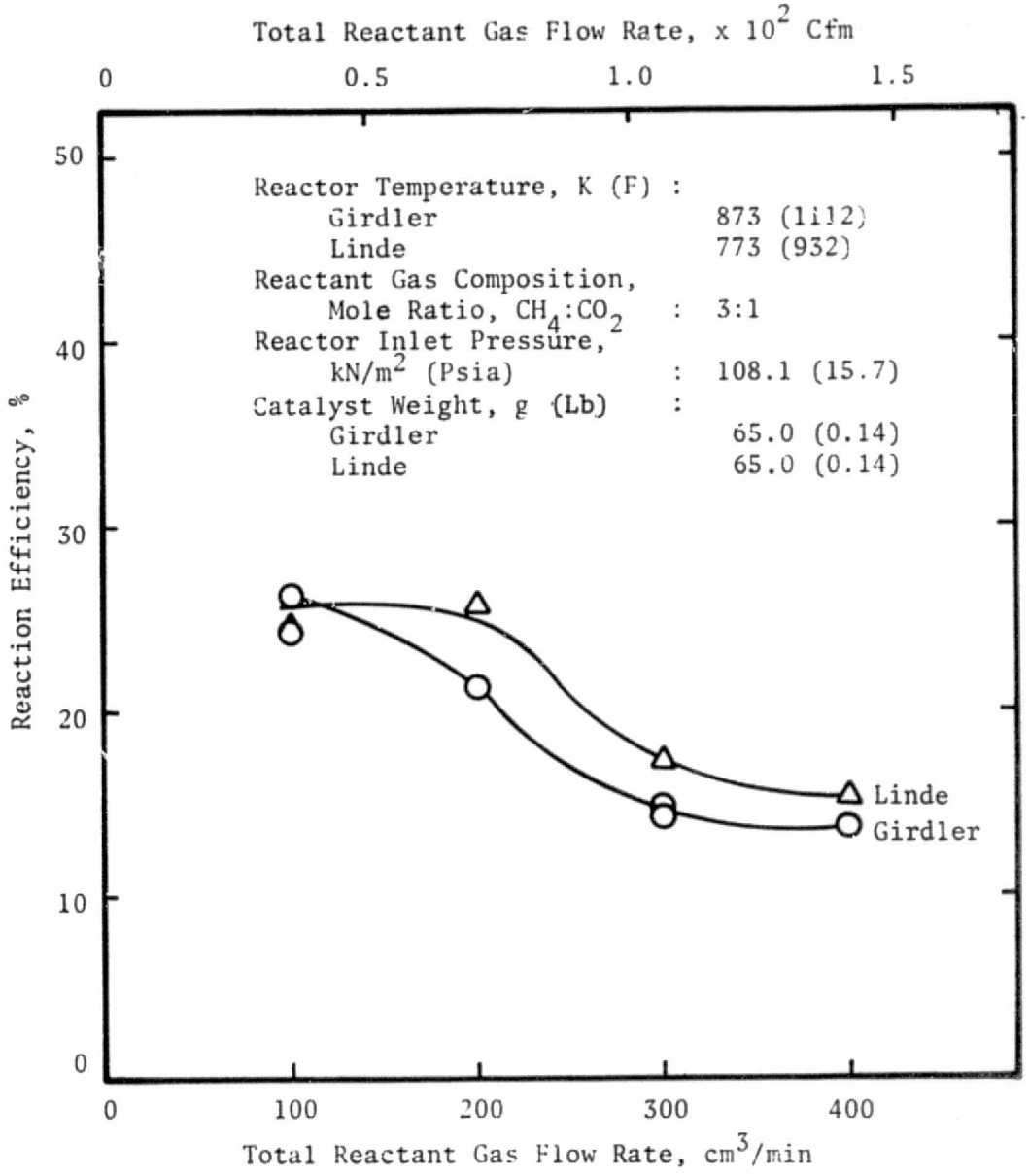

FIGURE 20 REACTION EFFICIENCIES OF GIRDLER AND LINDE CATALYST VERSUS TOTAL REACTANT GAS FLOW RATE

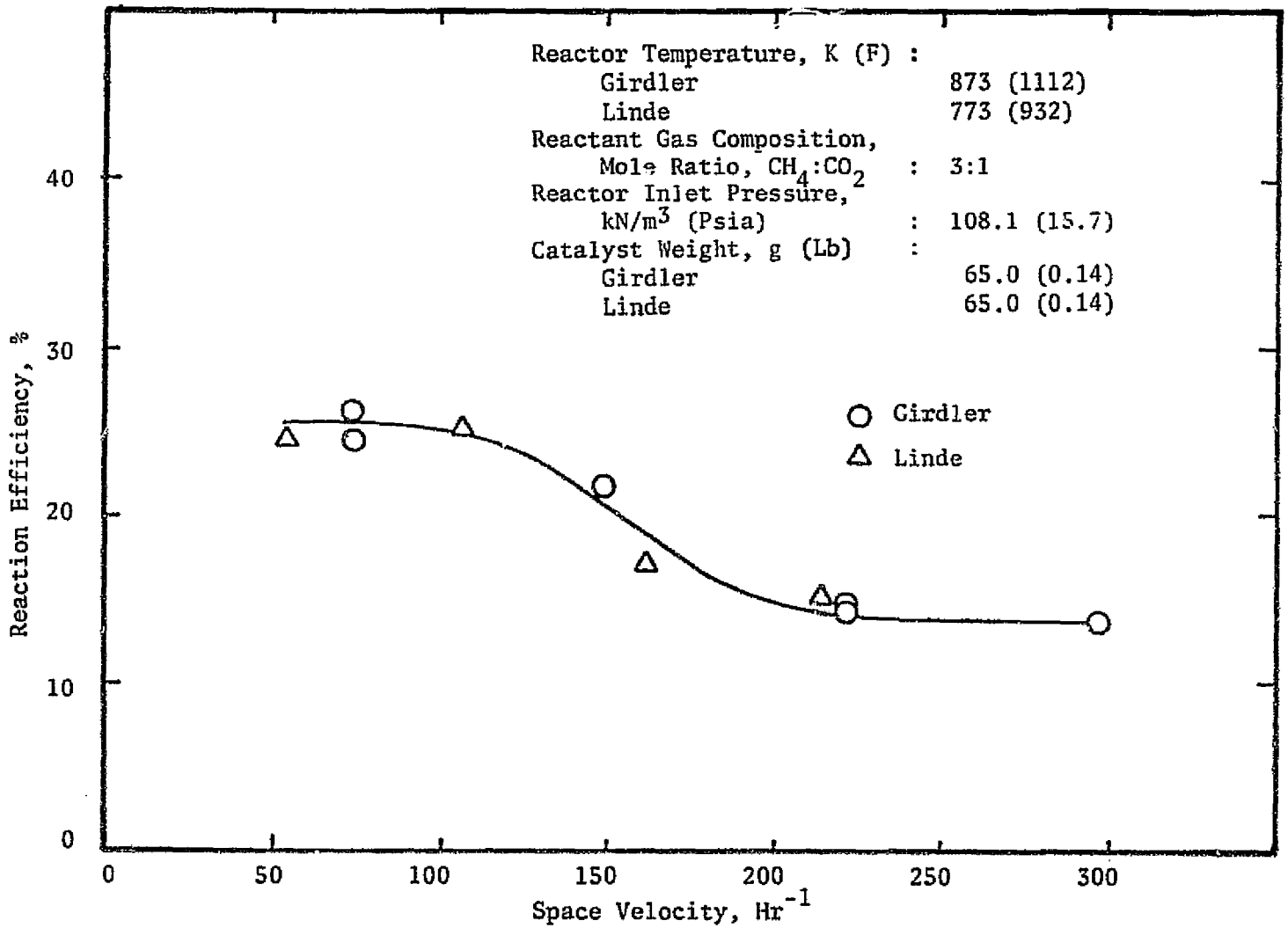

FIGURE 21 REACTION EFFICIENCIES OF GIRDLER AND LINDE CATALYSTS VERSUS SPACE VELOCITY

reaction efficiencies. An increase in the CH_4 concentration of the reactant gas mixture shifts the equilibrium of the CO_2 reduction toward higher CO_2 consumption and higher reaction efficiencies.

Figure 22 shows the efficiency of CO_2 conversion for the catalysts as a function of the mole ratio of CH_4 to CO_2 in the reactant gas stream. The efficiency of the Linde catalyst increases rapidly from a value of 8.2% at the stoichiometric mole ratio of 1:1 to a value of 39.2% at 7:1.

The Girdler catalyst is less affected by changes in the gas composition. The efficiency increases from 9.2% to only 26.0%. Also, the efficiency for the Girdler catalyst is nearly constant over the range of mole ratios between 3.5:1 and 5.0:1.

The composition of the reactant gas stream of a CO_2/CH_4 reactor integrated into an ARS would be determined by the efficiency of the Sabatier reactor feeding the CO_2/CH_4 reactor. The composition of the CO_2/CH_4 mixture is not a variable that can be adjusted independently of the overall system operation. This study does show, however, that the Linde catalyst would more efficiently remove trace quantities of CO_2 from the exhaust of an efficiently operating Sabatier reactor in which the mole ratio of CH_4 to CO_2 is three or greater.

Reactor Inlet Pressure. The inlet pressure of the CO_2/CH_4 reactor was varied to quantify the efficiency of CO_2 conversion at pressures other than the baseline value of 108 kN/m^2 (15.7 psia). Figure 23 shows the reaction efficiency for the catalysts at reactor pressures of 108 to 445 kN/m^2 (15.7 to 64.7 psia). The reaction efficiency of the catalysts decreases linearly with pressure. The reaction efficiency produced by the Linde catalyst decreases from 25.7% at 108 kN/m^2 (15.7 psia) to 18.7% at 446 kN/m^2 (64.7 psia). Over the same range in pressures, the efficiency of the Girdler catalyst decreased from 21.7% to 17.2%. These values correspond to a decrease of reaction efficiency with reactor pressure at rates of only -0.021% per kN/m^2 (-0.14% psi) and -0.013% kN/m^2 (-0.092 psi) for the Linde and Girdler catalysts, respectively. Small fluctuations in the reactor inlet pressure, therefore, have little effect on the reaction efficiency.

Ultraviolet Activation Studies

The UV activation studies completed the test program.

Objective

The objective of the UV activation studies was to quantify the improvement, if any, in the reaction efficiencies of the Ni on molecular sieve catalysts by irradiating the CO_2/CH_4 reactant gas mixture with UV light at a wavelength of 2537 A. The effect of UV activation without the use of a catalyst was also quantified.

Procedure

The procedure used is given below.

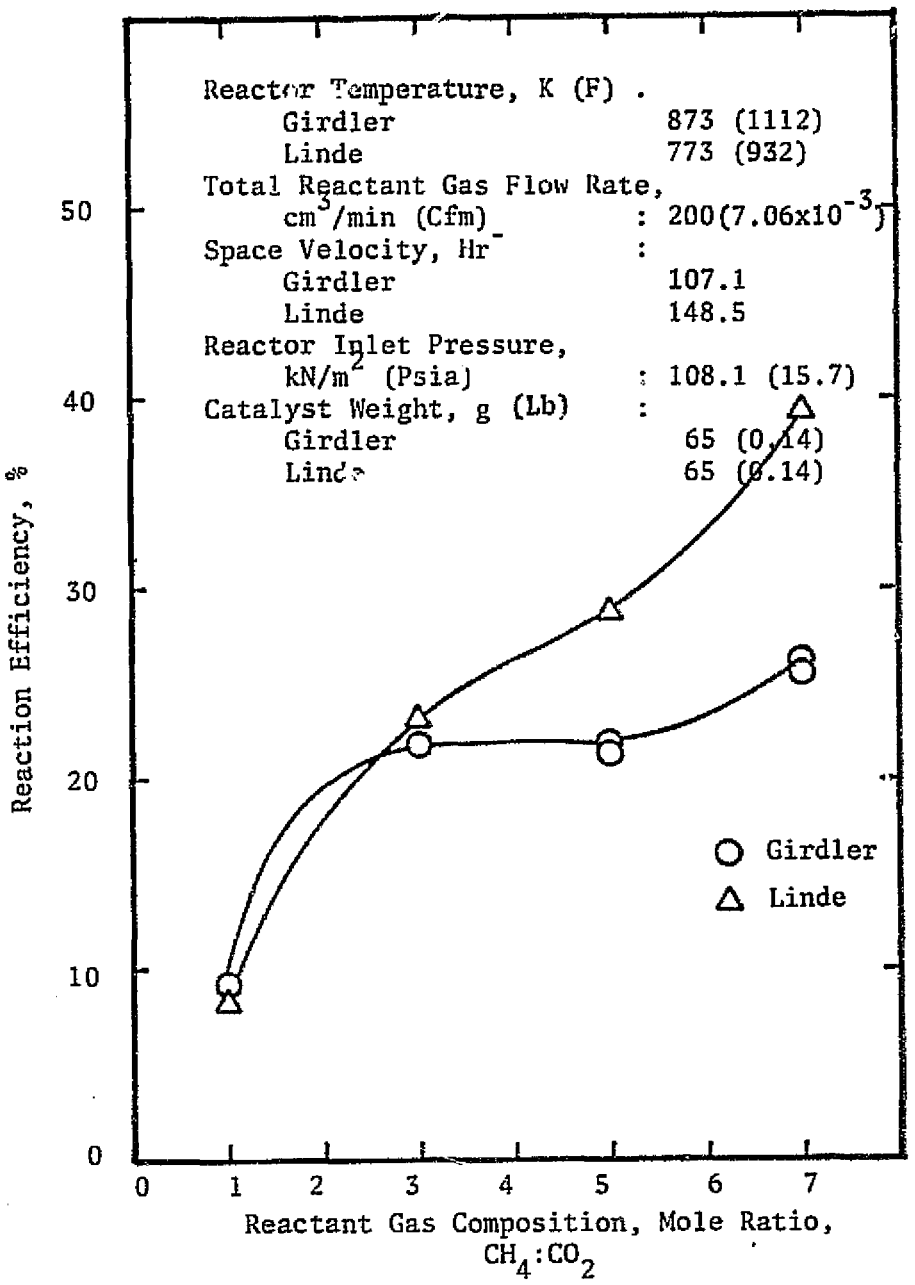

FIGURE 22 REACTION EFFICIENCIES OF GIRDLER AND LINDE CATALYSTS VERSUS REACTANT GAS COMPOSITION

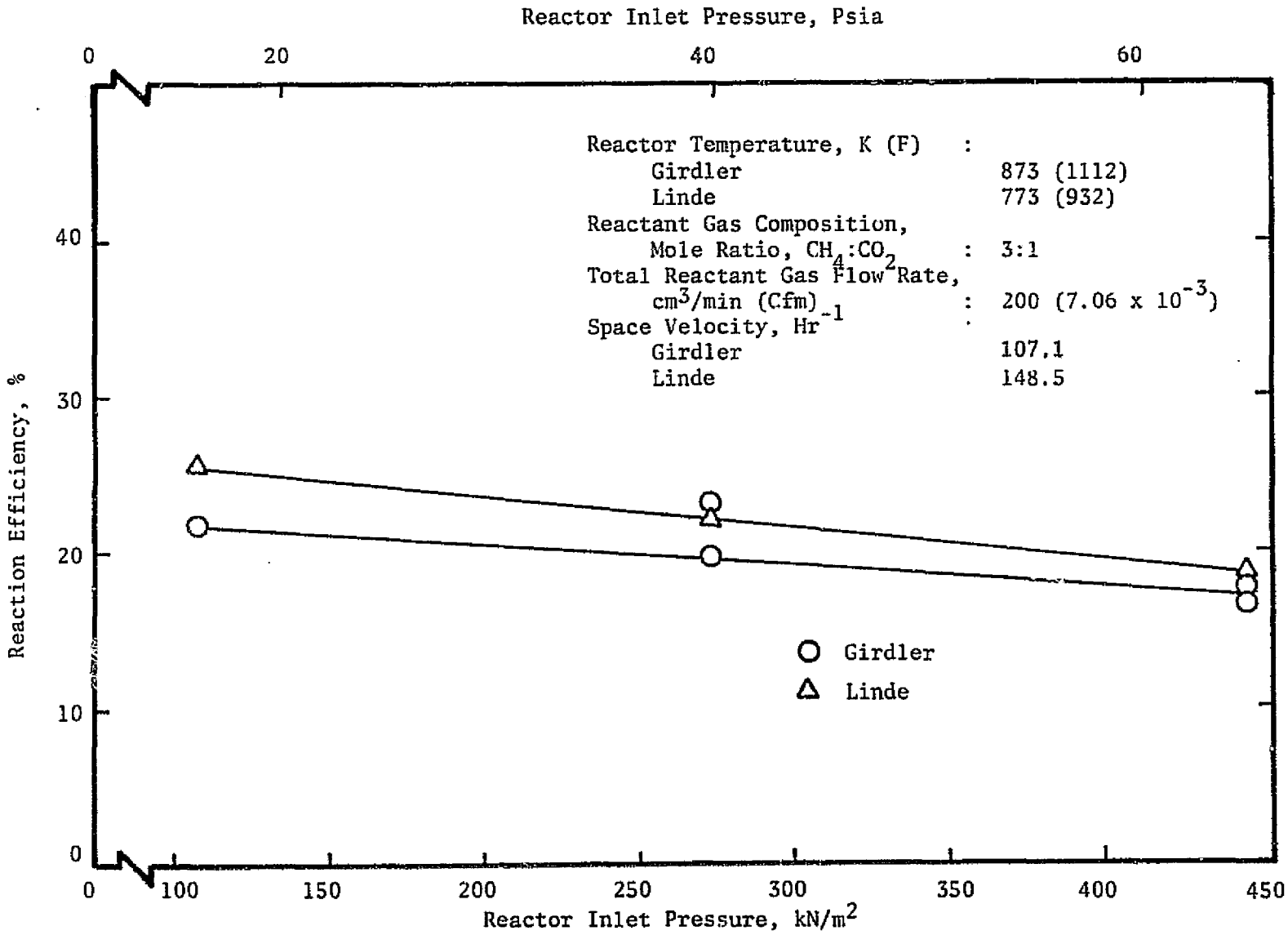

FIGURE 23 REACTION EFFICIENCIES OF GIRDLER AND LINDE CATALYSTS VERSUS REACTOR INLET PRESSURE

1. If a catalyst is to be used, weigh out 65 g (0.14 lb) of catalyst and pack it in the quartz tubular reactor.

2. Pre-treat the catalyst, if used, using the baseline pre-treatment procedure.

3. Adjust the oven to the required temperature, 773K (932F) for the Linde catalyst and 873K (1112F) for the Girdler catalyst.

4. With the UV lamp off, operate the reactor for 30 minutes with the product gases and water vapor bypassing the gas drying tube. Weigh the drying tube and attach it to the test stand.

5. Direct the product gases and water vapor through the drying tube for a one hour water collection period. Obtain chromatograms of the dried product gases.

6. After one hour, direct the product gases and water vapor through the bypass, remove and weigh the drying tube.

7. Turn on the UV lamp and operate the system 30 minutes. Reinsert the drying tube.

8. Repeat Steps 5 and 6 to obtain water generation rate data and product gas analysis for the UV activated reduction.

9. Repeat Steps 4 through 8 for second data point with and without UV activation.

10. Shut down test stand, turn off UV lamp and chromatograph, and close all gas cylinder valves.

Results

Ultraviolet activation of the reactant gases produces some changes in the composition of the product gases. For instance, with the Linde catalyst, the mole percent of CH_4 in the reactor effluent increases from 40 to 45.8% with UV activation, as shown in Figure 24. Simultaneously, the H_2 content decreases from 18.9 to 16.5% and the carbon formation decreases from 16.2 to 14.5%. Apparently, the rate of CH_4 decomposition is slower with UV activation. However, the water production is essentially unchanged.

The composition of the product gases from the Girdler catalyst are changed less by UV activation (Figure 25). The carbon formation is decreased from 12.5 to 12.1%, but the water output is decreased from 6.0 to 5.2%.

Ultraviolet activation does not increase the reaction efficiencies of the catalysts. In fact, in the case of the Girdler catalyst, the reaction efficiency is decreased slightly. However, the rate of carbon formation is also decreased.

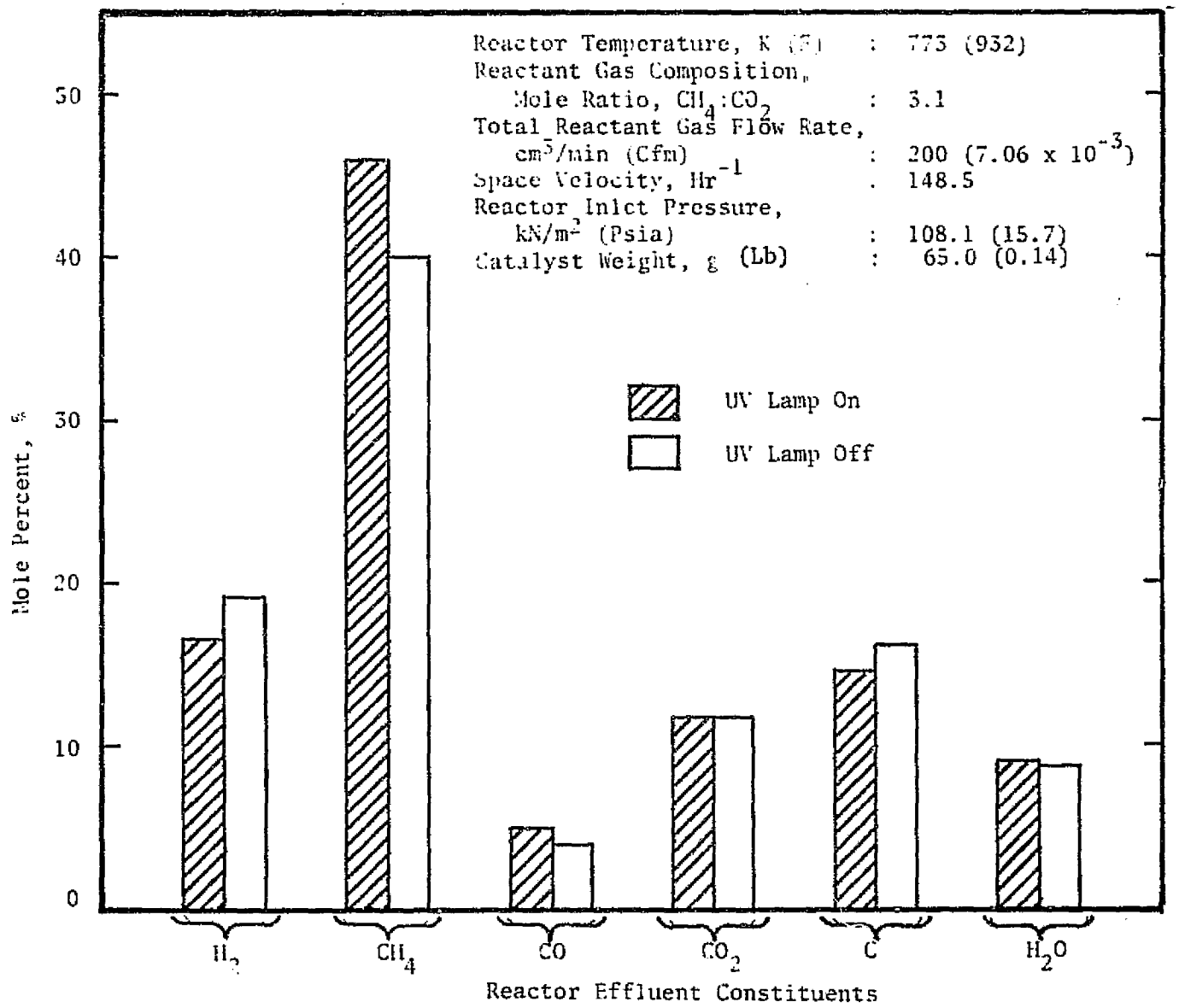

FIGURE 24 EFFECTS OF UV ACTIVATION ON REACTOR EFFLUENT COMPOSITION, LINDE CATALYST

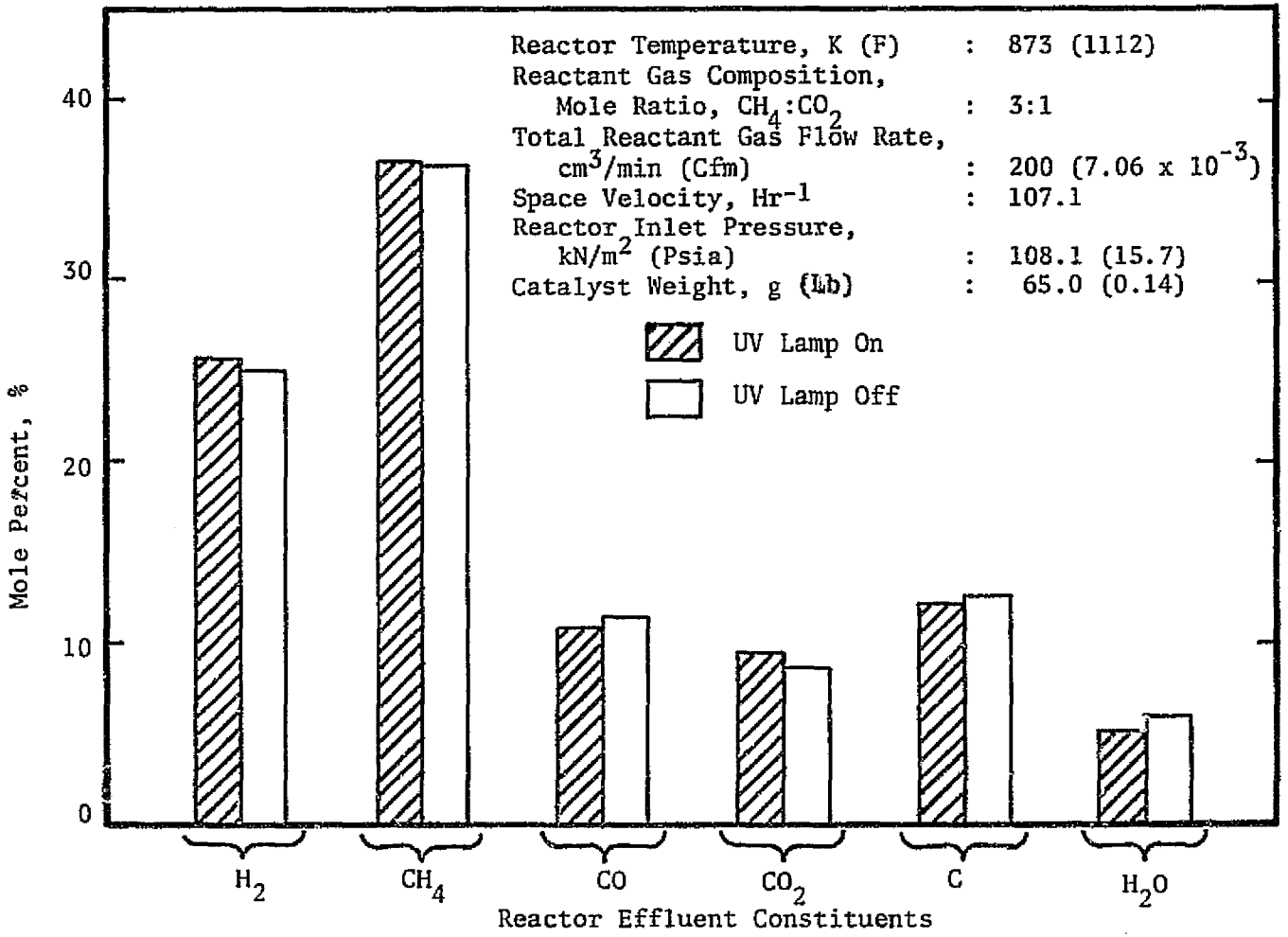

FIGURE 25 EFFECTS OF UV ACTIVATION ON REACTOR EFFLUENT COMPOSITION, CIRDLER CATALYST

To study the effects of UV activation without the use of catalysts, aluminum mirrors were positioned in the quartz reactor to produce repeated reflections of the UV radiation through the heated length of the reactor, as shown in Figure 26. The UV activation of the CO_2/CH_4 mixture caused some decomposition of the CH_4 and produced a trace quantity of H_2 and carbon (Figure 27). However, O_2 or water were not produced, as had been anticipated from the results of the literature review.

O_2 REGENERATION SYSTEM EMPLOYING THE CO_2/CH_4 REACTOR

The results of the experimental work revealed that a CO_2/CH_4 reactor employing Linde Ni on molecular sieves catalyst will yield a CO_2 conversion efficiency of 29% when operated under optimum conditions, using a larger reactor. The 29% reaction efficiency in the CO_2/CH_4 reactor, combined with the anticipated CO_2 conversion efficiency in the Sabatier reactor of 75%, results in a total O_2 recovery of 82.5%. The decrease in the water weight penalty associated with the use of the CO_2/CH_4 reactor, in conjunction with the Sabatier Reactor in a once-through flow scheme, is shown in Figure 28. For a 180-day, six-man mission, a weight savings of 84.91 kg (187.2 lb) of water is realized.

It is anticipated that the CO_2/CH_4 reactor would weigh less than 84.9 kg (187.2 lb), resulting in a net weight saving at launch. In order to recover the remaining CO_2 in the CO_2/CH_4 reactor exhaust, it will be necessary to incorporate a recycle loop into the ORS. This will allow an additional weight reduction of 220 kg (484 lb) of water but would require the addition of ancillary equipment for the recycle loop. The ancillary equipment is anticipated to weigh much less than 220 kg (484 lb). Therefore, the total weight reduction achieved using the recycle loop would be greater than the weight reduction obtained using the CO_2/CH_4 reactor integrated with the Sabatier reactor in a once-through flow scheme.

A conceptual block diagram of an O_2 Regeneration System (ORS) employing a CO_2/CH_4 Reactor in conjunction with a Sabatier Reactor, was prepared. The ORS block diagram and mass balance is presented in Figure 29. The proposed ORS consists of five major units: an Electrochemical Depolarized Concentrator (EDC), a Sabatier Reactor, a Solid Electrolyte Water Electrolysis Unit, a H_2 Separator, and a CO_2/CH_4 Reactor. The Water Electrolysis Unit is shown as two blocks in the diagram. This is done to illustrate that two banks of water electrolysis cells are required. One bank in the recycle loop are the solid electrolyte cells that electrolyze the water vapor formed in the Sabatier and CO_2/CH_4 Reactors. The second bank is completely independent of the recycle loop and electrolyzes feed water from spacecraft water storage. The second bank of cells can be a conventional liquid electrolyte water electrolysis unit or if a water vapor generator is included, can be the solid electrolyte cells. The EDC removes CO_2 from the cabin atmosphere. The Sabatier Reactor accomplishes partial CO_2 reduction, with the remaining CO_2 being reduced in a recirculation loop consisting of a Solid Electrolyte Water Electrolysis Unit, a H_2 Separator, and a CO_2/CH_4 Reactor.

The unique aspect of this system is the incorporation of the high temperature Solid Electrolyte Water Electrolysis Unit which eliminates the need for regen-

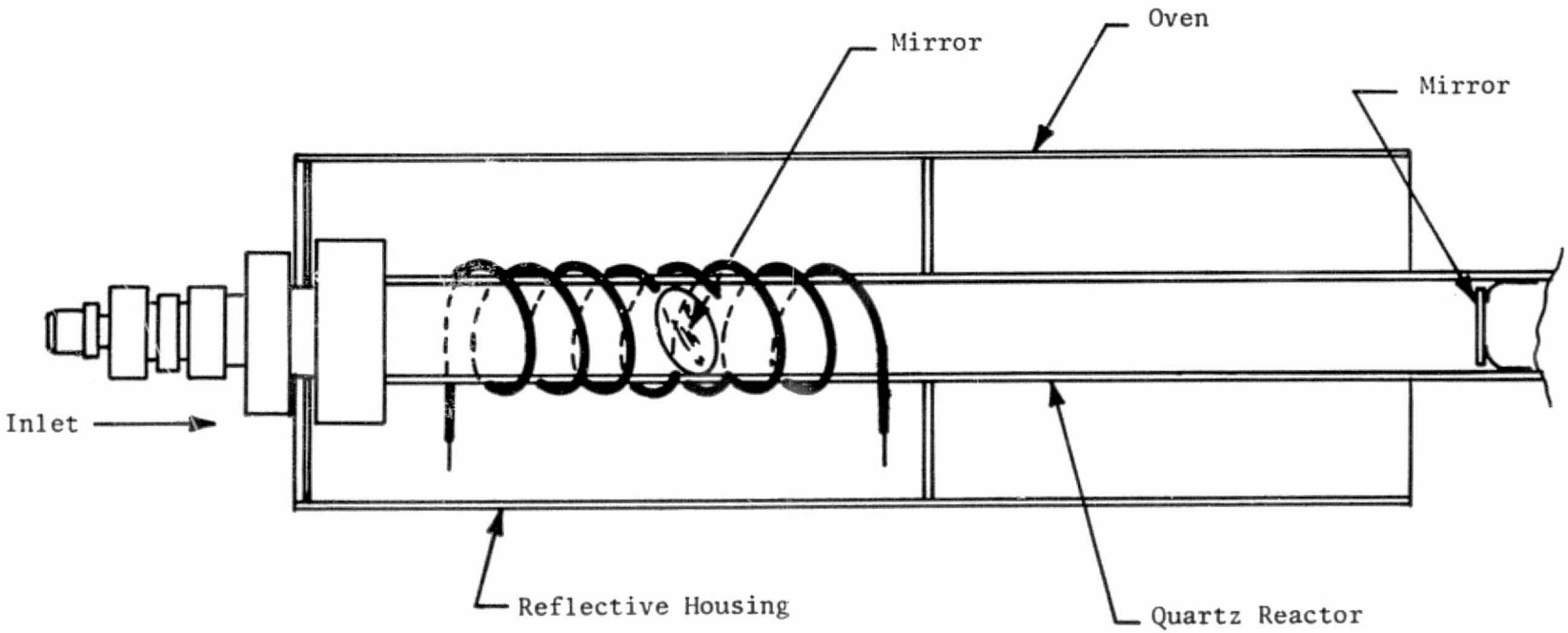

FIGURE 26 SCHEMATIC OF UV ACTIVATION APPARATUS WITHOUT CATALYST

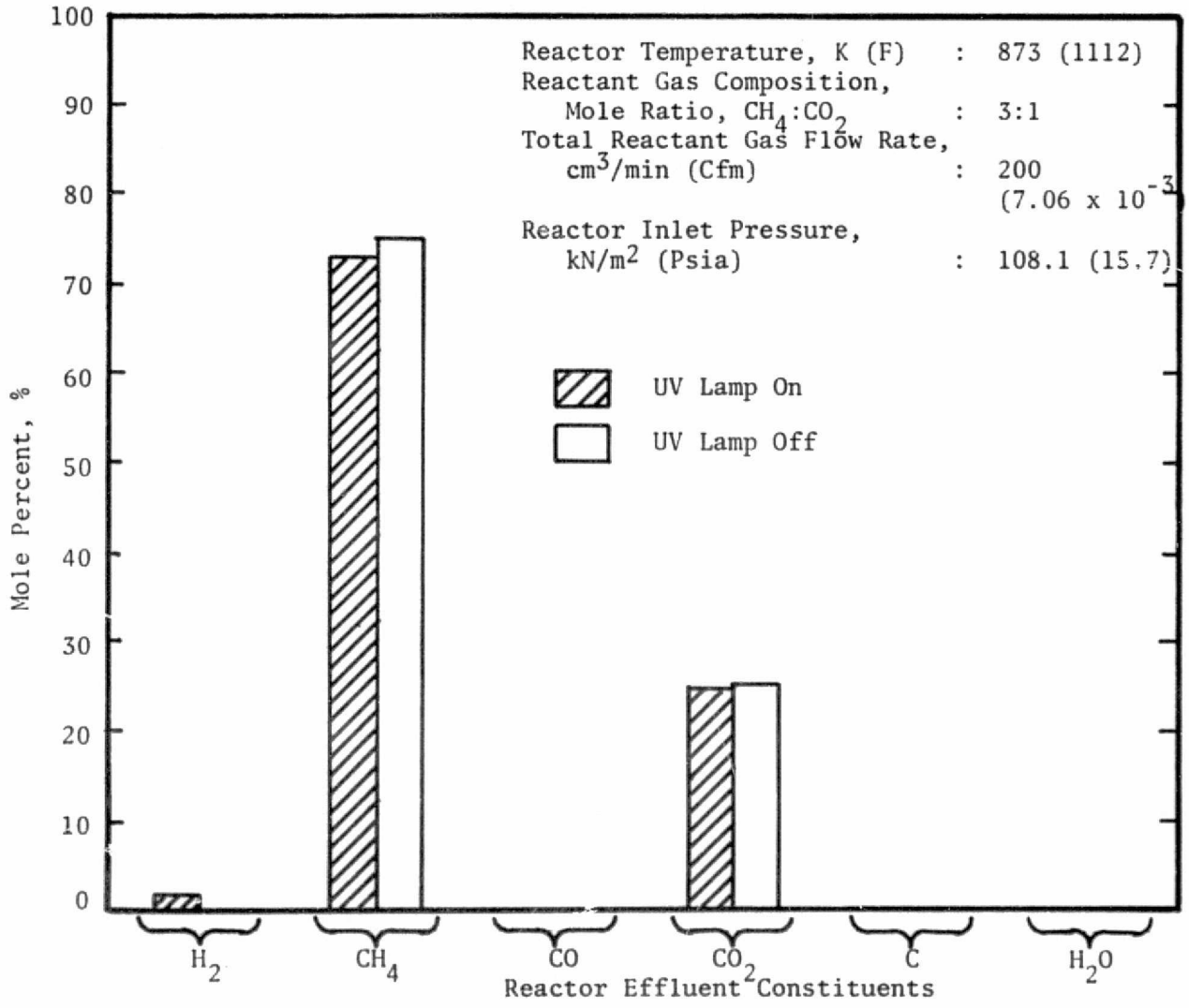

FIGURE 27 EFFECTS OF UV ACTIVATION WITHOUT CATALYST ON REACTOR EFFLUENT COMPOSITION

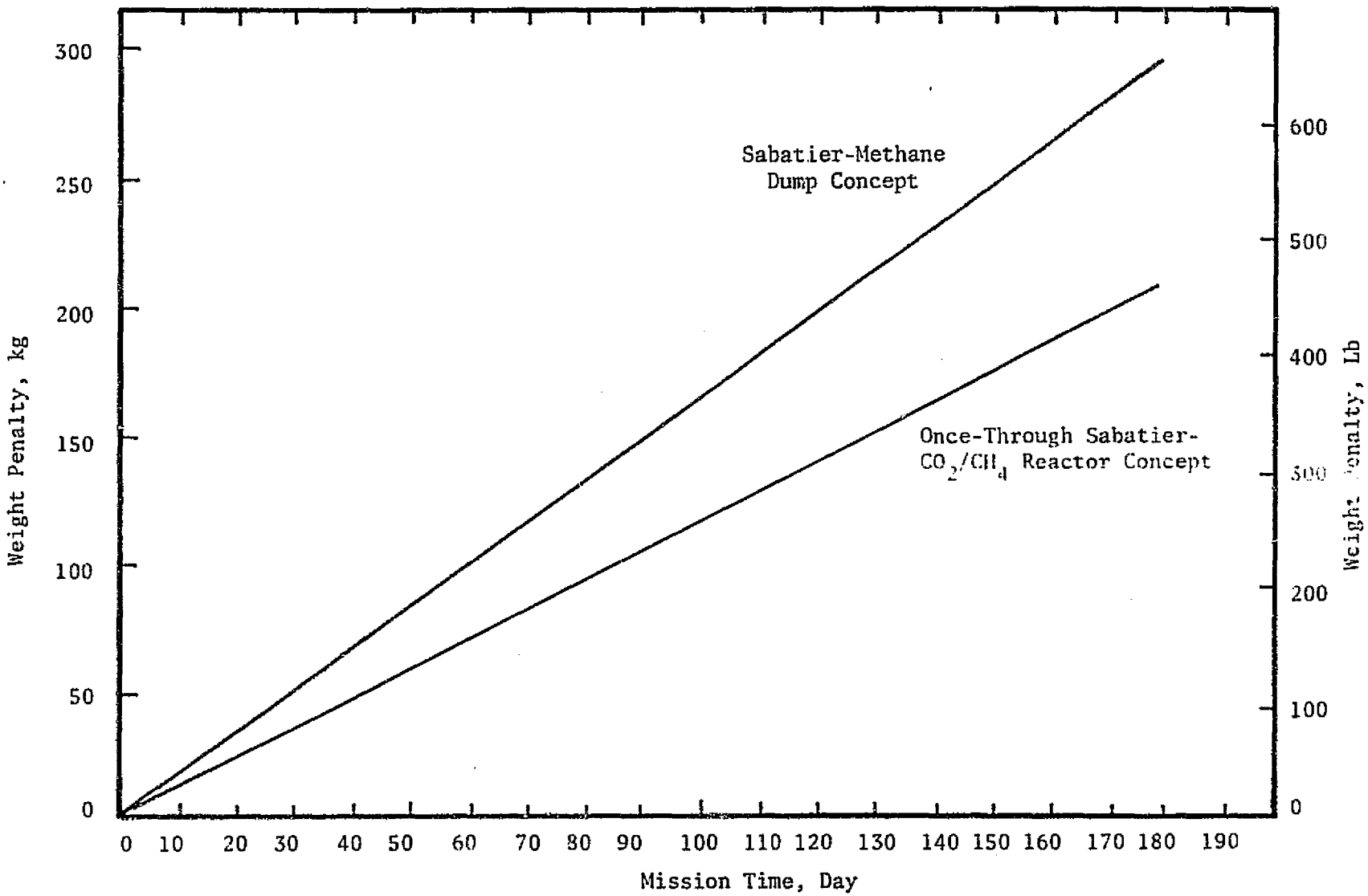

FIGURE 28 COMPARISON OF WATER WEIGHT PENALTY FOR TWO PARTIAL O_2 REGENERATION CONCEPTS

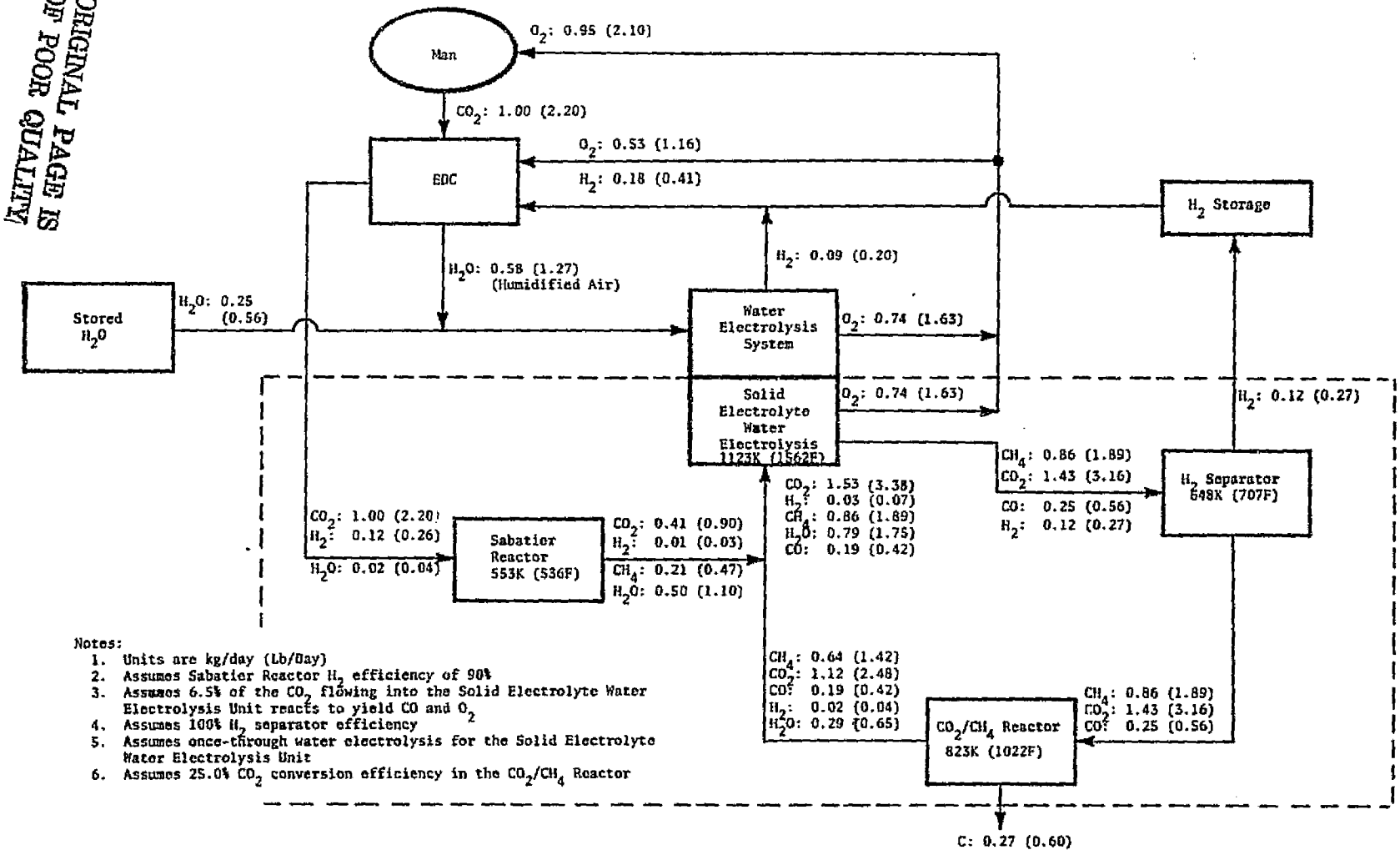

Notes:
1. Units are kg/day (Lb/Day)
2. Assumes Sabatier Reactor H_2 efficiency of 90%
3. Assumes 6.5% of the CO_2 flowing into the Solid Electrolyte Water Electrolysis Unit reacts to yield CO and O_2
4. Assumes 100% H_2 separator efficiency
5. Assumes once-through water electrolysis for the Solid Electrolyte Water Electrolysis Unit
6. Assumes 25.0% CO_2 conversion efficiency in the CO_2/CH_4 Reactor

FIGURE 29 ORS BLOCK DIAGRAM AND MASS BALANCE

erative heat exchangers and condenser/separators and also increases the CO_2/CH_4 Reactor efficiency by removing the product water that forms in the reactor. The reaction is thereby shifted toward more complete reduction of CO_2. It should be noted that the high temperature Solid Electrolyte Water Electrolysis Unit is a concept that can be applied to other CO_2 reduction type life support systems for eliminating the need for regenerative heat exchangers and condenser/separators. Table 5 describes the operation of each of the major system components as sized for a one-man system. A discussion of each of the major units of the ORS follows.

Electrochemical Depolarized Concentrator (EDC)

The CO_2 expired by man is removed from the cabin atmosphere by the EDC. The EDC employs an electrochemical cell which transfers CO_2 from the process air to a H_2 gas stream. During the process, O_2 reacts with the H_2 to produce water and electrical power.[28] A schematic depicting the operation of the EDC cell is shown in Figure 30. The anode exhaust of the EDC will interface with the Sabatier Reactor. The EDC exhaust gas composition is shown in Figure 29. The operating characteristics of the EDC are described in Table 5.

Sabatier Reactor

In the proposed ORS, the EDC anode exhaust will interface with the Sabatier Reactor. In the Sabatier Reactor, CO_2 is reduced with H_2 to CH_4 and water vapor in a heterogeneous exothermic catalytic reaction (Equation 1). In previously proposed life support systems the water vapor is condensed and supplied to an electrolysis system in liquid form which, in turn, supplies O_2 to the cabin atmosphere.[29] The operating characteristics of the Sabatier Reactor are listed in Table 5. The exhaust gas composition of the Sabatier Reactor is shown in Figure 29. For the sake of calculating the mass balances for the ORS, a H_2 conversion efficiency of 90% was assumed for the Sabatier Reactor. The basic configuration of a Sabatier Reactor is shown in Figure 31.

Solid Electrolyte Water Electrolysis Unit

The exhaust gas from the Sabatier Reactor and the exhaust gas from the CO_2/CH_4 Reactor join together and provide the inlet gas to the high temperature Solid Electrolyte Water Electrolysis Unit. The Solid Electrolyte Water Electrolysis Unit electrolyzes the water formed in the Sabatier Reactor and in the CO_2/CH_4 Reactor, thereby completing the O_2 recovery process. In the ORS, the specific advantage of the high temperature Solid Electrolyte Water Electrolysis Unit is that the need for regenerative heat exchangers and condenser/separators are eliminated and the size of the conventional water electrolysis unit can be reduced since O_2 is directly generated.

The principal of operation of the Solid Electrolyte Water Electrolysis Unit is that at elevated temperatures the solid electrolyte material allows the oxide ion ($O^{=}$) to migrate through its crystal lattice because it has a defect structure, i.e., the lattice is deficient in $O^{=}$ and all the anion sites are not filled. If two electrodes are separated by the heated solid electrolyte, water vapor contacting the cathode can be electrolyzed. Hydrogen is formed

TABLE 5 OPERATING CHARACTERISTICS OF THE MAJOR ORS UNITS

Electrochemical Depolarized Concentrator	
Operating Temperature, K (F)	296 (73)
Reactions Occurring	
Anode: $H_2 + 2OH^- = 2H_2O + 2e$	
$H_2O + CO_3^= = CO_2 + 2OH^-$	
Cathode: $2e + \frac{1}{2}O_2 + H_2O = 2OH^-$	
$CO_2 + 2OH^- = H_2O + CO_3^=$	
Net: $CO_2 + H_2 + \frac{1}{2}O_2 = H_2O + CO_2$	
Volume and Mass of Gases Reacting	
H_2: Sccm (Scfm)	551.8 (19.48×10^{-3})
kg/Day (Lb/Day)	0.07 (0.15)
O_2: Sccm (Scfm)	275.9 (9.74×10^{-3})
kg/Day (Lb/Day)	0.53 (1.16)
Transfer Index, Lb CO_2 Transferred/ Lb O_2 Consumed	1.9
Cell Current, A	4.88
Module Size, Cell/Man	15
Sabatier Reactor	
Operating Temperature, K (F)	553 (536)
Reaction Occurring: $CO_2 + 4H_2 = CH_4 + 2H_2O$	
Volume and Mass of Gases Reacting	
CO_2: Sccm (Scfm)	233.6 (8.25×10^{-3})
kg/Day (Lb/Day)	0.73 (1.35)
H_2: Sccm (Scfm)	934.6 (33.0×10^{-3})
kg/Day (Lb/Day)	0.11 (0.25)
Conversion Efficiency	
CO_2, %	61.5
H_2, %	90.0
Feed Gas, H_2/CO_2 Ratio	2.7
High Temperature Water Electrolysis Unit	
Operating Temperature, K (F)	1123 (1562)

continued-

Table 5 - continued

High Temperature Water Electrolysis Unit - continued

Reactions Occurring

$$2H_2O = 2H_2 + O_2$$
$$2CO_2 = 2CO + O_2$$

Volume and Mass of Gas Reacting

H_2O	
(a) from H_2O in Sabatier Reactor Exhaust,	
Sccm (Scfm)	463.6 (16.37×10^{-3})
kg/Day (Lb/Day)	0.50 (1.10)
(b) from H_2O in CO_2/CH_4 Reactor Exhaust,	
Sccm (Scfm)	272.8 (9.63×10^{-3})
kg/Day (Lb/Day)	0.29 (0.65)
CO_2: Sccm (Scfm)	38 (1.34×10^{-3})
kg/Day (Lb/Day)	0.10 (0.22)

Conversion Efficiency

H_2O, % (Once-Through)	100
CO_2, %	6.5(a)

CO_2/CH_4 Reactor

Operating Temperature, K (F)	823 (1022)

Reactions Occurring

$$CO_2 + CH_4 = 2H_2O + 2C$$
$$CH_4 = 2H_2 + C$$
$$2CO = CO_2 + C$$

Volume of Gases Reacting

CO_2: Sccm (Scfm)	136.4 (4.82×10^{-3})
kg/Day (Lb/Day)	0.36 (0.79)
CH_4: Sccm (Scfm)	224.2 (7.92×10^{-3})
kg/Day (Lb/Day)	0.21 (0.47)
CO: Sccm (Scfm)	38.0 (1.34×10^{-3})
kg/Day (Lb/Day)	0.06 (0.14)

Conversion Efficiency

CO_2, %	25
CH_4, %	25
CO, %	25
CH_4/CO_2 Inlet Mole Ratio	1.64

(a) It is projected that 6.5% of the CO_2 that enters the unit will react.

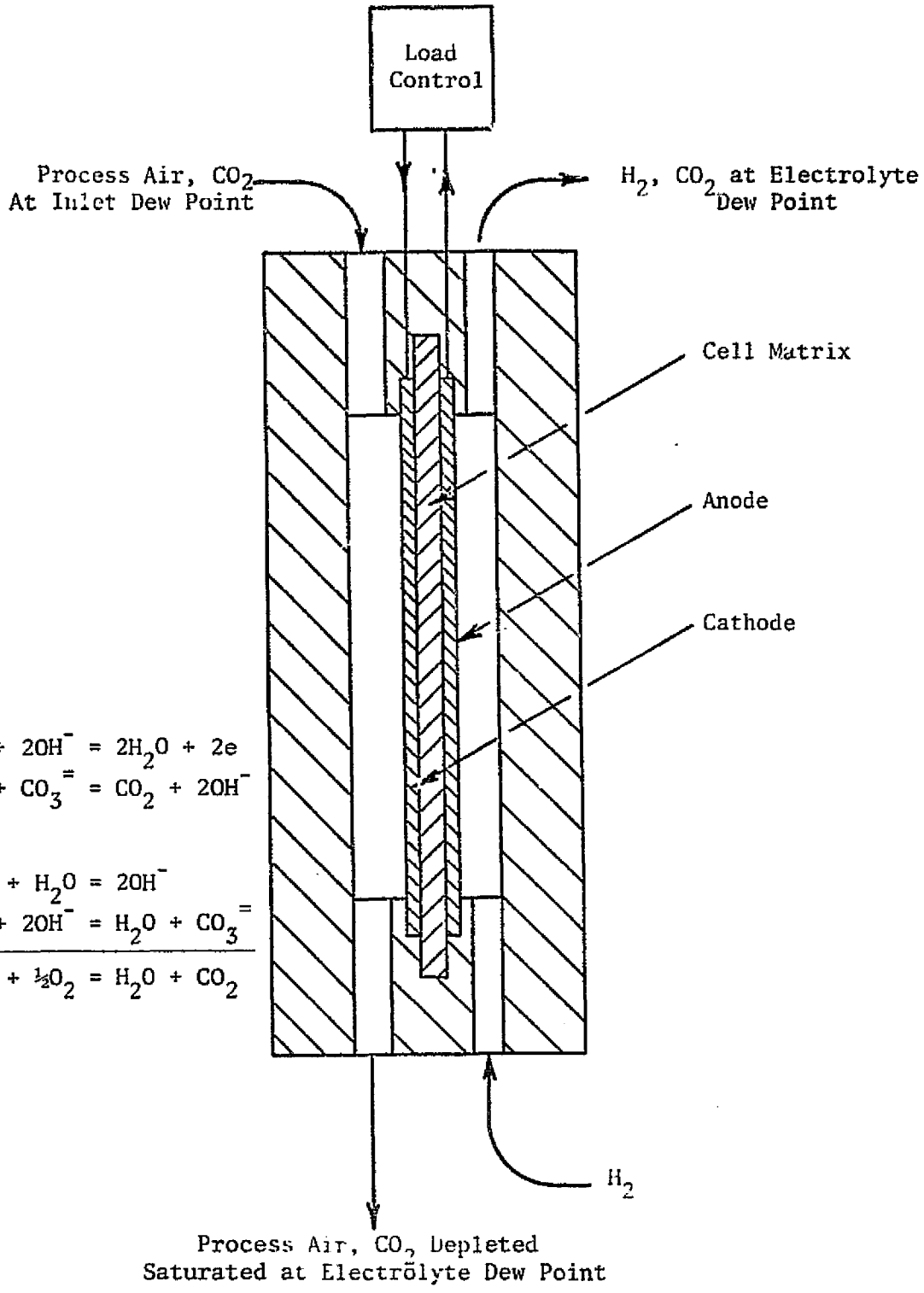

Anode:

$$H_2 + 2OH^- = 2H_2O + 2e$$
$$H_2O + CO_3^{=} = CO_2 + 2OH^-$$

Cathode:

$$2e + \tfrac{1}{2}O_2 + H_2O = 2OH^-$$
$$CO_2 + 2OH^- = H_2O + CO_3^{=}$$

Net: $CO_2 + H_2 + \tfrac{1}{2}O_2 = H_2O + CO_2$

FIGURE 30 EDC CELL SCHEMATIC

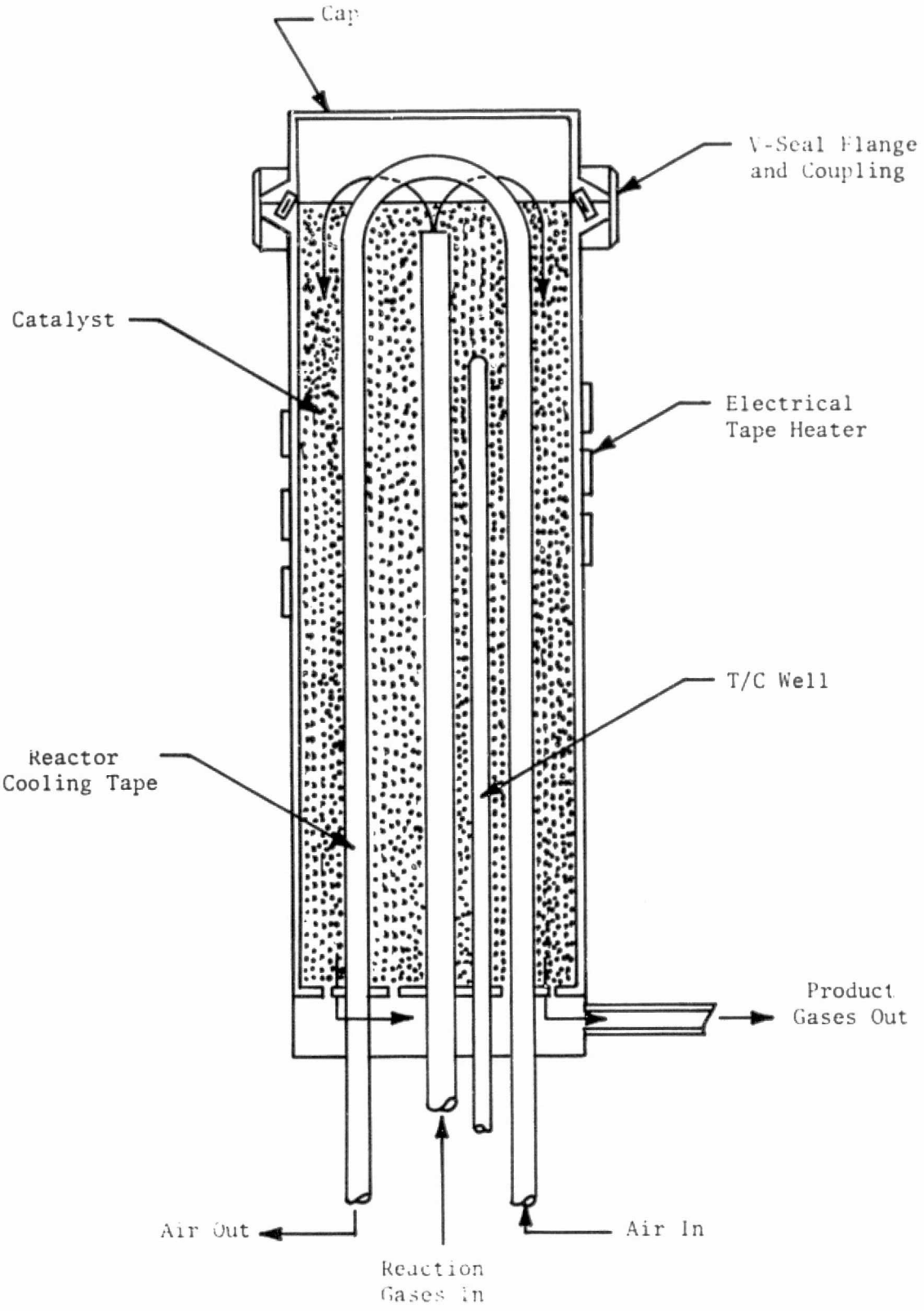

FIGURE 31 SABATIER REACTOR CONFIGURATION

at the cathode, $O^{=}$ carries the current through the electrolyte, and is oxidized to O_2 at the anode.[30] A sketch of the operation of a solid electrolyte water electrolysis cell is presented in Figure 32. A description of the high temperature Solid Electrolyte Water Electrolysis Unit is presented in Table 5. A parellel reaction that will occur in this unit is the electrolysis of CO_2 to CO and O_2. For the purpose of this discussion, it was assumed that 6.5% of the CO_2 entering the Solid Electrolyte Water Electrolysis Unit will react to form CO.

H_2 Separator

The exhaust from the high temperature Solid Electrolyte Water Electrolysis Unit interfaces with the H_2 separator which removes the excess H_2 formed in the recycle loop of the ORS. The H_2 is removed from the recycle loop gas stream by selective diffusion through palladium/silver (Pd/Ag) tubes. The configuration of a typical H_2 separator is shown in Figure 33. The principal of operation is that H_2 diffuses into the tubes under a H_2 partial pressure driving force and exhausts through the Pd/Ag tube manifold.

CO_2/CH_4 Reactor

The exhaust gas from the H_2 separator interfaces with the CO_2/CH_4 Reactor. The CO_2/CH_4 Reactor is required to recover the O_2 from the CO_2 that does not react in the Sabatier Reactor because the Sabatier is H_2-poor. The exhaust gas composition from the Sabatier Reactor (Figure 29) reveals that 155.4 cm^3/min (5.49×10^{-3} cfm) of CO_2 (41% of that produced in one man-day) will not be reacted. The total H_2 available at the Sabatier is based upon the byproduct H_2 produced from water electrolysis in satisfying man's and the EDC's O_2 need minus the H_2 that is consumed in the EDC. In the CO_2/CH_4 Reactor, the remaining CO_2 is reduced by the CH_4 (see Equation 3).

Two other reactions may occur in the CO_2/CH_4 reactor as indicated in Table 5. The reactions that occur depend on the relative gas composition at the reactor inlet which in turn depend on the characteristics of both the Sabatier and CO_2/CH_4 Reactors and the Solid Electrolyte Water Electrolysis Unit. For the mass balance calculations, the results of which are shown in Figure 29, it was assumed that all three reactions take place. It is in this reactor that the carbon present in CO_2 exhaled by man is deposited in a cartridge for removal in the form of a solid. In the analysis that resulted in Figure 29, 5% of the carbon is formed by the $2CO = CO_2 + C$ reaction, 23% of the carbon is formed as a result of the CH_4 decomposition reaction, and the remainder is formed by the CO_2/CH_4 reaction. The configuration of a CO_2/CH_4 reactor is shown in Figure 6.

CONCLUSIONS

Based on the results of this program, the following conclusions are drawn:

1. The reduction of CO_2 with CH_4 is a possible technique which may decrease the launch weight expendables of manned spacecraft by recovering O_2, in the form of water, from the exhaust gases of a Sabatier Reactor. A CO_2/CH_4 reactor when integrated with a Sabatier Reactor

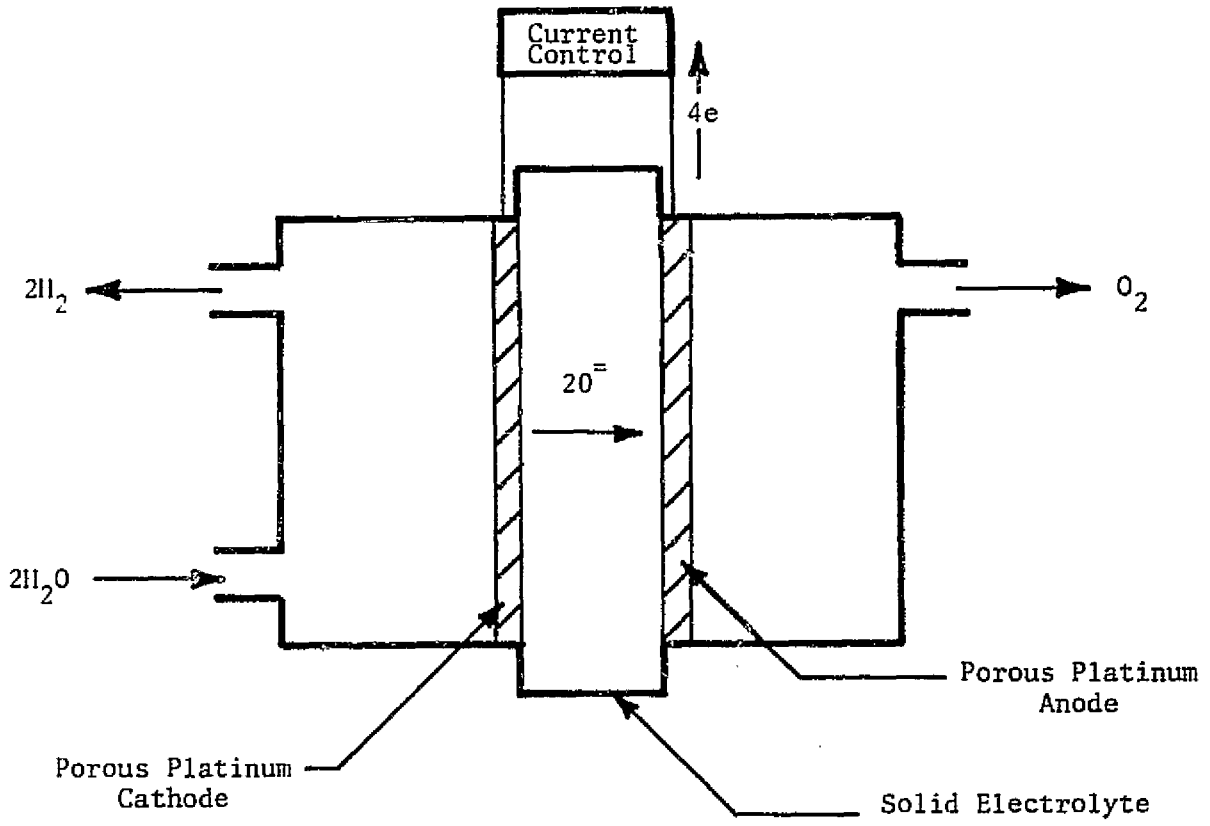

Water Electrolysis Reaction

Anode: $2O^= = O_2 + 4e$

Cathode: $2H_2O + 4e = 2H_2 + 2O^=$

Net: $2H_2O = 2H_2 + O_2$

FIGURE 32 HIGH TEMPERATURE WATER ELECTROLYSIS UNIT CELL SCHEMATIC

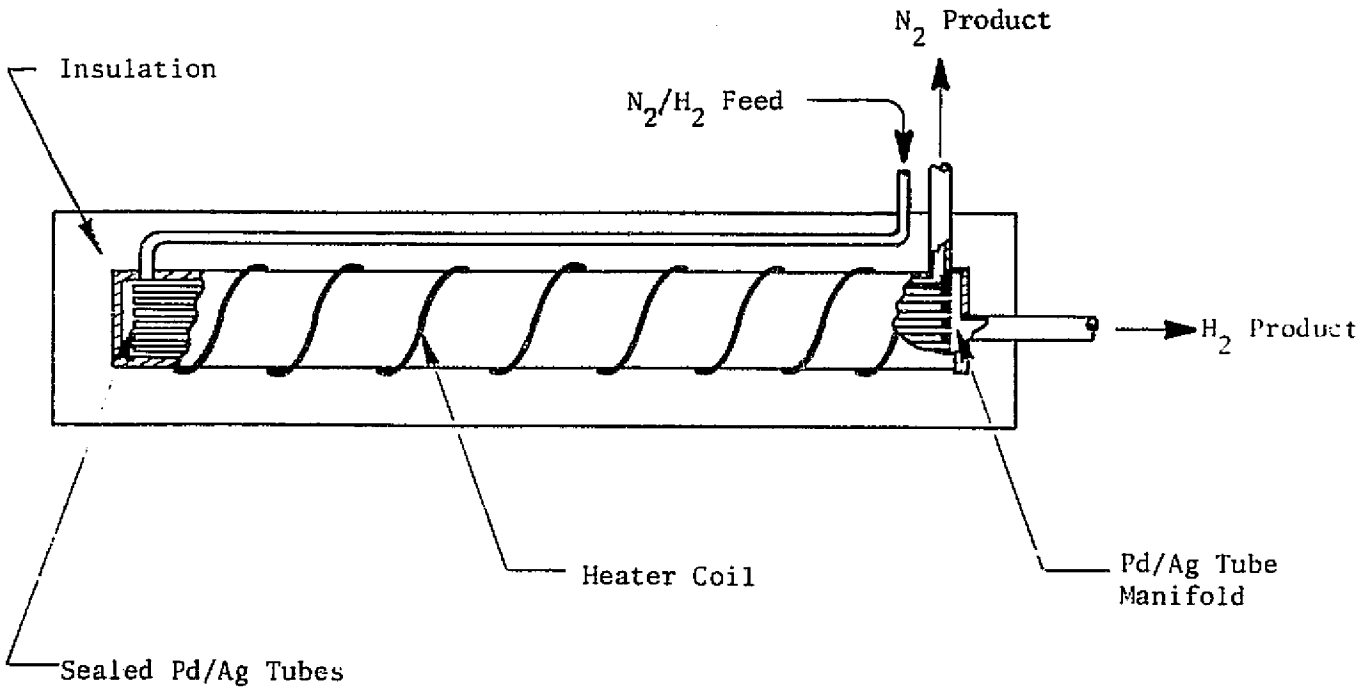

FIGURE 33 H_2 SEPARATOR CONFIGURATION

in a once-through flow scheme increases the percentage of metabolic CO_2 reduced from 75% for the Sabatier Reactor itself, to 82.5% for the Sabatier and CO_2/CH_4 combination. This represents an 84.9 kg (187 lb) reduction in stored water for six-man, 180-day mission.

2. The minimum CO_2/CH_4 reactor temperature that can be used without greatly sacrificing reaction efficiency is 773K (932F). At this temperature with Linde Ni on molecular sieves catalyst a reaction efficiency of 25% was attained.

3. A CO_2/CH_4 Reactor can be employed in a closed-loop O_2 regeneration system by recycling the effluent of the reactor and incorporating a high temperature water electrolysis unit and H_2 Separator in the recycle loop. For this configuration, a total savings of 304 kg (671 lb) in stored water at launch is possible for a six-man, 180-day mission.

4. Heterogeneous catalysis at temperatures greater than 773K (932F) is the technique that can be applied most successfully to the reduction of CO_2 with CH_4 for the recovery of O_2. Gamma ray radiation methods, UV photolysis, and homogeneous catalysis are not considered feasible alternatives because of their very low reaction efficiencies and, in the case of the homogeneous catalysts, high catalyst consumption rate.

5. Nickel (Ni) supported on molecular sieves is the most active catalyst for the reduction of CO_2 with CH_4. Of the six heterogeneous catalysts evaluated, Ni on molecular sieve catalysts were also the most reactive catalysts at low temperatures. A Linde Ni on molecular sieve catalyst achieved a maximum conversion efficiency of 29.9% at 950K (1251F) while a similar Girdler catalyst achieved a maximum conversion efficiency of 21.7% at 873K (1112F).

6. Linde Ni on molecular sieve catalyst should not be used at temperatures above 773K (932F) due to catalyst degradation within several hours of operation.

7. The use of UV radiation in conjunction with Ni on molecular sieve catalysts for temperatures up to 873K (1112F) did not improve the CO_2/CH_4 reaction efficiency (based on a production of water). In fact, at 873K (1112F) the reaction efficiency of the Girdler catalyst decreased from 18.7 to 16.5% when UV radiation was used. The reaction efficiency of the Linde catalyst was not significantly affected.

8. The use of UV radiation by itself for temperatures up to 873K (1112F) is not a means of activating the CO_2/CH_4 reaction. Only 2.7% of the CH_4 reacted and no water was produced when UV was used at 873K (1112F).

9. Iron wool can be added downstream of a Ni on molecular sieve catalyst to increase the overall reaction efficiency by reducing residual

CO in the reactor effluent with H_2. A 5.5% increase in reaction efficiency, based on the production of water, was observed.

10. The data obtained during the analytical and experimental activities of this program can be used to size and design a CO_2/CH_4 reactor for a once-through or recycle loop application to recover O_2 from the CO_2 contained in the effluent of a Sabatier Reactor as used in an Environmental Control/Life Support System of a manned spacecraft.

RECOMMENDATIONS

Based on the results of this study, it is recommended that further work in the following areas be performed:

1. Design, fabricate, assemble, and test a Breadboard Integrated Oxygen Recovery System (BIORS) that includes a Sabatier Reactor for partial CO_2 reduction and a recycle loop, including a CO_2/CH_4 reactor, a H_2 separator, and a Solid Electrolyte Water Electrolysis Unit for reduction of the remaining CO_2. The BIORS to be assembled and tested would include those units contained in the dashed line boundary in Figure 29. Ground Support Accessories would be fabricated and utilized to simulate the EDC anode exhaust. Testing would involve parametric tests and a 30-day endurance test.

2. Conduct a study aimed at defining a continuous carbon collection technique. This study would involve the identification of alternate techniques for collecting the carbon formed during CO_2 reduction processes. The goal of this study will be to identify possible techniques which will allow the solid carbon to be collected in a continuous manner. Such a technique would enable a decrease in the size of the reactor with a resulting decrease in weight, volume, and heat loss and would eliminate the need for frequent cartridge changes, thus reducing the need for expendables.

   As seen in Figure 2, carbon collection is an ultimate requirement for all CO_2 reduction systems and therefore the results of this study would find wide application. At NASA's option, this study could be expanded to include the fabrication and testing of the recommended continuous carbon collection technique.

REFERENCES

1. United Aircraft Corporation, "Trade-Off Study and Conceptual Designs of Regenerative Advanced Integrated Life Support Systems (AILSS)," NASA CR 1458, January, 1970.

2. Mills, E. S., Linzey, T. J., and Harkee, J. F., "Oxygen Recovery for the 90-Day Space Station Simulator Test," Paper No. 71-Av-18, SAE/ASME/AISS Life Support and Environmental Control Conference, San Francisco, California, July 12-14, 1971.

3. Trusch, R. B., Brose, H. F., and Thompson, C. D., "Atmosphere Revitalization in the Space Station Prototype," Paper No. 72-ENAv-24, Environmental Control and Life Support Systems Conference, San Francisco, California, August 14-16, 1972.

4. Holmes, R. F., Keller, E. E., and King, C. D., "A Carbon Dioxide Reduction Unit Using Bosch Reaction and Expendable Catalyst Cartridges," Convair Div. of General Dynamics Corp., NASA CR 1682, November, 1970.

5. Life Systems, Inc., "Solid Electrolyte Oxygen Regeneration System," First Quarterly Report, ER-190-4-1, Contract NAS2-7862, April, 1974.

6. Rousseau, J., "Atmospheric Control Systems for Space Vehicles," AiResearch Manufacturing Co., Contract AF33(657)953, March, 1963.

7. Hummel, L. E. and Rousseau, J., "Project RAW," Final Report, AiResearch Manufacturing Co., November, 1964.

8. Kurganova, S. Ya., Kulakova, I. I., Rudenko, A. P., and Balandin, A. A., Dokl. Akad. Nauk SSSR, 167, 350, 1960.

9. Stecher, P. G., Ed., "The Merck Index," Eighth Edition, Merck & Co., Inc., Rahway, N. J., 1968.

10. Wynveen, R. A., Schubert, F. H., and Powell, J. D., "One-Man Self-Contained CO_2 Concentrating System," Final Report, NASA CR-114426, March, 1972.

11. Schubert, F. H., "Study of the Integration of the Electrochemical Depolarized CO_2 Concentrator with the Bosch CO_2 Reduction Subsystem," Final Report, NAS8-29623, June, 1974.

12. Constant, R., Lecocg, R., Provoost, F., and Vasilescu, P., At.-Euratom, EUR-3496.f, 1967.

13. Hummel, R. W., "U. K. At. Energy Authority, Research Group, At. Energy Research Establishment," Report AERE-R, 4838, 1965.

14. Black, G. and Porter, G., Proc. Roy. Soc. (London), Ser. A266, 185, 1962.

15. Mahan, B. H. and Mandal, R., J. Chem. Phys., 37, 207, 1962.

16. Walker, D. C. and Black, R. A., J. Chem. Phys., 38, 1526, 1963.

17. Braun, W., Welge, K. H., and McNesby, J. R., J. Chem. Phys., 45, 2650, 1966.

18. Black, R. A. and van der Auwera, D., Can. J. Chem., 40, 2339, 1962.

19. Miller, G. A. and Steffgen, F. W., Catalyst Reviews, 8, 159, 1973.

20. Thompson, Jr., E. B., "Investigation of Catalytic Reactions for CO_2 Reduction," Part III, AF Flight Dynamics Laboratory, No. FDL TDR 64-22, October, 1965.

21. Thompson, Jr., E. B., "Investigation of Catalytic Reactions for CO_2 Reduction," Part IV, AF Flight Dynamics Laboratory, No. FDL TDR 64-22, February, 1966.

22. Ames, R. K., "Sabatier Reactor Performance Using Ruthenium and Nickel Catalysts at Sea Level and Reduced Pressure," 4th Space and Flight Equipment Symposium, San Diego, California, October 4-7, 1966.

23. Sigov, S. A. and Abdullaeva, U. A., Uzbeksk. Khim. Zh., 9, 63, 1965.

24. Bodrov, I. M. and Apel'baum, L. D., Kinet. Katal., 8, 379, 1967.

25. Shankle, J. D., "Evaluation of Life Support Chemical Techniques," Vol. 3, Final Report, AiResearch Manufacturing Co., NASA-1043, August, 1965.

26. Kim, B. C., Zupan, J., Hillenbrand, L., and Clifford, J. E., "Continous Catalytic Decomposition of Methane," Final Report, Battelle Memorial Inst., NASA CR-1662, October, 1970.

27. Hedden, K. and Ruch, S., Chem.Ing.Tech., 39, 1017, 1967.

28. Powell, J. D., Schubert, F. H., Marshall, R. D., and Shumar, J. W., "Six-Man, Self-Contained Carbon Dioxide Concentrator Subsystem," Final Report, NASA CR-114743, June, 1974.

29. Verostko, C. E., Forsythe, R. K., "A Study of the Sabatier-Methanation Reaction," Paper No. 740933, Intersociety Conference on Environmental Systems, Seattle, Washington, July 29 August 1, 1974.

30. Sproule, Richard T., "Solid Electrolytes: New Applications for ZrO_2," Microtecnic, Vol. XXVII, February, 1973.

APPENDIX 1 CALIBRATION DATA

FIGURE		PAGE
A1-1	Calibration of Reactor Inlet Pressure Gauge, PG1 (Low Range)	A1-2
A1-2	Calibration of Reactor Inlet Pressure Gauge, PG1 (High Range)	A1-3
A1-3	Calibration of Reactor Differential Pressure Gauge, PG2	A1-4
A1-4	Calibration of CO_2 Flowmeter, FM1	A1-5
A1-5	Calibration of CH_4 Flowmeter, FM2	A1-6
A1-6	Calibration of Reactor Oven Temperature Readout .	A1-7

PRECEDING PAGE BLANK NOT FILMED

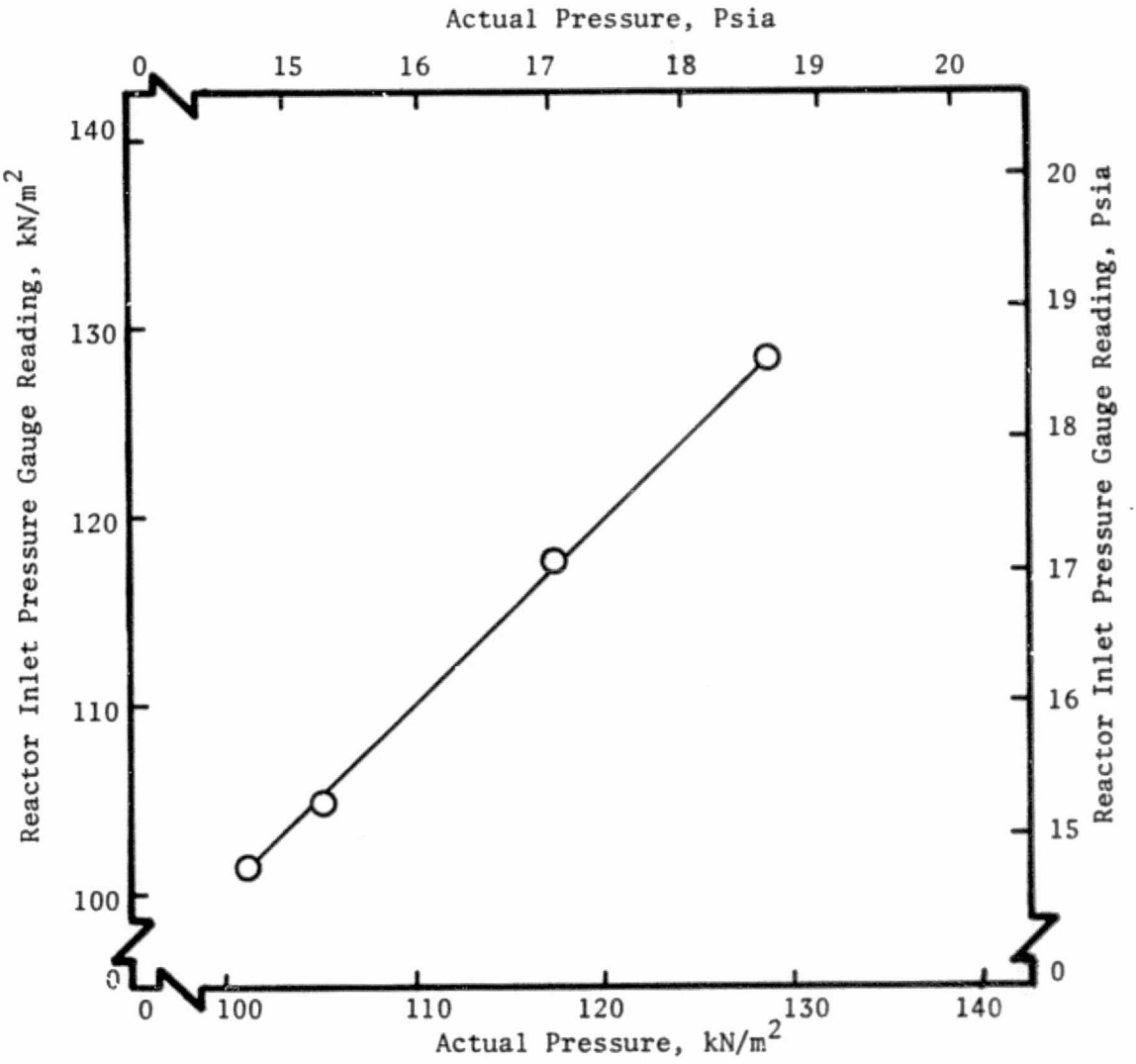

FIGURE A1-1 CALIBRATION OF REACTOR INLET PRESSURE GAUGE, PG1 (LOW RANGE)

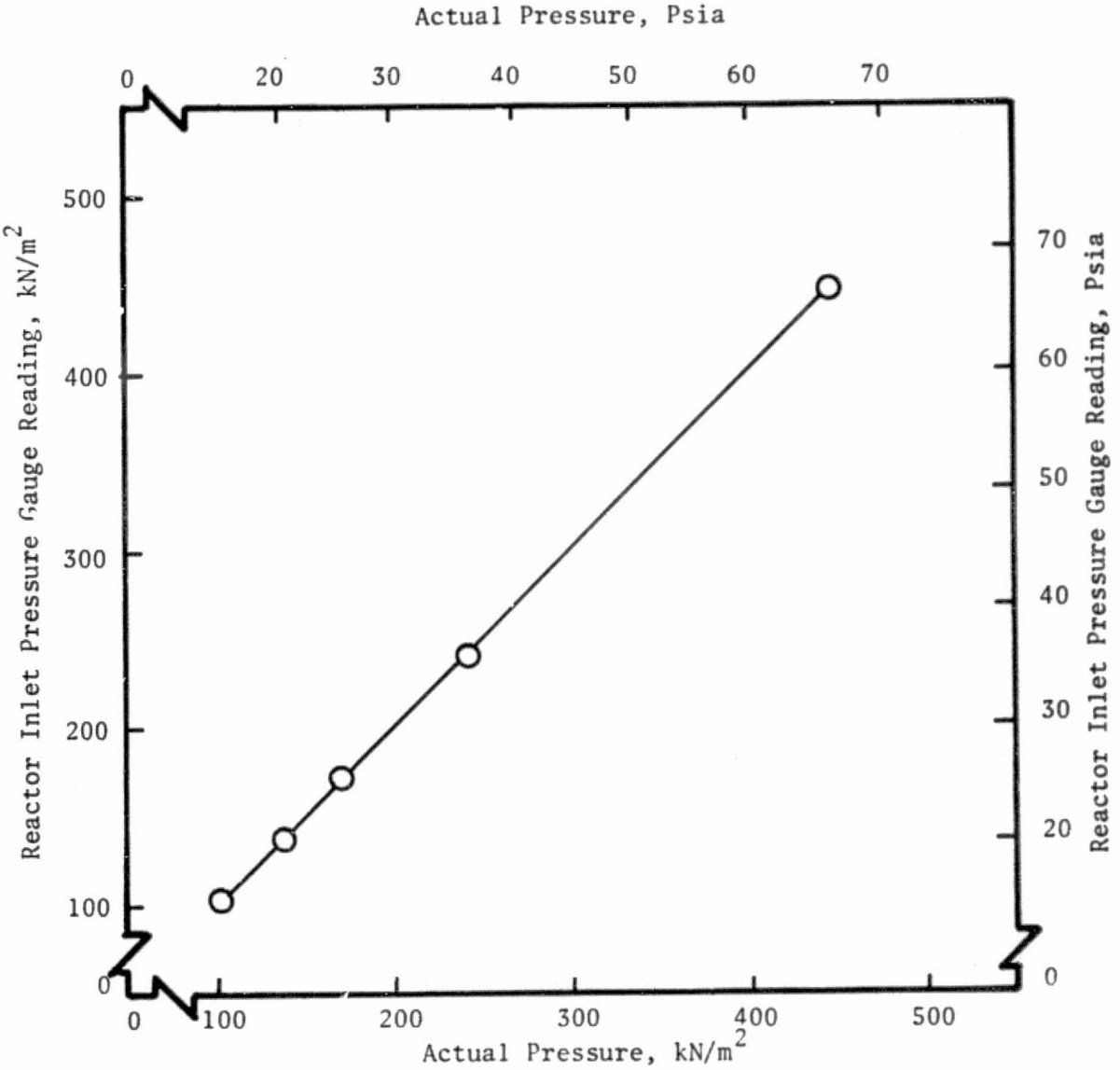

FIGURE A1-2 CALIBRATION OF REACTOR INLET PRESSURE GAUGE, PG1 (HIGH RANGE)

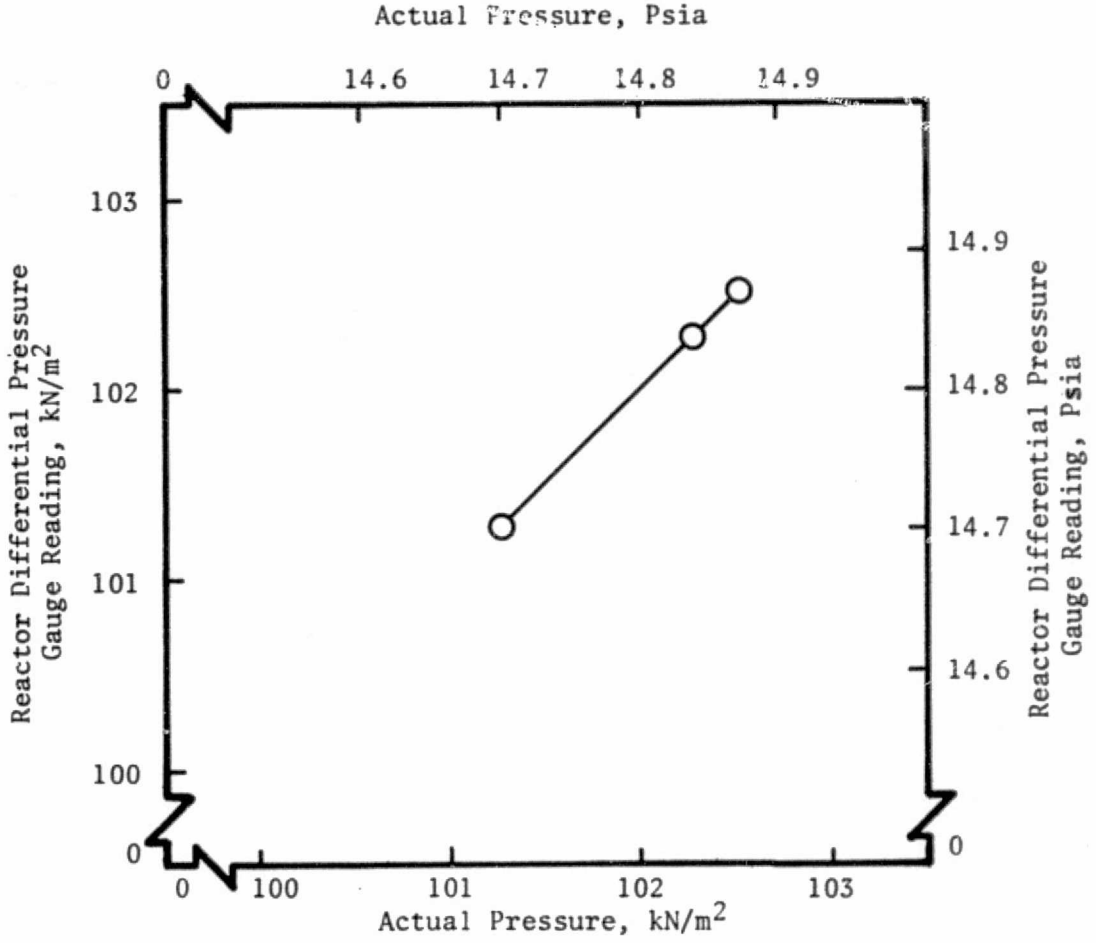

FIGURE A1-3 CALIBRATION OF REACTOR DIFFERENTIAL PRESSURE GAUGE, PG2

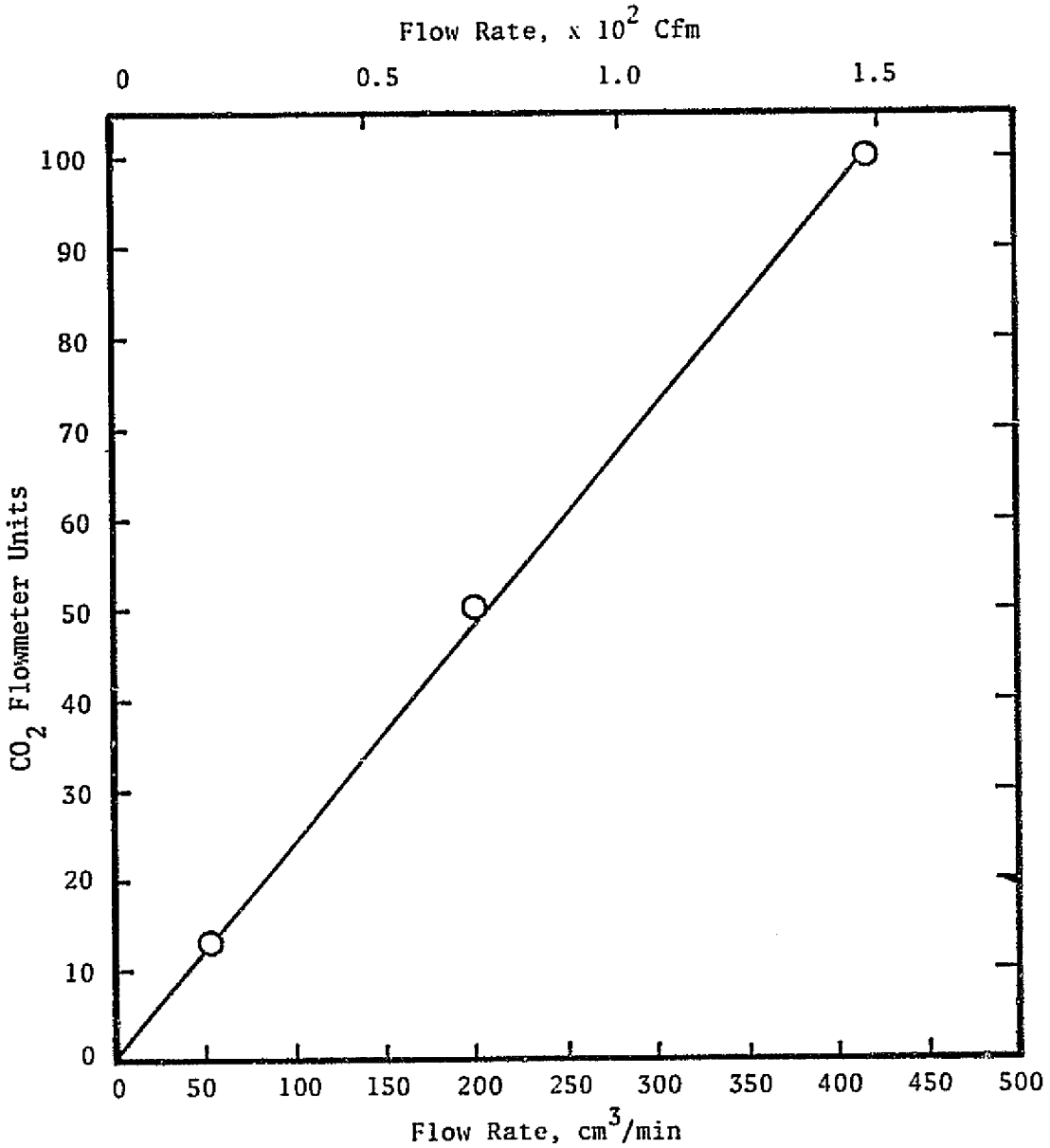

FIGURE A1-4 CALIBRATION OF CO_2 FLOWMETER, FM1

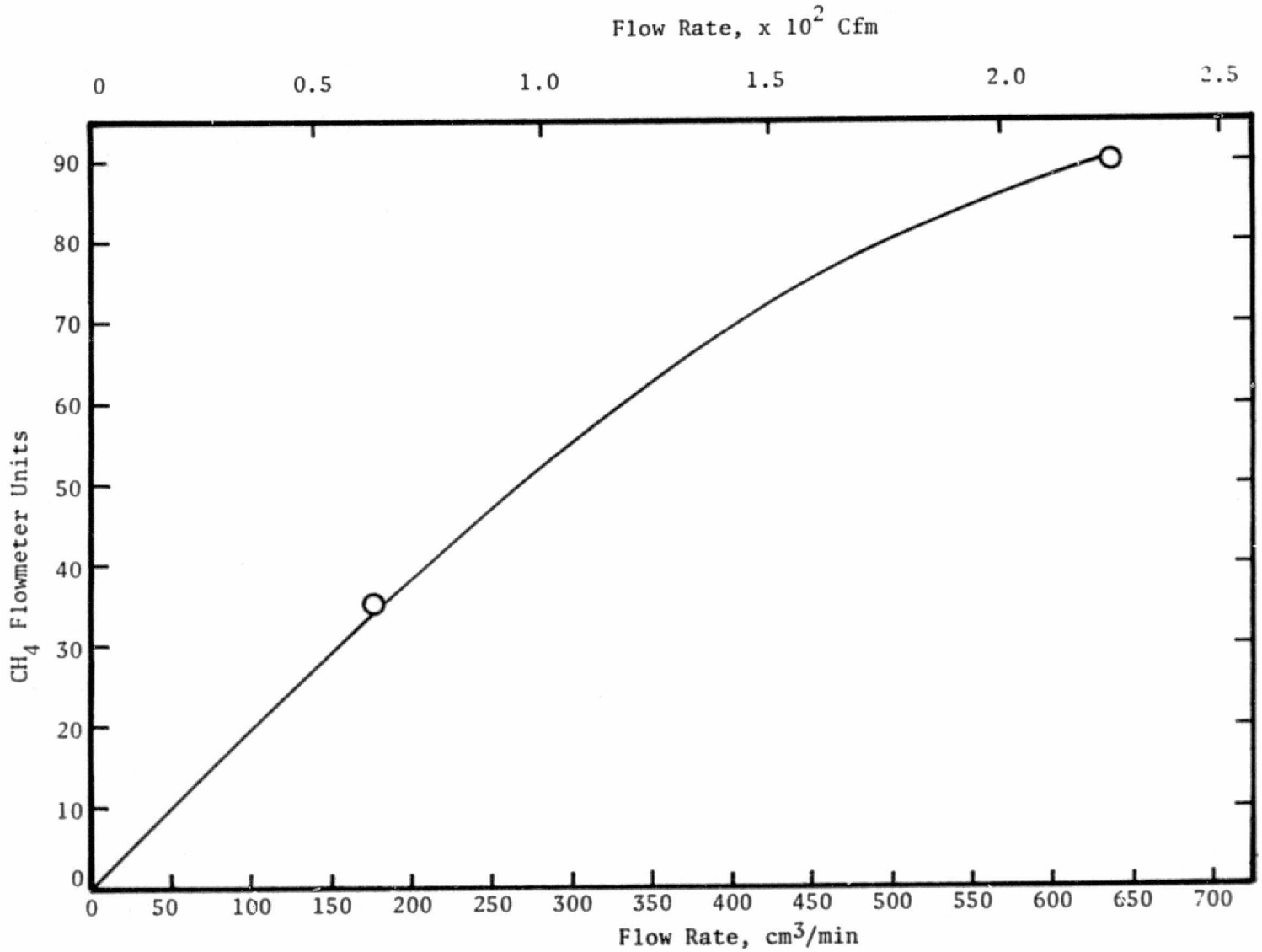

FIGURE A1-5 CALIBRATION OF CH_4 FLOWMETER, FM2

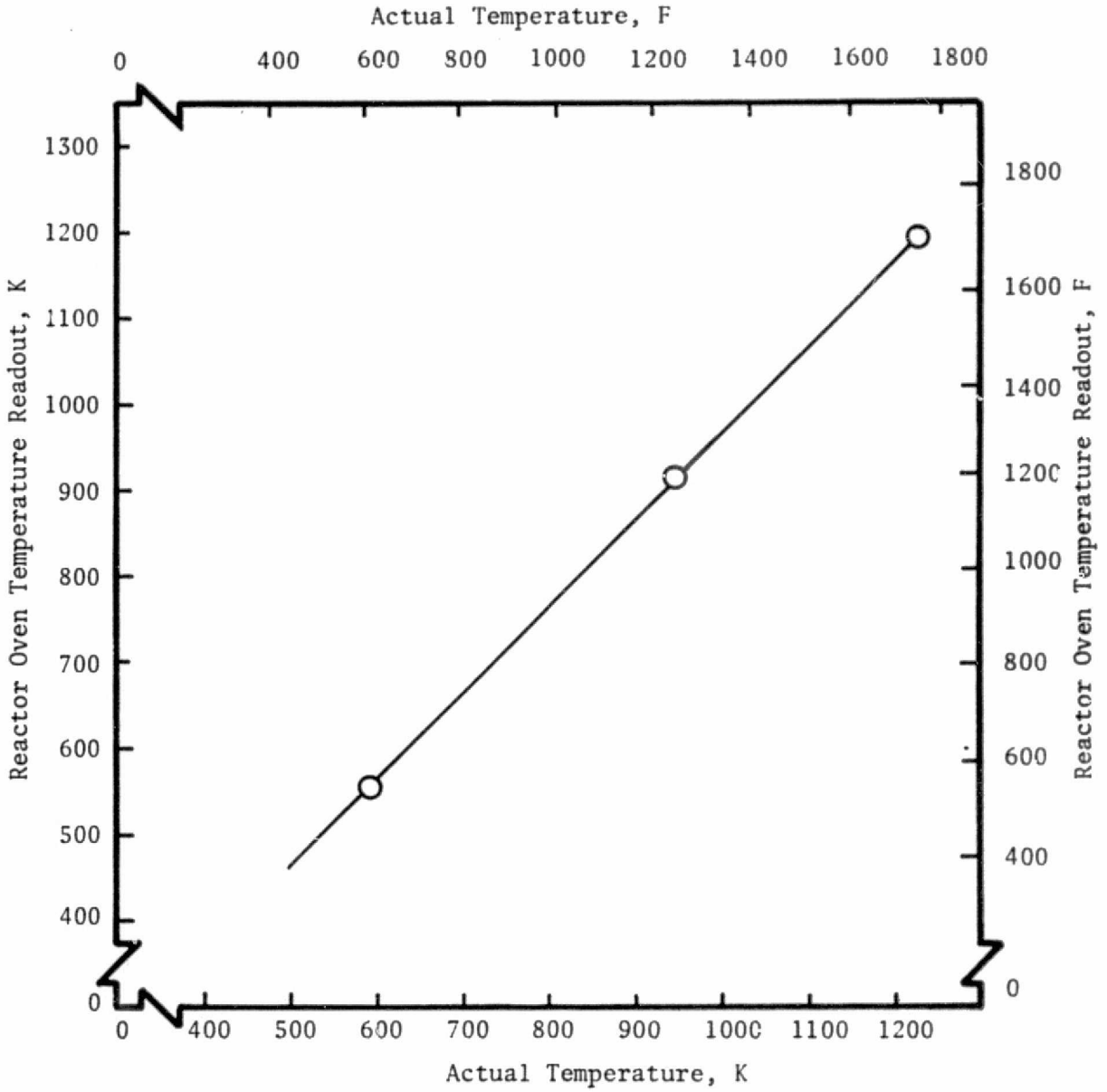

FIGURE A1-6 CALIBRATION OF REACTOR OVEN TEMPERATURE READOUT